URINARY AND BLOOD-DERIVED BIOMARKERS INDICATIVE OF RECOVERY FROM TRAUMATIC BRAIN INJURY AND SPINAL CORD INJURY

ELANI ANN BYKOWSKI
Bachelor of Science, **University of Lethbridge, 2018**

A thesis submitted
in partial fulfilment of the requirements for the degree of

MASTER OF SCIENCE

in

NEUROSCIENCE

Department of Neuroscience
University of Lethbridge
LETHBRIDGE, ALBERTA, CANADA

URINARY AND BLOOD-DERIVED BIOMARKERS INDICATIVE OF RECOVERY FROM TRAUMATIC BRAIN INJURY AND SPINAL CORD INJURY

ELANI BYKOWSKI

Date of Defense: April 14, 2020

Dr. Gerlinde Metz	Professor	Ph.D.
Tony Montina	Instructor	M.Sc.
Thesis Co-Supervisors		
Dr. Chantel Debert	Assistant Professor	M.D./M.Sc.
Thesis Examination Committee Member		
Dr. Artur Luczak	Professor	Ph.D.
Thesis Examination Committee Member		
Dr. Sergio Pellis	Professor	Ph.D.
Chair, Thesis Examination Committee		

DEDICATION

I would like to dedicate my MSc. Thesis to the professors who have mentored me as well as my friends and family for their enduring support throughout my Bachelor's and Master's degrees at the University of Lethbridge.

ABSTRACT

Background: This study aims to determine if a proton nuclear magnetic resonance-based quantitative metabolic profiling approach can identify novel biomarkers in clinically accessible biofluids that are indicative of both the repair processes and treatment efficacy during recovery from traumatic brain injury and spinal cord injury. The main hypotheses of this study are (a) that changes in the metabolic profiles following injury can be correlated to the extent of recovery of patients and (b) that biological pathway analysis will provide an insight into the mechanisms behind the repair process.

Methods: Patients with spinal cord injury and traumatic brain injury were recruited through the Foothills Medical Centre in Calgary, Alberta. Urine and blood samples were collected from patients initially and again at 6 months post-injury for NMR spectral acquisition.

Impact: Metabolomic analysis provides a window into the pathophysiological processes that underlie the recovery process, with insight for clinical application.

PREFACE

I wish to acknowledge the contributions of authors in the following manuscript-based thesis:

Elani Bykowski - primary author of all 4 studies and incorporated edits/revisions from Dr. Chantel Debert, Tony Montina, and Dr. Gerlinde Metz.

The authors would like to thank the Eric Paxman, Regan King, Janis Yajure and Mark Piitz for assistance with recruitment and collections of clinical measures and urine.

This research was supported by the Hotchkiss Brain Institute at the University of Calgary (Chantel Debert, Tony Montina, Gerlinde Metz) CIHR Project Scheme #363195 (G.M.) and NSERC Discovery Grant #5519 (Gerlinde Metz). E.B. was supported by a CIHR CGS-M studentship.

ACKNOWLEDGEMENTS

I would like to acknowledge Jamie Petersson for all her support during sample preparation and analysis. I extend gratitude to Dr. Gerlinde Metz for her endless encouragement, mentorship, and support for the past 2 years. I also extend gratitude to Tony Montina for his constant guidance and mentorship, and for imparting “nothing ventured, nothing gained.” I also extend appreciation to Michael Opyr for his brilliance with technical trouble shooting and to Dr. Sandy Shultz for his guidance while working alongside the Monash Trauma Group in Melbourne, Australia for 2 months.

TABLE OF CONTENTS

LIST OF TABLES

LIST OF FIGURES

LIST OF ABBREVIATIONS

SCI	Spinal Cord Injury
TBI	Traumatic Brain Injury
PCA	Principal Component Analysis
OPLS-DA	Orthogonal Projections to Latent Structures Discriminant Analysis
VIAVC	Variable Importance Analysis Based on Random Variable Combination
TBO	Triple Resonance Broadband
UCAN	University of Calgary Advising Network

CHAPTER 1: INTRODUCTION

"Some people are walking around with full use of their bodies and they're more paralyzed than I am."

- Christopher Reeve (spinal cord patient)

Metabolomics is a powerful approach to capture the metabolic fingerprint of an individual based on endogenous small molecules within biological fluids (Nicholson et al., 2008). Nuclear magnetic resonance (NMR) spectroscopy is a tool that permits identification of novel compounds and it has been used to study metabolic disturbances following stroke (Jung et al., 2011), severe traumatic brain injury (TBI) (Glenn et al., 2013), and spinal cord injury (SCI) (Peng et al., 2014). Metabolomic NMR studies of clinically accessible bio-fluids, such as blood and urine, provides an intricate and relatively non-invasive snapshot into the metabolic response. Urine is a non-invasive, easily accessible bio-fluid, and NMR has the most number of detectable (209) and unique (108) metabolites in human urine when compared to chromatography and mass spectroscopy techniques (Bouatra et al., 2013). Furthermore, NMR can detect 49 metabolites in human serum and plasma samples, 20 of which are unique to NMR (Psychogios et al., 2011). Our research question is to determine if a proton NMR based quantitative metabolic profiling approach can identify novel biomarkers that are indicative of both the repair processes and treatment efficacy following recovery from TBI and SCI. We hypothesize that (a) each of the different neurological conditions will yield changes in the metabolic profiles that can be correlated to the extent of recovery of a patient, and (b) that biological pathway analysis will provide an insight into the mechanisms behind the repair process (Xia et al., 2010). These techniques will advance the objective of my MSc project, to provide a greater

understanding of the biochemical processes that mediate injury repair in the central nervous system.

TBI is a prevalent issue, with an incidence that is 10 times greater than SCI (Khan et al., 2003). Primary causes of TBI are the result of mechanical forces at the time of trauma, including rapid acceleration, contusion, and tearing of cranial nerve figures (Meaney & Smith, 2011). This stage is followed by delayed, secondary pathology which is characterized by oxidative stress, inflammation, and changes in cerebral metabolism (Siesjo & Siesjo, 1996). Intervention during the secondary phase could lead to attenuation of these symptoms. TBI can be classified as severe (GCS less than 8), moderate (GCS 8-12), and mild (GCS 13-15)., (Sternbach et al., 2000). There are four sub-types of TBIs present within our patient cohort: subdural hematoma (n=5), subarachnoid hemorrhage (n=3), diffuse axonal injury (n=2), and intraparenchymal hemorrhage (n=1). Subdural hematoma results from formation of a blood clot between the inner layer of the dura mater and arachnoid mater of the brain (Shim et al., 2007). As it increases in size, it exerts pressure on the brain which can result in headaches. Subarachnoid hemorrhage occurs when blood is released into the space between the brain and the skull, which exerts pressure on the brain against the bone (Sobey & Faraci, 2007). Diffuse axonal injury (DAI) occurs when the head is rapidly accelerated or decelerated, due to traumatic shearing forces (Adams et al., 1989). DAI results in damage to the white matter tracts of the brain, such as the corpus callosum and within the brainstem (Mesfin et al., 2020). Lastly, intraparenchymal hemorrhage is a form of intracerebral bleeding, which can lead to subarachnoid hemorrhage and subdural hematoma (Chang et al., 2006).

Reduced ATP production due to mitochondrial dysfunction and brain tissue hypoxia underlie these neurodegenerative changes (Werner & Engelhard, 2007). Due to low oxygen levels, anaerobic glycolysis is the primary means of ATP production, and ensuing depletion of ATP leads to failure of ion pumps. Additional downstream pathological changes include oedema and subsequent increases in intracranial pressure, efflux of excitatory amino acid neurotransmitters leading to prolonged depolarization, and inflammation. Brain oedema is a consequence of increased blood-brain-barrier permeability, and ensuing infiltration of leukocytes which trigger inflammation (Readnower et al., 2010). Secondly, excessive release of excitatory neurotransmitters, predominantly glutamate, creates overstimulation of glutamate receptors, which lead to fluctuations in calcium, sodium, and potassium ion levels. Neuronal attempts to correct these ion balances results in over-activity of Na+/K+ ATPase pumps, which also contributes to the ATP deficit. Lastly, inflammation following TBI is attributed to the release of pro-inflammatory cytokines, such as interleukin-1-beta and interleukin-6, which mobilize immune and glial cells (Woodcock & Morganti-Kossmann, 2013). This up-regulation takes places within hours of insult.

There are three primary ways of measuring TBI severity. The first is the Glasgow Coma Scale (GCS). However, the GCS has been shown to suffer from low accuracy when tested for inter-rater reliability amongst healthcare professionals of different levels of experience (Rowley & Fielding, 1991). The second is measuring the length of post-traumatic amnesia, which has been shown to be related to loss of memory and verbal fluency (Hart et al., 2017). Thirdly, clinicians use the length of loss of consciousness, as evidenced by the presence of intercranial abnormalities (Blyth & Bazarian, 2010). In the

case of the Functional Independence Measure (FIM) which provides an overall assessment of physical, social, and psychological function, it has been shown to suffer from a "ceiling effect", even amongst inpatients in rehabilitation (Hall et al., 1996). Although it has been validated that the Montreal Cognitive Assessment (MoCA) is a superior metric for measuring cognitive reserve compared to the Mini Mental State Examination (Kang et al., 2018), this is purely a behavioral assessment and does not reveal pathological consequences. Thus, there are several shortcomings to subjective assessments (the GCS, FIM, and MoCA), as they do not provide reveal biological processes that lead to the observed signs and symptoms presented by the patient. NMR metabolomics explored within this thesis attempts to present objective biomarkers with the potential to serve as proxy tools for these traditional measures.

SCI results when all or some of the 31 nerve fibers that form the spinal cord are torn or compressed, leading to homeostatic disturbances that afflict the entire body. A complete SCI means there is full loss of motor and sensory functions, and the potential for functional recovery is very unlikely. The brain and the spinal cord are comprised of nerve fibers incapable of regeneration following a complete injury due to the presence of inhibitory growth factors controlling central nervous system myelination (Nicholls et al., 1999). However, restoration of some sensory and motor function below the level of injury is possible after an incomplete injury (Marino et al., 2016). Thus, for an incomplete SCI, there is greater potential for recovery and restoration of function. The level of the lesion is also a determinant of functional recovery; the higher the SCI, the more severe it is, and the worse the prognosis. Cervical lesions of the C1-C7 segments results in tetraplegia, which refers to paralysis of all four limbs (Kirshblum et al., 2011). Injury to the thoracic, lumbar,

and sacral segments results in paraplegia, a less severe form of SCI which leads to paralysis of the legs and lower body (Nas et al., 2015). Even lower-level injuries, resulting from damage to the lumbar or sacral regions, produces some loss of function in the hips and legs. Pathological changes arise from the lack of mobility below the level of injury, causing alterations to the bone. For instance, there is increase in osteoclast activity, and consequently there is an increased risk for the development of osteoporosis (Ragnarsson, 2015). Although SCI patients often show the greatest reduction in bone below the level of injury, they also experience bone loss throughout the body (Maimoun et al., 2005). In a previous study, it was shown that SCI leads to severe bone loss in a rodent model, since the central nervous system is an important regulator of bone metabolism via its innervating pathways (Morse et al., 2008). Since SCI rapidly induces severe bone loss leading to an abundance of calcium in the bloodstream (del Rivero & Bethea, 2016), damage to the spinal cord also has implications for the overall health of the skeletal system.

Tissue necrosis and mechanical tissue disruption are primary mechanisms of damage following an SCI. Of greater relevance are the insidious secondary damage mechanisms, which include inflammation and oxidative stress (Xiu et al., 2005). In the wake of a SCI, there is an inflammatory response as cytokines cross the blood-brain-barrier (Popovich et al., 2008). This initial swelling can trigger further secondary damage, resulting in neuronal and glial apoptosis and increased blood-CNS barrier permeability, which can persist for months or years after the initial trauma (Donnelly & Popovich, 2007). Changes in metabolism accompany the inflammatory response. This is the main physiological response that occurs in the wake of a SCI, where severe atrophy of denervated musculature leads to marked changes in body composition (Baumann & Spungen, 2000; Gorgey et al.,

2013). Metabolic rates decline due to the loss of metabolically active lean body mass below the level of the lesion and a corresponding increase in adiposity (Giangregorio & McCartney, 2016). SCI leads to a marked reduction in whole body glucose transport, proportional to the reduction in muscle mass amongst spinal cord injured patients (Bauman & Spungen, 2016), which can provoke disorders in carbohydrate and lipid metabolism. Particularly, individuals with tetraplegia/cervical level lesions have decreased glucose homeostasis and altered muscle morphology. This results in down-regulation of the expression of genes needed for lipid oxidation and glycogen storage in skeletal muscle (Long et al., 2011). A NMR-based, metabolomics perspective on disruptions to carbohydrate and lipid metabolism resulting from SCI could help inform appropriate rehabilitation paradigms to promote activity and limit the extent of skeletal atrophy. A biomarker that could inform these metabolic changes would be useful for predicting the trajectory of recovery of patients in the wake of a SCI.

The American Spinal Cord Injury Association (ASIA) Impairment Scale is the gold standard for diagnosing as well as determining the level and type of injury following SCI. This instrument assesses sensory levels and motor levels for right and left sides, then determines the neurological level of injury to determine whether the injury is complete or incomplete (International Standards for Neurological Classification of Spinal Cord Injury, 2019). There is also the Spinal Cord Independence Measure (SCIM), which is traditionally used for assessing patients' functional ability. Although it has proven to be a reliable measure when observing patient performance, it has been shown to have variability when used as a tool to interview patients by raters from different professions (Itzkovich et al., 2018). Thus, the inherent inaccuracies when using a subjective tool is a strong argument

for finding a reliable, objective measure- namely a fluid-derived biomarker- that can provide information on patients' trajectory for recovery. Furthermore, robotic-based rehabilitation is an important tool for locomotor functional training, with positive implications for cardiorespiratory, urinary, musculoskeletal, neuronal, and somatosensory systems (Holanda et al., 2017). However, what the spinal cord rehabilitation field lacks is the ability to triage patients to the appropriate rehabilitation paradigm, based on knowing injury severity and a patient's prognosis. Since very little is known about which rehabilitation types and dosages produce the best outcomes for SCI patients (Teeter et al., 2012), an informative biomarker could assist planning therapies for patients to produce the best recovery outcomes.

Metabolomics studies involving SCI represents a relatively unexplored frontier. There have only been a few studies to date that have employed magnetic resonance or chromatography-mass spectrometry techniques to characterize metabolic disturbances following SCI. Previous studies that characterized metabolomic profiles of human SCI patients collected serum and cerebrospinal fluid samples which were analyzed using chemical isotope-labeling liquid chromatography-mass spectrometry (Wu et al., 2016), dietary interventions in an SCI rat model and measured using gas chromatography-mass spectrometry (Figueroa et al., 2013), use of ^{31}P magnetic resonance spectroscopy to study experimental SCI (Vink et al., 1987), and using ^{1}H-NMR to investigate changes in an SCI rat model (Peng et al., 2014). Thus there is a paucity of studies examining SCI in humans using ^{1}H NMR spectroscopy and urine as a bio-fluid. Thus, the present thesis fills this gap in the literature.

A gap also exists for ^{1}H NMR studies of patients with TBI. Although there have been studies examining metabolic changes in cerebrospinal fluid using ^{1}H NMR (Glenn et al., 2013; Toczylowska et al., 2006), using ^{1}H magnetic resonance spectroscopy (1H-MRS), (Garnett et al., 2000; Harris et al., 2012), and using 1H NMR to examine metabolites harvested from the blood (Cohen et al., 2010) and cortical tissue (Rubin et al., 1997), there is a scarcity of studies using ^{1}H NMR to examine metabolic changes in the blood, let alone in the urine of patients with TBI. The present thesis also attempts to close this gap.

Metabolomics is still in its infancy, with a plethora of studies recently emerging focussing on a variety of neurological conditions ranging from Alzheimer's disease (Wilkins & Trushina, 2018), multiple sclerosis (Bhargava & Calabresi, 2016), amyotrophic lateral sclerosis, (Kumar et al., 2013), and Parkinson's disease (Lei & Powers, 2013). Despite this rapid growth of metabolomics knowledge, the rehabilitation field is lacking a single "gold standard" diagnostic marker with the ability to objectively determine the severity of SCI or TBI. Imaging technologies such as computerized tomography and magnetic resonance imaging provide quick acute diagnosis at the cost of being expensive (Goeree, 2005; Krueger et al., 2013; Tator et al., 2016). The field is lacking an efficient tool for prognosticating outcomes, which can aid in determining patients' potential for recovery. Developing efficient tools is especially important for the treatment of neurological patients, since the central nervous system is incapable of regenerating itself due to the presence of inhibitory growth factors (Nicholls et al., 1999), which are not present in the peripheral nervous system. The insidious, delayed secondary injury response that occurs in the days to week following an TBI or SCI exacerbates inflammatory and oxidative stress damage beyond the initial injury (Donnelly & Popovich, 2008; Bedreag et

al., 2014). The demand for a high-throughput method that can rapidly diagnose patients' conditions to optimize the potential for TBI and SCI patients' recovery is explored in the following four pilot studies.

REFERENCES

Adams, J., Doyle, D., Ford, I., Gennarelli, A., Graham, D., & Mclellan, D. (1989). Diffuse axonal injury in head injury: Definition, diagnosis and grading. *Histopathology*, *15*(1): 49-59.

Asken, B.M., Houck, Z.M., Bauer, R.M., & Clugston, J.R. (2019). SCAT5 vs. SCAT3 symptoms reporting differences and convergent validity in collegiate athletes. *Archives of Clinical Neuropsychology*, acz007, https://doi.org/10.1093/arclin/acz2007

Barua, B. (2017). Waiting Your Turn: Wait Times for Health Care in Canada, 2017 Report. *Fraser Institute.* Retrieved September 30, 2018 from https://www.fraserinstitute.org/studies/waiting-your-turn-wait-times-for-health-care-in-canada-2017

Baumann, W., & Spungen, A. (2000). Metabolic changes in persons after spinal cord injury. *Physical Medicine and Rehabilitation Clinics of North America, 11*(1): 109-140.

Baumann, W., & Spungen, A. (2016). Invited Review Carbohydrate and Lipid Metabolism In Chronic Spinal Cord Injury. *The Journal of Spinal Cord Medicine, 24*(4): 266-277.

Bedreag, O., Rogobete, A., Sarandan, M, Cradigati, A., Papurica, M., Rosu, O.,… Sandesc, D. (2014). Oxidative stress and antioxidant therapy in traumatic spinal cord injuries. *Romanian Journal of Anaesthesia and Intensive Care, 21*(2): 123-129.

Bhargava, P., & Calabresi, P.A. (2016). Metabolomics in multiple sclerosis. *Multiple Sclerosis, 22*(4): 451-60. Doi: 10.1177/1352458515622827.

Blyth, B.J., & Bazarian, J.J. (2010). Traumatic alterations in consciousness: traumatic brain injury. *Emergency Medicine Clinics of North America, 28*(3): 571-594. Doi: 10.1016/j.emc.2010.03.003.

Bouatra, S., Aziat, F., Mandal, R., Guo, A., Wilson, M., Knox, C., Wishart, D. (2013). The Human Urine Metabolome. *PLOS ONE, 8*(9), 1-28.

Chang, E., Meeker, M., & Holland, M. (2006). Acute Traumatic Intraparenchymal Hemorrhage: Risk Factors for Progression in the Early Post-injury Period. *Neurosurgery*, *58*(4): 647-656.

Chan, M., Vielleuse, J.V., Vokaty, S., Wener, M.A., Pearson, I., & Gagnon, I. (2012). Test-retest reliability of the sport concussion assessment tool 2 (SCAT2) for uninjured children and young adults. *British Journal of Sports Medicine, 47*(5). Doi:10.1136/bjsports-2012-092101.18

Cohen, M.J., Serkova, N.J., Wiener-Kronish, J., Pittet, J.F., & Niemann, C.U. (2012). 1H-NMR-based metabolic signatures of clinical outcomes in trauma patients—beyond

lactate and base deficit. *The Journal of Trauma, 69*(1): 31-40. Doi: 10.1097/TA.0b013e3181e043fe.

del Rivero, T., & Bethea, J.R. (2016). The effects of spinal cord injury on bone loss and dysregulation of the calcium/parathyroid hormone loop in mice. *Osteoporosis Sarcopenia, 2*(3): 164-169. Doi: 10.1016/j.afos.2016.06.003.

Donnelly, D., & Popovich, P. (2007). Inflammation and its role in neuroprotection, axonal regeneration and functional recovery after spinal cord injury. *Experimental Neurology, 209*(2): 378-388.

Donnelly, D., & Popovich, P. (2008). Inflammation and its role in neuroprotection, axonal regeneration and functional recovery after spinal cord injury. *Experimental Neurology, 209*(3): 378-388.

Figueroa, J.D., Cordero, K., Serrano-Illan, M., Almeyda, A., Baldeosingh, K., Almaguel, F.G., & De Leon, M. (2013). Metabolomics uncovers dietary omega-3 fatty acid-derived metabolites implicated in anti-nociceptive responses after experimental spinal cord injury. *Neuroscience, 255*(26): 1-18. https://doi.org/10.1016/j.neuroscience.2013.09.012.

Garnett, M.R., Blamire, A.M., Corkill, R.G., Cadoux-Hudson, T.A.D., Rajagopalan, B., & Styles, P. (2000). Early proton magnetic resonance spectroscopy in normal-appearing brain correlates with outcome in patients following traumatic brain injury. *Brain, 123*(10): 2046-2054. https://doi.org/10.1093/brain/123.10.2046.

Giangregorio, L., & McCartney, N. (2016). Bone Loss and Muscle Atrophy in Spinal Cord Injury: Epidemiology, Fracture Prediction, and Rehabilitation Strategies. *The Journal of Spinal Cord Medicine, 29*(5): 489-500.

Glenn, T, Hirt, D., Mendez, G., McArthur, D.L., Sturtevant, R., Wolahan, S.,…Martin, N.A. (2013). Metabolomic analysis of cerebral spinal fluid from patients with severe brain injury. *Acta Neurochirurgica Supplement, 118*, 115-119.

Goeree, R., Blackhouse, G., Petrovic, R., & Salama, S. (2005). Cost of stroke in Canada: a 1-year prospective study. *Journal of Medical Economics, 8*(4): 147-167. DOI: 10.3111/200508147167

Gorgey, A., Dolbow, D., Dolbow, J., Khalil, R., Castillo, C., & Gater, D. (2013). Effects of spinal cord injury on body composition and metabolic profile. *Journal of Spinal Cord Medicine, 37*(6): 693-702.

Hall, K.M., Mann, N., High, W.M., Wright, J., Kreutzer, J.S., & Wood, D. (1996). Functional measures after traumatic brain injury: ceiling effects of FIM, FIM+FAM, DRS, and CIQ. *The Journal of Head Trauma Rehabilitation, 11*(5): 27-39. https://doi.org/10.1097/00001199-199610000-00004.

Harris, J.L., Yeh, H.W., Choi, I.Y., Lee, P., Berman, N.E., Swerdlow, R.H.,…Brooks, W.M. (2012). Altered neurochemical profile after traumatic brain injury: (1)H-

MRS biomarkers of pathological mechanisms. *Journal of Cerebral Blood Flow and Metabolism, 32*(12): 2122-34. Doi: 10.1038/jcbfm.2012.114.

Hart, T., Novack, T.A., Temkin, N., Barber, J., Dikmen, S.S., Diaz-Arrastia, R.,…Zafonte, R. (2017). Duration of post-traumatic amnesia predicts neuropsychological and global outcome in complicated mild traumatic brain injury. *Journal of Head Trauma Rehabilitation, 31*(6): E1-E9. Doi: 10.1097/HTR.0000000000000210.

Holanda, L., Silva, P., Amorim, T., Lacerda, M., Simao, C., & Morya, E. (2017). Robotic assisted gait as a tool for rehabilitation of individuals with spinal cord injury: a systematic review. *Journal of NeuroEngineering and Rehabilitation, 14*: 126.

International Standards for Neurological Classification of Spinal Cord Injury. (2019). Retrieved from https://asia-spinalinjury.org/isncsci-2019-revision-released/ , April 17, 2020.

Itzkovich, M., Shefler, H., Front, L., Gur-Pollack, R., Elkayam, K., Bluvshtein, V.,…Catz, A. (2017). SCIM III (Spinal Cord Independence Measure version III): reliability of assessment by interview and comparison with assessment by observation. *Spinal Cord, 56*: 46-51.

Jung, J.Y., Lee, H.S., Kang, D.G., Kim, N.S., Cha, M.H., Bang, O.S.,…Hwang, G.S. (2011). ^{1}H-NMR-based metabolomics study of cerebral infarction. *Stroke. 42*(5), 1282-1288.

Kang, J.M., Cho, Y.S., Park, S., Lee, B.H., Sohn, B.K., Choi, C.H.,…Lee, J.Y. (2018). Montreal cognitive assessment reflects cognitive reserve. *BMC Geriatrics, 18*:261. Doi: 10.1186/s12877-018-0951-8.

Kirshblum, S., Burns, S., Biering-Sorenson, F., Donovan, W., Graves, D., Jha, A.,…Waring, W. (2011). International standards for neurological classification of spinal cord injury. *The Journal of Spinal Cord Medicine, 34*(6): 535-546.

Krueger, H., Noonan, V., Trenaman, L., Joshi, P., & Rivers, C. (2013). The economic burden of traumatic spinal cord injury in Canada. *Chronic Diseases and Injuries in Canada, 33*(3): 113-122.

Kumar, A., Ghosh, D., & Singh, R.L. (2013). Amyotrophic lateral sclerosis and metabolomics: clinical implication and therapeutic approach. *Journal of Biomarkers, 2013*: 538765. Doi: 10.1155/2013/538765.

Lei, S., & Powers, R. (2013). NMR metabolomics analysis of Parkinson's disease. *Current Metabolomics, 1*(3): 191-209. Doi: 10.2174/2213235X113019990004.

Long, Y., Kostovski, E., Boon, H., Hjeltnes, N., Krook, A., & Widegren, U. (2011). Differential expression of metabolic genes essential for glucose and lipid metabolism in skeletal muscle from spinal cord injured subjects. *Journal of Applied Physiology, 110*(5): 1204-1210.

Maimoun, L., Couret, I., Mariano-Goulart, D., Dupuy, A.M., Micallef, J.P., Peruchon, E.,…Leroux, J.L. (2005). Changes in osteoprotegerin/RANKL system, Bone Mineral Density, and Bone Biochemical Markers in Patients with Recent Spinal Cord Injury. *Calcified Tissue International, 76*(6): 404-411. Doi: 10.1007/s00223-004-0048-6.

Marino, R., Barros, T., Biering-Sorensen, F., Burns, S., Donovan, W., Graves, D.,…Priebe, M. (2016). International Standards for Neurological Classification of Spinal Cord Injury. *The Journal of Spinal Cord Medicine, 26*: sup1, S50-S56, doi:10.1080/10790268.2003.11754575.

Meaney, D.F. & Smith, D.H. (2011). Biomechanics of concussion. *Clinics in Sports Medicine, 30*(1): 19-vii. Doi: 10.1016/j.csm.2010.08.009

Mesfin, F.B., Gupta, N., Shapshak, A.H., & Taylor, R.S. (2020). Diffuse axonal injury (DAI). In: *StatPearls* [Internet]. Treasure Island (FL): StatPearls Publishing. https://www.ncbi.nlm.nih.gov/books/NBK448102/

Morse, L., Teng, Y.D., Pham, L., Newton, K., Yu, D., Liao, W.L.,…Battaglino, R. (2007). Spinal cord injury causes rapid osteoclastic resorption and growth plate abnormalities in growing rats (SCI- induced bone loss in growing rats). *Osteoporosis International, 19*: 645-652. https://doi.org/10.1007/s00198-007-0494-x.

Nas, K., Yazmalar, L., Sah, V., Ayudin, A., & Ones, K. (2015). Rehabilitation of spinal cord injuries. *World Journal of Orthopedics, 18*(6): 8-16.

Nicholls, J., Adams, W., Geiser, R., Lepre, M., Lugue, J., & Wintzer, M. (1999). Why does the central nervous system not regenerate after injury*? Survey of Ophthamology,* 43. Suppl 1: S136-141.

Nicholson, J.K., Lindon, J.C., & Holmes, E. (1999) 'Metabonomics': understanding the metabolic responses of living systems to pathophysiological stimuli via multivariate statistical analysis of biological NMR spectroscopic data. *Xenobiotica, 29,* 1181–1189.

Peng, J., Zeng, J., Cai, B., Yang, H, Cohen, M., Chen, W.,…Jiang, H. (2014). Establishment of Quantitative Severity Evaluation Model for Spinal Cord Injury by Metabolomic Fingerprinting. *PLOS ONE, 9*(4): e93736.

Popovich, P., Guan, Z., McGaughy, V., Fisher, L., Hickey, W., & Basso, D. (2002). The neuropathological and behavioral consequences of intraspinal microglial/macrophage activation. *Journal of Neuropathology and Experimental Neurology, 61*(7): 623-633.

Psychogios, N., Hau, D, Peng, J., Guo, A., Mandal, R., Bouatra, S., & Wishart, D. (2011). The Human Serum Metabolome. *PLOS ONE, 6*(2), 1-23.

Ragnarsson, K.T. (2015). Bone loss and fractures in limbs paralyzed by spinal cord injury: Prevention, diagnosis, and treatment. *The Journal of Spinal Cord Medicine, 38*(1): 10-12.

Readnower, R., Chavko, M., Adeeb, S., Conroy, M., Pauly, R., McCarron, R., & Sullivan, P. (2010). Increased in blood-brain barrier permeability, oxidative stress, and activated microglia in a rat model of blast-induced traumatic brain injury. *Journal of Neuroscience Research*, *88*(16), 3530-3539.

Rowley, G., & Fielding, K. (1991). Reliability and accuracy of the Glasgow Coma Scale with experienced and inexperienced users. *The Lancet*, *337*: 535-538.

Rubin, Y., Cecil, K., Wehrli, S., McIntosh, T.K., Lenkinski, R.E., & Smith, D.H. (1997). High-resolution 1H NMR spectroscopy following experimental brain trauma. *Journal of Neurotrauma, 14*(7): 441-9. Doi: 10.1089/neu.1997.14.441.

Shim, Y.S., Park, C.O., Hyun, D.K., Park, H.C., & Yoon, S.H. (2007). What are the causative factors for a slow, progressive enlargement of a chronic subdural hematoma? *Yonsei Medical Journal, 48*(2): 210-217. https://doi.org/10.3349/ymj.2007.48.2.210

Siesjo, B.K, & Siesjo, P. (1996). Mechanisms of secondary brain injury. *European Journal of Anaesthesiology, 13*(3): 247-268. Doi: https://doi.org/10.1046/j.1365-2346.1996.00976.x

Sobey, C.G., & Faraci, F.M. (2007). Subarachnoid hemorrhage: what happens to the cerebral arteries? *Clinical and Experimental Pharmacology and Physiology, 25*(11): 867-876. https://doi.org/10.1111/j.1440-1681.1998.tb02337.x

Sternbach, G. (2000). The Glasgow Coma Scale. *Journal of Emergency Medicine*. *19*(1):67-71. Doi: 10.1016/s0736-4679(00)00182-7.

Tator, C., Logan, L., & Stringer, K. (2016). Action needed to address the rising cost of concussions in Canada. Published in *The Ottawa Sun.* Retrieved September 30, 2018.

Teeter, L., Gassaway, J., Taylor, S., LaBarbera, J., McDowell, S., Backus, D.,…Whiteneck, G. (2012). Relationship of physical therapy inpatient rehabilitation interventions and patient characteristics to outcomes following spinal cord injury: The SCI Rehab Project. *The Journal of Spinal Cord Medicine, 35*(6): 503-526.

Toczylowska, B., Chalimoniuk, M., Wodowska, M., & Mayzner-Zawadzk, E. (2006). Changes in concentration of cerebrospinal fluid components in patients with traumatic brain injury. *Brain Research, 1104*(1): 183-9. Doi: 10.1016/j.brainres.2006.05.057.

Valovich McLeod, T.C., & Leach, C. (2012). Psychometric properties of self-report concussion scales and checklists. *Journal of Athletic Training, 47*(2): 221-223.

Vink, R., Knoblach, S.M., & Faden, A.I. (1987). 31P magnetic resonance spectroscopy of traumatic spinal cord injury. *Magnetic Resonance in Medicine, 5*(4): 390-394.

Werner, C., & Engelhard, K. (2007). Pathophysiology of Traumatic Brain Injury. *British Journal of Anasthesia, 99*(1), 4-9.

Wilkins, J.M., & Trushina, E. (2018). Application of metabolomics in Alzheimer's disease. *Frontiers in Neurology, 12*(8): 719. Doi: 10.3389/fneur.2017.00719.

Woodcock, T., & Morganti-Kossmann, M.C. (2013). The role of markers of inflammation in traumatic brain injury. *Frontiers in Neurology, 4*(18): doi: 10.3389/fneur.2013.00018.2

Wu, Y., Streijger, F., Wang, Y., Lin, G., Christie, S., Mac-Thiong, J.M.,…Li, L. (2016). Parallel metabolomic profiling of cerebrospinal fluid and serum for identifying biomarkers of injury severity after acute human spinal cord injury. *Scientific Reports, 6*: 38718, doi: 10.1038/srep38718

Xia, J., & Wishart, D. (2010). MSEA : a web-based tool to identify biologically meaningful patterns in quantitative metabolomic data. *Nucleic Acids Research, 38,* doi : 10.1093/nar/gkq329

Xiu, W., Chi, L., Xu, R., Ke, Y., Luo, C., Cai, J.,…Liu, R. (2005). Increased production of reactive oxygen species contributed to motor neuron death in a compression mouse model of spinal cord injury. *Spinal Cor*d, 43: 204-213.

CHAPTER 2: Urinary Metabolomic Signatures are Correlated to Severity in Males and Females with Traumatic Brain Injury

INTRODUCTION

Traumatic brain injury (TBI), which occurs as a result of a blow or jolt to the head, is a leading cause of death and disability worldwide (Popescu et al., 2015). The incidence of TBI is increasing in Canada; a recent cross-sectional analysis revealed that the proportion of Canadians who reported having a TBI in 2014 was 3.2% compared to 1.4% in 2005 (Rao et al., 2017). Although studies have shown that TBI afflicts disproportionately more men than women (Colantonio et al., 2010; Mollayeva et al., 2018), their vulnerabilities vary. For instance, the increased incidence amongst males may be due to greater participation in violent behavior and occupational hazards, whereas fall-related TBIs affect more females (Colantonio et al., 2010). Despite these differences, recent data show that there is no association between sex and outcome after severe TBI (Herrera-Melero et al., 2015); thus, it remains unclear whether sex is a determinant of TBI outcome. Despite advances in TBI biomarker research, no study has been able to find a fluid biomarker or biomarker signature that accurately correlates to severity, injury or functional recovery. Thus, new robust biomarkers would provide a valuable window into the better understanding the pathophysiological processes underlying TBI and how it relates to clinical outcomes.

Metabolomics is a powerful approach to provide quantitative assessment of endogenous small molecules within biological fluids (Beckonert et al., 2007). Nuclear magnetic resonance (NMR) spectroscopy is an amenable technique to studying metabolomics, as it permits identification of novel compounds and it needs no chemical derivatization (Emwas et al., 2015). NMR is capable of detecting 209 metabolites in human

urine, with 108 of these being unique to NMR (Bouatra et al., 2013). To date, metabolomics fingerprinting has been shown to be a useful biomarker tool for a variety of neurological conditions including stroke (Naccarato et al., 2010), SCI (Peng et al., 2014), and severe TBI (Paxman et al., 2018). Though recent studies hold promise, there is no fluid biomarker(s) that accurately reflects TBI recovery and inflammation.

The present study used a metabolomics approach in the identification of novel biomarkers through quantitative assessment of small molecules indicative of TBI and subsequent recovery (Nicholson et al., 2008). Although there have been predecessor studies in the literature that explored sex differences attributable to hormones (Bazarian et al., 2010; Espinoza et al., 2011) and gender differences (Colantonio et al., 2010; Slewa-Younan et al., 2004), there has yet to be identified a reliable biomarker with the potential to discriminate recovery outcomes as a function of sex and gender. Furthermore, awareness of the male bias when it comes to TBI research (Gupte et al., 2019) has prompted the present longitudinal pilot study, which involves analysis of urine samples from male and female patients with mild to severe TBI to elucidate whether there is an informative biomarker specific to sex. In addition, we pooled metabolomic data from both sexes to determine if there are common mechanisms of injury across both sexes. In line with a precision medicine approach, this study (1) determined sex-dependent differences in the initial and post-recovery metabolomics profile; (2) based on the list of significant metabolites, revealed the underlying biochemical pathways contributing to TBI outcome; (3) determined the predictive accuracy of the identified metabolites as biomarkers of TBI, and (4) how these changes correlate to clinical outcomes in male and female patients.

MATERIALS AND METHODS

Patient Characteristics and Sample Collection

This study was embedded in a larger study called Understanding Neurological Recovery: the role of resting state fMRI, biomarkers, and robotics after TBI, stroke, and SCI (UCAN) study funded by the Hotchkiss Brain Institute at the University of Calgary. The UCAN Study followed patients with TBI, stroke, and SCI throughout their recovery from one week to 6 months post injury. Patients with TBI were recruited through the Foothills Medical Centre, Calgary (n=8 males, average age 45 +/- 18.4 years; n=4 females, average age 36 +/- 18.9 years); (Table 1). Pairs of fasting morning urine samples (acquired between 6am and 9am) were collected at two different time points: within 7 days after TBI and again at 6 months post-injury. Pairing the samples for this within-subject control study allows exclusion of confounding factors, such as diet and lifestyle factors, increasing the validity of the analysis to attribute changes in the metabolic profiles throughout recovery. Urine samples were stored at -80°C until further processing. This study was reviewed and approved by the University of Calgary Conjoint Health Research Ethics Board (CHREB) and the University of Lethbridge Human Participant Research Committee in accordance to the standards set forth by the Tri-Council Policy Statement: Ethical Conduct for Research Involving Humans.

Clinical Assessments

The Glasgow Coma Scale (GCS) was used to rate the initial severity of TBI for each patient. It measures three different functions: eye opening, verbal response, and motor responses, where higher scores indicate better function (Sternbach et al., 2000). The final GCS score was the sum of these numbers, with the following ranges: severe (GCS less than

8), moderate (GCS 8-12), and mild (GCS 13-15). The Montreal Cognitive Assessment (MoCA) was used to screen for short term memory, visuospatial abilities, executive functions, and language (Nasreddine et al., 2005). A score of 26 and higher was considered to be normal, whereas a score below 26 indicated impairment. In addition, the Functional Independence Measure (FIM) served as a global assessment of physical, social, and psychological function (Kidd et al., 1995). It included six areas of evaluation including self-care, continence, mobility, transfers, communication, and cognition. Each item was graded on a scale from 1-7, where 1 indicates total dependence and 7 indicates complete independence.

NMR Sample Preparation, Data Acquisition, and Processing

Urine samples were prepared for nuclear magnetic resonance (NMR) spectroscopy as described previously (Paxman et al., 2018). A 700 MHz Bruker Avance III HD NMR spectrometer and a room-temperature TBO probe was used to acquire the NMR data. Three-dimensional and one-dimensional shimming experiments were conducted prior to NMR data acquisition on the urine samples to correct for any inhomogeneities in the static magnetic field. The data were acquired using a one-dimensional 1H Nuclear Overhauser Effect Spectroscopy experiment with water suppression, 128k points, and 128 scans. The data was processed using zero filling to 256k points, line broadening to 0.3 Hz, and automatic phase and baseline correction. The spectra obtained from the NMR experiment were then imported into MATLAB where they underwent dynamic adaptive binning (Anderson et al., 2011), followed by manual inspection and correction of the bins, and recursive segment-wise peak alignment (Veselkov et al., 2009). In total, 354 bins were created for this analysis.

Metabolites were identified using a combination of resources: Chenomx 8.2 NMR Suite (Chenomx Inc., Edmonton, Alberta, Canada), the Human Metabolome Database (HMDB) (Wishart et al., 2018), and Table 3 from The Human Urine Metabolome paper (Bouatra et al., 2013). Once the significant metabolites were identified, they were used to carry out metabolic pathway topology and visualization tests in MetaboanalystR (Chong et al., 2019). Pathway topology analysis was conducted using the list of significant metabolites, the Kyoto Encyclopedia of Genes and Genomes (KEGG), and the HMDB (Xia et al., 2010), to provide metabolite pathways that have been potentially altered.

Statistical Analysis

Multivariate statistical analysis was used to determine if urinary metabolite profiles could be used to distinguish between the initial and post-recovery samples. Prior to modelling, the data were pareto-scaled and mean-centered (Wiklund et al., 2008). Bins containing significant metabolites were sorted according to the F-ranked Variable Importance Analysis based on random Variable Combination (VIAVC) analysis (Yun et al., 2015). This MATLAB based statistical programming algorithm enables identification of significant metabolites based on the Receiver Operator Characteristic (ROC) test and the subsequent Area-Under-the-Curve (AUC) analysis (Fawcett, 2005). It also employs a binary matrix resampling method, which is a more robust method for randomly sampling the data, and all multivariate supervised models were double ten-fold cross-validated (Szymanska et al., 2012).

An orthogonal projection to latent structures discriminant analysis (OPLS-DA) was also conducted to visualize between-group separation as a function of within-group separation (Wiklund et al., 2008). This was complemented by a Principal Components

Analysis (PCA) which demonstrated the degree of separation between groups without the presence of an algorithm (unsupervised). In addition, either a paired T-tests or paired Wilcoxon-Mann-Whitney U test was used in the case of parametric or non-parametric data, respectively.

Pearson R correlations were performed between concentrations of urinary metabolites and the GCS, MoCA, and FIM measures (Table 2). The significance is assessed based on the Bonferroni corrected p-value, obtained by dividing alpha<0.05 by the number of VIAVC F-ranked bins tested for each analysis. The % difference for scores at the two different time points were computed as follows, based on the clinical data provided in Table 1:

$$\left(\frac{Post\ Recovery\ Score - Initial\ Score}{\left(\frac{Post\ Recovery\ Score + Inital\ Score}{2}\right)}\right) * 100\%$$

RESULTS

Patient Characteristics

The number of patients with severe (n=4), moderate (n=4), and mild GCS (n=4), MoCA (this test was conducted initially (n=4 patients with normal scores, n=8 patients with impairment) and at post-recovery (n=10 patients with normal scores, n=2 patients with impairment), and FIM scores are summarized in Table 1.

Metabolomic Analysis

The spectral binning found to be significant by either the paired T-test/Wilcoxon Mann-Whitney test (134 bins for males, 14 for females, and 94 for both males and females) or the VIAVC best subset (27 bins for males, 2 for females, and 6 for both males and females) were used for the analysis. PCA demonstrated a large degree of unsupervised group separation for the males, but a smaller one for the females, and even smaller for males and females combined (Figures 1A, B, C). The OPLS-DA plot illustrates significant group separation between the initial injury and post-recovery samples for males (R^2Y=0.959, p<0.0005; Q^2=0.785, p<0.0005), females (R^2Y=0.898, p=0.0265; Q^2=0.762, p=0.0265), and males combined with females (R^2Y=0.806, p=0.002; Q^2=0.594, p=0.0005; Figures 1D, E, F). This supervised model indicates a change in the metabolic profiles of patients over the course of the recovery process. Metabolites that contributed the most to the group separation for males, females, and combined are provided in Appendix 1. Metabolites are ranked in order of significance according to the paired T-test/Wilcoxon Mann Whitney analysis.

Receiver Operator Characteristic (ROC) curves were also generated for males and females separately and combined. For males an area-under-the-curve equal to 0.996 was achieved, with a 95% confidence interval of 1-1 (Figure 2A). For females there were not enough variables generated by VIAVC to generate a ROC curve (n=2 bins). When males and females were combined, an area-under-the-curve equal to 0.99 was achieved, with a 95% confidence interval of 0.938-1 (Figure 2B).

Pathway topology analysis conducted separately for males, females, and both sexes combined (Figures 3A, B, C) illustrates the potential pathway impact based on changes to the patients' urinary metabolic profiles, presented in increasing order of impact. Metabolic

pathways significantly affected amongst the male patients were purine metabolism (p<0.01), and phenylalanine, tyrosine, & tryptophan biosynthesis (p<0.05). The pathways significant amongst the female patients were riboflavin metabolism (p<0.05) followed by purine metabolism, which nearly achieved significance (p=0.075). When male and female data were combined, the top three most significant pathways were purine metabolism (p<0.01), histidine metabolism (p<0.01), and phenylalanine, tyrosine, & tryptophan biosynthesis (p<0.01). Pathway analysis was based on bins significant by the VIAVC best subset, the paired T-test, and the Wilcoxon-Mann-Whitney test.

Metabolomic Signatures Correlate with Injury severity

Table 2 provides the Pearson R correlation values when comparing the change in concentration of each metabolite initially following injury and at 6-months to the GCS scores. Homovanillate (R= -0.74, p=0.001), L-methionine (R= -0.78, p<0.001), and thymine (R= -0.85, p<0.001) negatively correlated to injury severity in males. Mevalonic acid (R= -0.96, p<0.001) and methylamine (R= -0.98, p<0.001) negatively correlated to injury severity in females. When males and females were combined, there were no metabolites significant based on the Bonferroni threshold for this comparison.

DISCUSSION

The present study evaluated the feasibility of finding metabolomic signatures in urine that correlate to initial injury severity and recovery from injury. The male and female patient population ranged from mild to severe TBI. Purine metabolism was altered amongst males, females, and when combined, suggesting a sex-independent injury mechanism.

Furthermore, we show that metabolomics signatures have potential value for reflecting initial injury severity and clinical assessments. These findings suggest that a metabolomics approach combined with machine learning analysis of urine samples is feasible, and specific metabolite profiles can be correlated to injury severity.

Metabolite Signatures

Metabolites that are Altered Following TBI

Adenosine. It was the most significant purine derivative within the male samples. A previous study has suggested that adenosine, derived from the breakdown of ATP, mitigates ischemia and that following traumatic insult, there is a concomitant increase in brain interstitial adenosine levels (Kochanek et al., 2013). Several studies support the presence of adenosine in cerebrospinal fluid as an endogenous neuroprotective agent. For instance, adenosine may reduce excitotoxicity and inhibit microvascular thrombosis (Clark et al., 1997). Adenosine has also been experimentally proven to inhibit the generation of toxic oxygen metabolites and play a role in regulating neutrophil activity during the immune response (Cronstein, 1994). To date, there is a paucity of evidence in the literature supporting the presence of adenosine in the urine as an additional marker of this phenomenon. Findings from this study may fill this gap.

Inosine: As a major degradation product of adenosine, the metabolite inosine has also been shown to have neuroprotective and immunomodulatory effects. As the only purine derivative present within the female samples, it's up-regulation may support its postulated roles in suppressing macrophage, neutrophil, and lymphocyte activity and attenuating levels of pro-inflammatory mediators (Hasko et al., 2004).

Deoxyinosine: It was the most significant metabolite within the male combined with female samples. Deoxyinosine (part of DNA) is the equivalent of inosine (found in RNA), both resulting from the deamination of adenine to hypoxanthine (Novotny et al., 2000). Thus, deoxyinosine may have a similar neuroprotective role to inosine, although this hasn't been discretely explored in the literature. Thus, metabolomics signatures confirm previous evidence implicating adenosine and associated purine derivatives in pathological processes following TBI.

Metabolite Based Classification of Recovery

A high predictive accuracy and near-perfect classification of the metabolomic profiles initially compared to post-recovery is shown by the ROC model (Figures 2A and B). This demonstrates that the TBI profiles of the patients are separated with a high degree of sensitivity, and that the model is nearly a perfect predictor of the group separation shown within the OPLS-DA analysis (figures D, E, F). Thus, there are profound differences in the types of metabolites found in urine over the course of the patients' recovery.

Metabolic Pathway Regulation in Participants with TBI

The metabolomics analyses revealed purine metabolism as the common pathway significantly changed across males, females, and both combined. Ample previous evidence supports the neuroprotective role of purines in the nervous system (Stone, 2002; Jackson et al., 2016). Derivatives of purines including xanthine, xanthosine, ADP, deoxyinosine, inosine, and adenosine have the ability to restore tissue perfusion and down-regulate inflammation (Morelli et al., 2011). Xanthine, xanthosine, ADP, deoxyinosine, and adenosine were present within the male samples, and were up-regulated. Inosine was the

only purine derivative present within the female samples, and was also up-regulated. All of the aforementioned purine derivatives were found up-regulated in the male combined with female samples suggesting that they are fulfilling a neuroprotective role (Appendix 1).

Metabolic Signatures as Indicators of Initial Injury Severity

Metabolic Signatures in Males Correlated to GCS

Homovanillate. Homovanillate presented with a significant negative correlation to male patients' initial injury severity as assessed by the GCS. Homovanillate is the major metabolite of dopamine, and therefore, its levels are also reflective of the brain's dopamine levels (Felice et al., 1976). TBI is usually associated with reduced brain dopamine levels; according to one study on in every five patients with moderate to severe TBI presents with reduced binding for dopamine transporters in the striatum (Jenkins et al., 2018). The present data corroborate this claim by showing that the change in homovanillate levels is negatively correlated to initial functional outcomes, thus homovanillate levels are higher initially than at post-recovery. This observation may indicate that dopamine abnormalities become more evident in later stages of TBI pathology, as the reduction in homovanillate in the urine indicates a concurrent reduction in dopamine levels. Thus, homovanillate has potential to serve as a biomarker of reduced dopamine and associated emotional changes, such as apathy and depression, experienced by patients with TBI (Starkstein et al., 2014; da Costa et al., 2013). Furthermore, the time-course of change in homovanillate levels may also reflect the finding that male patients generally report less successful recovery outcomes than females (Niemeier et al., 2014).

L-methionine. L-methionine also presented with a significant negative correlation to male patients' GCS scores. This essential amino acid is implicated in angiogenesis and vascular remodeling, which are processes stimulated by TBI (Zhang et al., 2013). In addition, it has been proposed that a decrease in blood methionine levels amongst patients with mild to severe TBI is related to injury severity (Dash et al., 2016). Accordingly, the opposite trend would be expected in urine, where increased levels of methionine would indicate greater severity. At 6 months recovery, the concentration of L-methionine was lower than the initial levels, suggesting attenuation of TBI pathology, and potentially indicating recovery.

Thymine. Lastly, thymine also revealed a significant negative correlation to GCS scores. It has been determined that raised urinary thymine levels are indicative of dihydrothymine dehydrogenase deficiency, which catabolizes thymine to beta-aminoisobutyric acid (Bakkeren et al., 1984). This by-product has been shown to down-regulate the production of proinflammatory cytokines in adipose tissue observed in obesity (Tanianskii et al., 2019). Since the concentration of thymine in initial samples were on average greater than at 6 months recovery, this may indicate that this pathway involving thymine is providing this neuroprotective role to attenuate inflammation in the later stages of brain injury.

Metabolic Signatures in Females Correlated to GCS

Mevalonic Acid: Mevalonic Acid presented with a significant negative correlation to female patients' initial injury severity as assessed by the GCS. Mevalonic acid is a precursor along the mevalonate pathway which produces terpenes and steroids. In a previous study, it was shown that total cholesterol synthesis is significantly correlated to

excretion of mevalonic acid and is detectable in urinary output (Lindenthal et al., 1996). Cholesterol is the central precursor to production of steroid hormones, including progesterone which in the past has been shown to have neuroprotective effects amongst females with TBI, reducing immune inflammation, stimulating axon remyelination and enhancing dendritic sprouting (Stein, 2001). A more recent phase 3 progesterone trial study refutes this earlier finding (Stein, 2015) and thus the neuroprotective role of progesterone is controversial. Therefore, significant levels of urinary mevalonic acid within the present female cohort may therefore be evidence of progesterone's action.

Methylamine: Methylamine also presented with a significant negative correlation to GCS scores. This endogenous aliphatic amine is cytotoxic at elevated concentrations and is implicated in oxidative stress (Mitchell and Zhang, 2001). Oxidative deamination of methylamine generates formaldehyde which severely affects neurons' metabolism by accelerating glycolytic flux (Tulpule and Dringen, 2013).Thus, significant levels of methylamine may indicate oxidative stress and changes in metabolism that underlie alterations in cognition following TBI, especially during the acute stages.

Sex Differences Associated with Injury Severity

The OPLS-DA comparisons likely indicate mechanisms that are unique to sex, as greater group separation was achieved when the sexes were considered separately than when they were combined (Figures 1D-F). Interestingly, when males and females were considered independently, changes in select metabolites significantly correlated to initial injury severity (GCS scores). However, when male and female data were combined and subjected to the same analysis, there were no significant correlations based on the

Bonferroni threshold. This likely indicates that there are unique mechanisms of TBI based on sex, which become obscured when the sexes are combined.

Conclusion and Limitations

The present study identified endogenous individual urine biomarkers that change over recovery following TBI and correlated the metabolic changes to injury severity. As well, we found sex differences in metabolite profiles, suggesting sex influences metabolites in urine which should be considered in future metabolomic studies. Although the sample size in the present study was small, the present within-subject design ensured that the regulation of metabolite concentrations provides a robust indicator of change in TBI symptom severity. Further validation will be needed to ascertain the prognostic potential of the identified metabolites in the clinical practice. Nevertheless, the present findings indicate the analysis of urinary metabolites is feasible following TBI and specific metabolic profile can be associated with symptom severity.

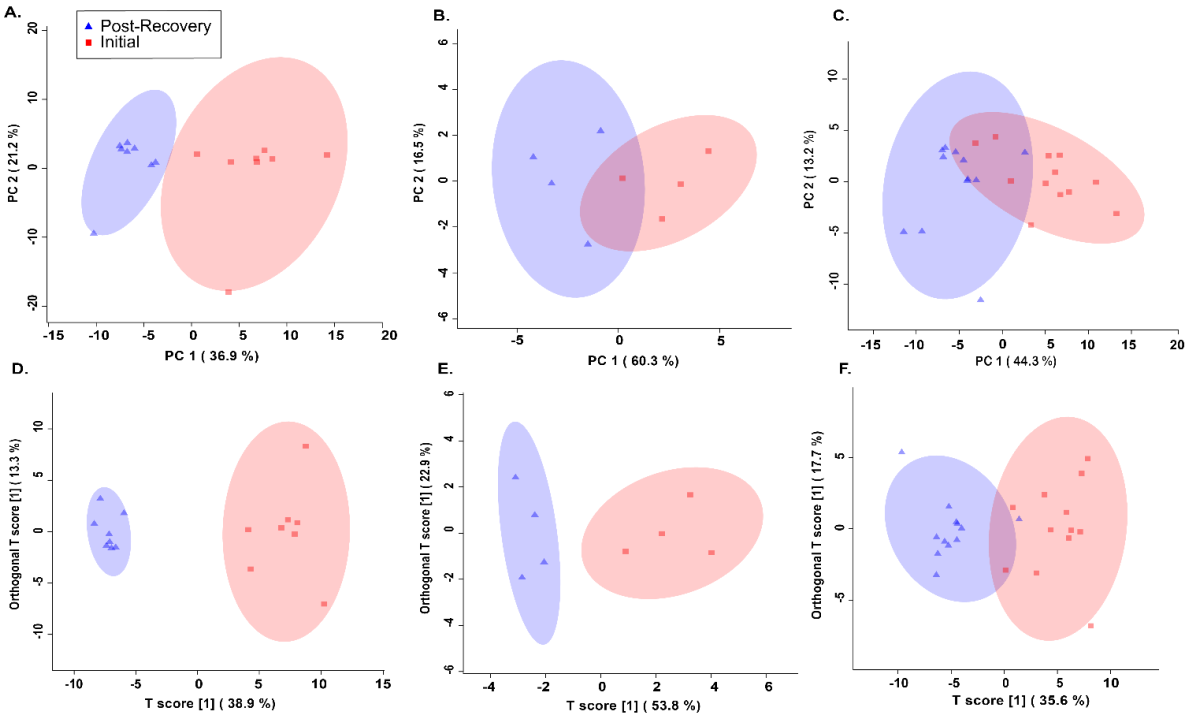

Figure 1. Principal Components Analysis (PCA) (A-C) and Orthogonal Projections to Latent Structures Discriminant Analysis (OPLS-DA) (D-F) scores plots for males (A and D), females (B and E) and both sexes combined (C and F). This analysis was carried out using a list of urinary metabolites found to be statistically significant by either paired t-test/Mann-Whitney or VIAVC testing. The 95% confidence interval is indicated by the shaded ellipses. In the case of the PCA scores plots the x- and y-axis show the data variance explained by principle component 1 and 2, respectively. In the case of the OPLS-DA scores plot the x- and y-axis show the predictive (between group) and orthogonal (within group) variation, respectively. The following are the cross-validation and permutation measures for the OPLS-DA figures: D - R^2Y=0.959 (p<0.0005), Q^2=0.785 (p<0.0005); E - R^2Y=0.898 (p=0.0265), Q^2=0.762 (p=0.0265); F - R^2Y=0.806 (p=0.002), Q^2=0.594 (p=0.0005).

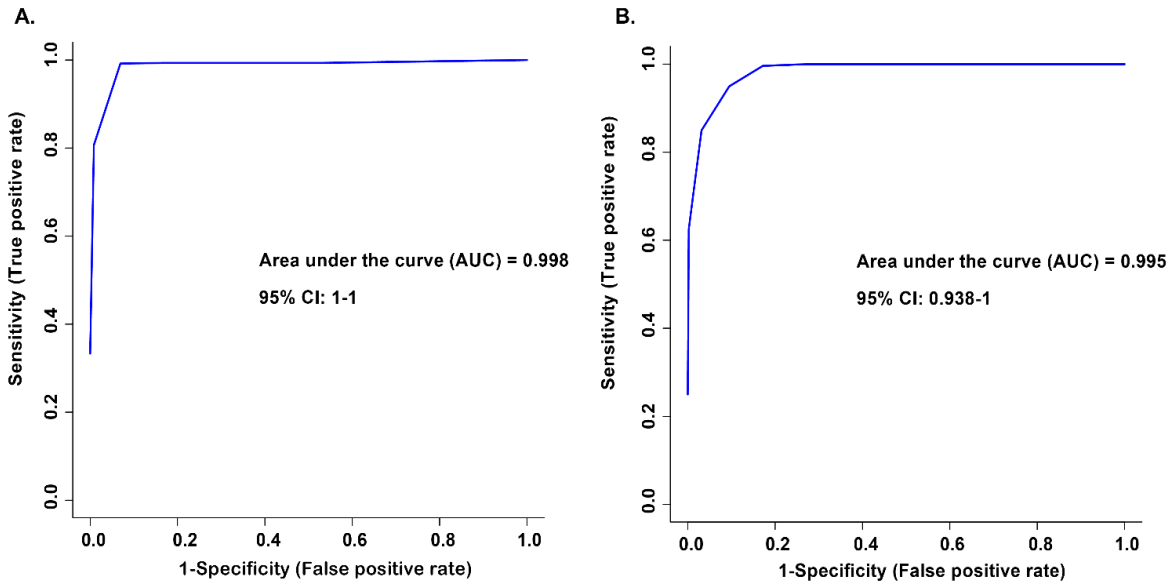

Figure 2. Receiver Operator Characteristic (ROC) curves for (A**)** males and (B) both sexes combined. The corresponding area under the curve (AUC) and confidence interval are indicated on each figure. These ROC curves were constructed using the metabolites determined to be significantly altered based on the VIAVC best subset which corresponds to 27 and 6 bins for figures A and B, respectively. The predictive accuracy of males (A) and the combined sexes (B) is 99.7% and 93.5%, respectively, when all bins from the best subset are considered.

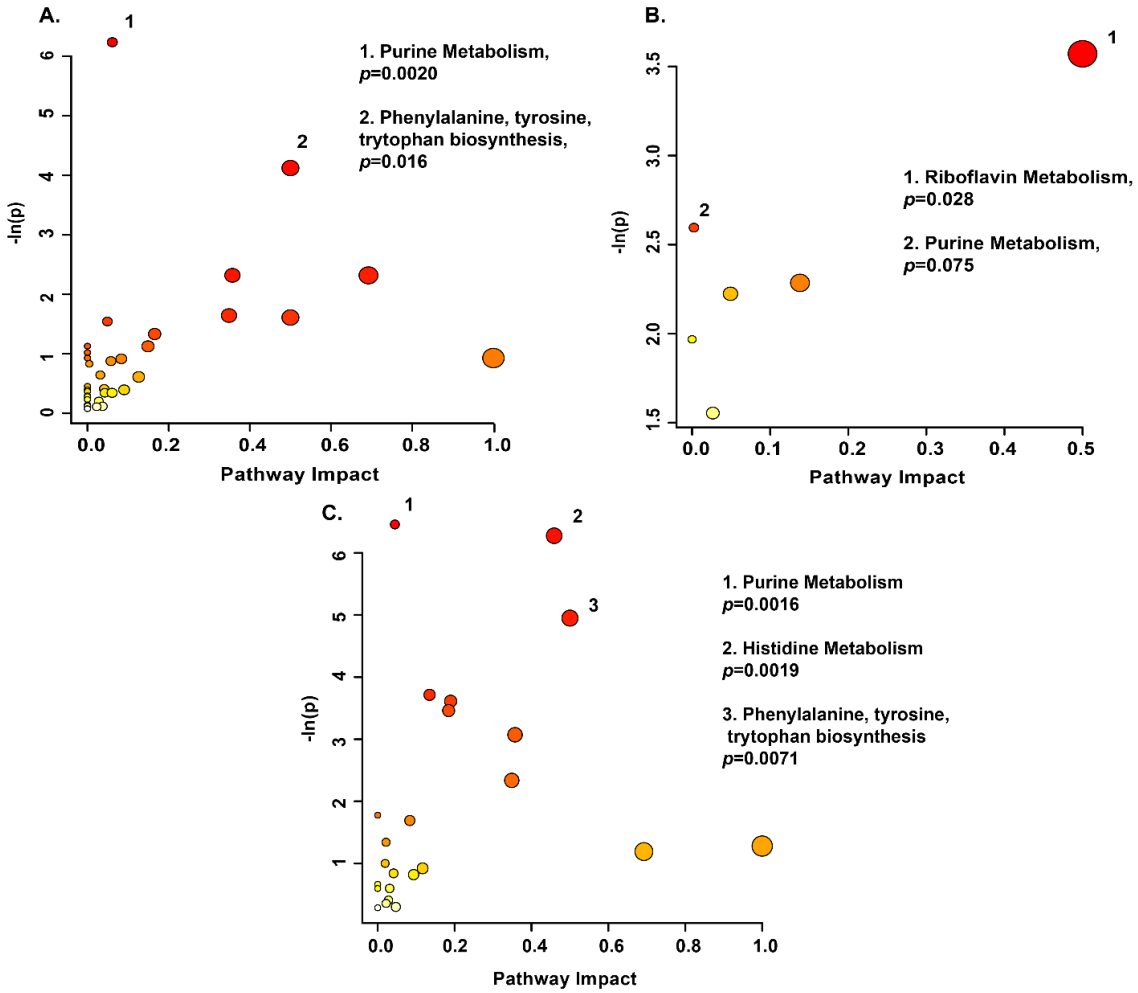

Figure 3. Metabolic Pathway Analysis for (A) males, (B) females, and (C) both sexes combined. A higher value on the y-axis indicates a lower p-value for the pathway and the x-axis provides the pathway impact, which is a measure of how affected each pathway is by the metabolites identified as significantly altered. Only pathways with a p-value less than 0.075 are labelled. This analysis was carried out using the list of metabolites that were identified to be significantly altered by either the paired t-test/Mann-Whitney or VIAVC test.

Table 1. Patient characteristics table indicating the sex, age, and TBI type, as well as the initial Glasgow Coma Scale score and both the initial and post-recovery Montreal Cognitive Assessment and Functional Independence Measure scores.

Patient Code	Sex	Age	Glasgow Coma Scale score	TBI Type	Initial Montreal Cognitive Assessment score	Post-Recovery Montreal Cognitive Assessment score	Initial FIM Score	Post-Recovery FIM score
TBI_02	M	18	3	Frontal	25	30	126	126
TBI_03	M	49	10	Frontal	23	26	113	122
TBI_04	F	17	3	SDH/Intraparenchymal hemorrhage	27	28	126	123
TBI_07	M	18	6	SDH	26	27	124	125
TBI_10	F	52	9	SAH-Right	25	26	NaN	125
TBI_13	M	64	13	DAI- Left	20	27	112	121
TBI_19	M	46	8	SDH/SAH bifrontal	25	26	113	124
TBI_24	M	68	15	SDH/SAH	21	23	126	123
TBI_26	M	48	14	SDH/SAH	27	27	124	126
TBI_28	F	52	15	SAH	27	26	120	125
TBI_29	M	48	12	SAH- right frontal	23	23	115	122
TBI_30	F	22	3	DAI- left	22	29	106	124

Abbreviations: SDH = subdural hematoma, SAH= subarachnoid hemorrhage, DAI= diffuse axonal injury

Table 2. Pearson R values and associated p-values displayed for males and females for the change in metabolites (post-recovery concentration – initial concentration) correlated to the Glasgow Coma Scale score. Reported metabolites are significant based on the Bonferroni corrected threshold for males (alpha<0.001) and for females (alpha<0.003125). For males combined with females, there were no significant correlations based on the Bonferroni threshold (alpha<0.00135).

SUBJECTS	CLINICAL TEST	Δ METABOLITES TO INITIAL INJURY SEVERITY (GCS)
MALES	Glasgow Coma Scale	Homovanillate R= -0.74, *p*= 0.001 L-methionine R= -0.78, *p*= 0.0004 Thymine R= -0.85, *p*= 0.00003
FEMALES	Glasgow Coma Scale	Mevalonic acid R= -0.96, *p*= 0.0001 Methylamine R= -0.98, *p*= 0.00003
MALES AND FEMALES	Glasgow Coma Scale	No significant metabolites by the Bonferroni threshold

REFERENCES

Anderson, P., Mahle, D., Doom, T., Reo, N., DelRaso, N., & Raymer, M. (2011). Dynamic Adaptive Binning: an Improved Quantification Technique for NMR Spectroscopic Data. *Metabolomics, 7*(2): 179-190. https://link.springer.com/article/10.1007/s11306-010-0242-7 Accessed January 15, 2020.

Bakkeren, J., De Abreu, R., Sengers, R., Gabreels, F., Maas, J., & Renier, W. (1984). Elevated urine, blood and cerebrospinal fluid levels of uracil and thymine in a child with dihydrothymine dehydrogenase deficiency. *Clinica Chimica Acta*: *140*(3):247-256. Doi: 10.1016/0009-8981(84)90206-7.

Bazarian, J., Blyth, B., & McDermott, M. (2010). Sex Differences in Outcome after Mild Traumatic Brain Injury. *Journal of Neurotrauma*, *27*(3): 527-539. Doi: 10.1089/neu.2009.1068.

Beckonert, O., Keun, H., Ebbels, T., Bundy, J., Holmes, E., Lindon, J.C., & Nicholson, J.K. (2007). Metabolic profiling, metabolomic and metabonomic procedures for NMR spectroscopy of urine, plasma. serum and tissue extracts. *Nature Protocols*, *2*(11):2692-2703. doi: 10.1038/nprot.2007.376

Bouatra, S., Aziat, F., Mandal, R., Guo, A.C., Wilson, M.R., Knox, C.,…Wishart, D.S. (2013). The Human Urine Metabolome. *PLoS ONE*, *8*(9), 1-28. Doi: 10.1371/journal.pone.0073076

Chong, J., Wishart, D.S., & Xia, J. (2019). Using MetaboAnalyst 4.0 for Comprehensive and Integrative Metabolomics Data Analysis. *Current Protocols in Bioinformatics*, *68*, e86 (128 pages). doi: 10.1093/nar/gky310.

Clark, R., Carcillo, J., Kochanek, P.M., Obrist, W.D., Jackson, E.K., Mi, Z.,…Marion, D.W. (1997). Cerebrospinal Fluid Adenosine Concentration and Uncoupling of Cerebral Blood Flow and Oxidative Metabolism after Severe Head Injury in Humans. *Neurosurgery*, *41*(6): 1284-1292. Doi: 10.1097/0000613-199712000-00010

Colantonio, A., Harris, J.E., Ratcliff, G., Chase, S., & Ellis, K. (2010). Gender differences in self reported long term outcomes following moderate to severe traumatic brain injury. *BMC Neurology*, *10*:102. Doi: 10.1186/1471-2377-10-102.

Cronstein, B. (1994). Adenosine, an endogenous anti-inflammatory agent. *Journal of Applied Physiology*, *76*(1): 5-13. Doi: 10.1152/jappl.1994.76.1.5

da Costa, R., Porto, F., & Marrocos, R. (2013). Dissociation of depression from apathy in traumatic brain injury: a case report. *Dementia & Neuropsychologia*, *7*(3): 312-315.

Dash, P., Hergenroeder, G., Jeter, C., Choi, H., Kobori, N., & Moore, A. (2016). Traumatic Brain Injury Alters Methionine Metabolism: Implications for Pathophysiology. *Frontiers in Systems Neuroscience*, *10*:36 doi: 10.3389/fnsys.2016.00036.

Emwas, A.H. (2015). The strengths and weaknesses of NMR spectroscopy and mass spectrometry with particular focus on metabolomics research. *Methods in Molecular Biology*, *1277*: 161-193. doi: 10.1007/978-1-4939-2377-9_13.

Espinoza, T., & Wright, D. (2011). The Role of Progesterone in Traumatic Brain Injury. *Journal of Head Trauma Rehabilitation*, *26*(6): 497-499. Doi: 10.1097/HTR.0b013e318230088fa

Fawcett, T. (2005). An introduction to ROC analysis. *Pattern Recognition Letters*, *72*(8):861-874. https://doi.org/10.1016/j.patrec.2005.10.010 Accessed January 17, 2020.

Felice, L., & Kissinger P. (1976). Determination of Homovanillic Acid in Urine by Liquid Chromatography with Electrochemical Detection. *Analytica; Chemistry*, *48*(6): 794-795. https://pubs.acs.org/doi/abs/10.1021/ac60370a018 Accessed January 21, 2020.

Gupte, R., Brooks, W., Vukas, R., Pierce, J., & Harris, J. (2019). Sex Differences in Traumatic Brain Injury: What We Know and What We Should Know. *Journal of Neurotrauma*, *36*(22): 3063-3091. doi: 10.1089/neu.2018.6171

Hasko, G., Sitkovsky, M., & Szabo, C. (2004). Immunomodulatory and neuroprotective effects of inosine. *Trends in Pharmacological Sciences, 25*(3):152-157. Doi: 10.1016/j.tips.2004.01.006

Herrera-Melero, M.C., Egea-Guerrero, J.J., Vilches-Arenas, A.A., Rincon-Ferrari, M.D., Flores-Cordero, J.M., Leon-Carrion, J., & Murillo-Cabezas, F. (2015). Acute predictors for mortality after severe TBI in Spain: Gender differences and clinical data. *Brain Injury*, *29*(12):1439-1444. Doi: 10.3109/02699052.2015.1071428.

Jackson, E., Boison, D., & Kochanek P. (2016). Purines: Forgotten Mediators in Traumatic Brain Injury. *Journal of Neurochemistry*, *137*(2): 142-153. Doi: 10.1111/jnc.13551

Jenkins, P., Simoni, S., Bourke, N., Fleminger, J., Scott,G., Towey, D.J.,…Sharp, D.J. (2018). Dopaminergic abnormalities following traumatic brain inury. *Brain*, *141*(3): 797-810. Doi: 10.1093/brain/awx357.

Kidd, D., Stewart, G., Baldry, J., Johnson, J., Rossiter, D., Petruckevitch, A., Thompson, A.J. (1995). The Functional Independence Measure: A comparative validity and reliability study. *Disability and Rehabilitation 17*(1): 10-14. Doi: 10.3109/09638289509166622

Kochanek, P.M., Verrier, J.D., Wagner, A.K., & Jackson, E.K. (2013). The Many Roles of Adenosine in Traumatic Brain Injury. In: Masino S, Boison D. (eds) Adenosine. Springer, New York, NY. Pp 307-322. https://doi.org/10.1007/978-1-4614-3903-5_15

Lindenthal, B., Simatupang, A., Dotti, M., Federico, A., Lutjohann, D., & Bermann, K. (1996). Urinary excretion of mevalonic acid as an indicator of cholesterol synthesis. *The Journal of Lipid Research*, *37*(10): 2193-201. https://www.ncbi.nlm.nih.gov/pubmed/8906596 Accessed January 14, 2020.

Mitchell, S., & Zhang, A. (2001). Methylamine in human urine. *Clinica Chimica Acta, 12*(1): 107-114. Doi: 10.1016/S0009-8981(01)00608-8.

Mollayeva, T., El-Khechen-Richandi, G., & Colantonio, A. (2018). Sex & gender considerations in concussion research. *Concussion, 3*(1):CNC51. Doi: 10.2217/cnc-2017-0015.

Morelli, M., Carta, A.R., Kachroo, A., & Schwarzschild, M.A. (2011). Pathophysiological roles for purines: adenosine, caffeine and urate. *Progress in Brain Research, 183*:183-208. Doi: 10.1016/S0079-6123(10)83010-9.

Naccarato, M., Pizzuti, D., Petrosino, S., Simonetto, M., Ferigo, L., Grandi, F.C.,…Di Marzo, V. (2010). Possible Anandamide and Palmitoylethanolamide involvement in human stroke. *Lipids in Health and Disease*. *9*, 47. doi: 10.1186/1476-511X-9-47.

Nasreddine, Z., Phillips, N., Bedirian, V., Charbonneau, S., Whitehead, V., Collin, I.,…Chertkow, H. (2005). The Montreal Cognitive Assessment, MoCA: A Brief Screening Tool for Mild Cognitive Impairment. *Journal of the American Geriatrics Society*, *53*(4): 695-699. Doi: 10.1111/j.1532-5415.2005.53221.x

Niemeier, J., Perrin, P., & Nersessova, K. (2014). Gender Differences in Awareness and Outcomes During Acute Traumatic Brain Injury Recovery. *Journal of Women's Health, 23*(7): 573-580. Doi: 10.1089/jwh.2013.4535.

Nicholson, J.K., & Lindon, J.C. (2008). Systems biology: metabonomics. *Nature, 455*(7216), 1054-1066. Doi: 1038/4551054a

Novotny, L., Abdel-Hamid, M., & Hamza, H. (2000). Inosine and 2'-deoxyinosine and their synthetic analogues: lipophilicity in the relation to their retention in reversed-phase liquid chromatography and the stability characteristics. *Journal of Pharmaceutical and Biomedical Analysis, 24*(1):125-132. Doi: 10.1016/s0731-7085(00)00403-9

Paxman, E.J., Boora, N.S., Kiss, D, Laplante, D.P., King, S., Montina, T., & Metz, G.A.S. (2018). Prenatal Maternal Stress from a Natural Disaster Alters Urinary Metabolomic Profiles in Project Ice Storm Participants. *Scientific Reports, 8*(1): 12932. https://doi.org/10.1038/se41598-018-31230-x

Peng, J., Zeng J, Cai B, Yang, H., Cohen, M.J., Chen, W.,…Jiang, H. (2014). Establishment of Quantitative Severity Evaluation Model for Spinal Cord Injury by Metabolomic Fingerprinting. *PLOS ONE, 9*(4): e93736. doi: 10.1371/journal.pone.0093736

Popescu, C., Anghelescu, A., & Onose, G. (2015). Actual data on epidemiological evolution and prevention endeavours regarding traumatic brain injury. *Journal of Medicine and Life, 8*(3): 272-277. https://www.ncbi.nlm.nih.gov/pmc/articles/PMC4556905/#__ffn_sectitle Accessed January 5, 2020.

Rao, D., McFaull, S., Thompson, W., & Jayaraman, G. (2017). Trends in self-reported traumatic brain injury among Canadians, 2005-2014: a repeated cross-sectional analysis. *CMAJ Open, 5*(2): E301-E307. doi: 10.9778/cmajo.20160115

Slewa-Younan, S., Green, A., Baguley, I., Gurka, J., & Marosszeky, J. (2004). Sex difference in injury severity and outcome measures after traumatic brain injury. *Archives of Physical Medicine and Rehabilitation*, *85*(3): 376-379. Doi: 10.1016/j.apmr.2003.05.007

Starkstein, S., & Pahissa, J. (2014). Apathy Following Traumatic Brain Injury. *Psychiatric Clinics of North America, 37*(1): 103-112. Doi: 10.1016/j.psc.2013.10.002.

Stein, D. (2001). Brain damage, sex hormones and recovery: a new role for progesterone and estrogen? *Trends in Neurosciences*, *24*(7): 386-391. Doi: 10.1016/s0166-2236(00)01821

Stein, D. (2005). Embracing failure: What the Phase III progesterone studies can teach about TBI clinical trials. *Brain Injury*, *29*(11):1259-1272. Doi: 10.3109/02699052.2015.1065344.

Sternbach, G. (2000). The Glasgow Coma Scale. *Journal of Emergency Medicine. 19*(1):67-71. Doi: 10.1016/s0736-4679(00)00182-7.

Stone, T.W. (2002). Purines and Neuroprotection. *Advances in Experimental Medicine and Biology, 513*:249-280. Doi: 10.1007/978-1-4615-0123-7.9

Szymanska, E., Saccenti, E., Smilde, A.K., & Westerhuis, J.A. (2012). Double-check: validation of diagnostic statistics for PLS-DA models in metabolomics studies. *Metabolomics*, *8*:S3-S16. doi: 10.1007/s11306-011-0330-3.

Tanianskii, D., Jarzebska, N., Birkenfeld, A., O'Sullivan, J., & Rodionov, R. (2019). Beta-Aminoisobutyric Acid as a Novel Regulator of Carbohydrate and Lipid Metabolism. *Nutrients, 11*(3):524. Doi: 10.3390/nu11030524.

Tulpule, K., & Dringen, R. (2013). Formaldehyde in brain: an overlooked player in neurodegeneration? *Journal of Neurochemistry*, *127*(1): 7-21. Doi: 10.1111/jnc.12356.

Veselkov, K., Lindon, J., Ebbels, T.M., Crockford, D., Volynkin, V.V., Holmes, E.,…Nicholson, J.K. (2009). Recursive Segment-Wise Peak Alignment of Biological 1H NMR Spectra for Improved Metabolic Biomarker Recovery. *Analytical Chemistry,* 2009:*81*(1): 56-66. Doi: 10.1021/ac8011544.

Wiklund, S., Johannsson, E., Sjostrom, L., Mellerowicz, E.J., Edlund, U., Shockcor, J.P.,…Trygg, J. (2008). Visualization of GC/TOF-MS-Based Metabolomics Data for Identification of Biochemically Interesting Compounds Using OPLS Class Models. *Analytical Chemistry, 80*(1): 115-122. Doi: 10.1021/ac0713510.

Wishart, D.S., Feunang, Y.D., Marcu, A., Guo, A.C., Liang, K., Vazquez-Fresno, R.,…Scalbert, A. (2018). HMBD 4.0- The Human Metabolome Database for 2018. *Nucleic Acids Research*, Jan 4;*46*(D1): D609-17. 29140435. Doi: 10.1093/nar/gkx.1080.

Xia, J., & Wishart, D.S. (2010). MetPA: a web-based metabolomics tool for pathway analysis and visualization. *Bioinformatics, 26*, 2342-2344. Doi: 10.1093/bioinformatics/btq418.

Yun, Y., Liang, F., Deng, B., Lai, G., Goncalves, C., Lu, H.,…Liang, Y. (2015). Informative metabolites identification by variable importance analysis based on random variable combination. *Metabolomics, 11*(6): 1539-1551.

Zhang, Y., Xiong, Y., Mahmood, A., Zhang, Z., & Chopp, M. (2013). Angiogenesis and Functional Recovery After Traumatic Brain Injury. In: Lo, E., Lok, J., Ning, M., Whalen, M (eds) *Vascular Mechanisms in CNS Trauma. Springer Series in Translational Stroke Research, 5*, 141-156.

CHAPTER 3: Blood-Derived Metabolomic Signatures are Correlated to Severity in Males and Females with Traumatic Brain Injury

INTRODUCTION

As the leading cause of death and disability worldwide, traumatic brain injury (TBI) is the "silent epidemic" that afflicts millions annually (Dewan et al., 2019). There are two distinct phases that characterize TBI. At first TBI results in primary injury, or the sequelae resulting from mechanical forces at the time of impact, leading to bruising, bleeding, and tearing of fibres within the cranial tissue. The delayed secondary injury phase provides opportunities for therapeutic intervention. This phase is characterized by disturbances in brain metabolism, can lead to neurodegeneration and loss of cognitive function beyond the effects of the primary injury. As a prevalent and rising health issue that currently relies upon subjective clinical guidelines for diagnosis and treatment, an informative and quantitative biomarker would be an essential tool and provide a window into the pathophysiological processes in the body, and with the ability to provide insight as to how to intervene most effectively to optimize patients' potential for recovery.

Awareness of the male bias in TBI research (Gupte et al., 2019) has prompted the present longitudinal pilot study, which involved analysis of blood samples from male and female patients with mild to severe TBI to elucidate whether there is an informative biomarker specific to sex. Although there have been previous efforts to identify biomarkers with diagnostic and prognostic potential, including S100B, glial fibrillary acidic protein, and neuron-specific enolase for assessing mild TBI (concussion), none of these biomarkers have been validated as reliable (Papa et al., 2015). As the search for an informative biomarker with potential for clinical use continues, our team has shown that metabolites in

urine samples collected from athletes with concussion results in significantly distinct metabolic profiles at baseline and post-injury (Paxman et al., 2017). Furthermore, this complements our previous work which examined urine samples for metabolic biomarkers from TBI patients using nuclear magnetic resonance (NMR) spectroscopy (Bykowski et al., submitted). NMR spectroscopy is a technique that is especially amenable to detecting metabolic changes in the blood, as it can detect 49 compounds, with 20 of these being unique to NMR (Psychogios et al., 2011).

Here, we pooled metabolomic data from both sexes to determine if there are common mechanisms of injury across males and females. This study addressed the following objectives: (1) to determine sex-dependent differences in the initial and post-recovery metabolomics profile; (2) based on the list of significant metabolites, to reveal the underlying biochemical pathways contributing to TBI outcome; (3) to determine the predictive accuracy of the identified metabolites as biomarkers of TBI, and (4) to examine how these changes correlate to clinical outcomes in male and female patients.

MATERIALS AND METHODS

Patient Characteristics and Sample Collection

This research was embedded in a larger study called Understanding Neurological Recovery: the role of resting state fMRI, biomarkers, and robotics after TBI, stroke, and SCI (UCAN) study funded by the Hotchkiss Brain Institute at the University of Calgary. The UCAN Study followed patients with TBI, stroke, and SCI throughout their recovery from one week to 6 months post-injury Patients with TBI were recruited through the Foothills Medical Centre, Calgary (n=8 males, average age 45 +/- 18.4 years; n=4 females,

average age 36 +/- 18.9 years); (Table 3). Pairs of fasting morning blood samples (acquired between 6am and 9am) were collected at two different time points: within 2 weeks after TBI and again at 6 months post-injury. Pairing the samples for this within-subject control study minimizes confounding factors, such as diet and lifestyle, increasing the validity of the analysis to attribute changes in the metabolic profiles throughout recovery. Whole blood samples were centrifuged and spun down to isolate the serum, which is the protein-rich component of the blood that does not contain fibrinogens, and therefore will not clot. Serum samples were transported to the University of Lethbridge and stored in a -80 degrees Celsius freezer until NMR data acquisition. This study was reviewed and approved by the University of Calgary Conjoint Health Research Ethics Board (CHREB) and the University of Lethbridge Human Participant Research Committee in accordance to the standards set forth by the Tri-Council Policy Statement: Ethical Conduct for Research Involving Humans.

Clinical Assessments

The Glasgow Coma Scale (GCS) was used to rate the initial severity of TBI for each patient. It measures three different functions: eye opening, verbal response, and motor responses, where higher scores indicate better function (Sternbach et al., 2000). The final GCS score was the sum of these numbers, with the following ranges: severe (GCS less than 8), moderate (GCS 8-12), and mild (GCS 13-15). The Montreal Cognitive Assessment (MoCA) was used to screen for short term memory, visuospatial abilities, executive functions, and language (Nasreddine et al., 2005). A score of 26 and higher was considered to be normal, whereas a score below 26 indicated impairment. In addition, the Functional Independence Measure (FIM) served as a global assessment of physical, social, and

psychological function (Kidd et al., 1995). It included six areas of evaluation including self-care, continence, mobility, transfers, communication, and cognition. Each item was graded on a scale from 1-7, where 1 indicates total dependence and 7 indicates complete independence.

NMR Sample Preparation, Data Acquisition, and Processing

Buffer was prepared to combine with the blood samples for use in Nuclear Magnetic Resonance Spectroscopy-based metabolomics. The buffer contained a 4:1 ratio of dibasic potassium phosphate (K_2HPO4) to monobasic potassium phosphate (KH_2PO4) with a combined concentration of 0.625M in dH_2O, 3.75mM NaN_3 anti-microbial agent and 0.375 M potassium fluoride (KF). It has been found that large variations in the pH and the cationic concentration of serum create positional noise within NMR-generated datasets (Smelter et al., 2017), which presents a confounding variable that interferes with multivariate statistics. The phosphate buffer carefully controls the pH of the sample, while the addition of KF reduces positional noise in the citrate peaks caused by divalent cations in blood, thereby correcting for chemical shift variation (Gil et al., 2016).

All serum samples were processed in a containment level two laboratory. Amicon 0.5 mL 3 kDa centrifuge filters were used to isolate the metabolite-rich, water soluble components from the protein-rich, potentially pathogenic component. The Millipore filters were washed 10 times with deionized water immediately prior to use in order to remove glycerol preservative from the filters. Reverse pipetting was used to add 300 µL of metabolomics buffer into each of the Amicon centrifuge filters. Then, 200 µL of plasma was pipetted from each sample into the correctly labelled tube. Tubes were centrifuged at 14,000 g for 30 minutes at 4 degrees Celsius. This caused the proteins and large

macromolecules to concentrate inside the filter, while the water-soluble metabolites passed through the filter, to be collected as the filtrate. Filtrate samples were stored in a -80 degrees Celsius freezer until NMR data processing. The filters containing the concentrated proteins were placed upside down inside a second centrifuge tube and spun for 2 minutes at 1000 g. This caused the concentrate solute macromolecules to come out of the filter and fall into the centrifuge tube for storage in a -80 degree Celsius freezer.

For NMR sample preparation, 380 µL of serum filtrate, 100 µL of metabolomics buffer and 120 µL of 0.02709 % weight/volume D2O with TSP were pipetted into a microfuge tube. The trimethylsilyl propanoic acid (TSP) in the D2O served as a chemical shift reference for the 1H NMR spectroscopy. Each microfuge tube was then centrifuged at 12000 rpm for 5 minutes at 4 degrees Celsius. This was done to eliminate any insoluble matter in the sample that would interfere with the NMR signal. 550 µL of buffered sample was transferred to an NMR tube to be loaded into the spectrometer. Samples were vortexed prior to loading to ensure that the serum was mixed prior to spectral acquisition.

A 700 MHz Bruker Avance III HD NMR spectrometer and a room-temperature TBO probe was used to acquire the NMR data. Three-dimensional and one-dimensional shimming experiments were conducted prior to NMR data acquisition on the urine samples to correct for any inhomogeneities in the static magnetic field. The data were acquired using a one-dimensional 1H Nuclear Overhauser Effect Spectroscopy experiment with water suppression, 128k points, and 128 scans. The data was processed using zero filling to 256k points, line broadening to 0.3 Hz, and automatic phase and baseline correction. The spectra obtained from the NMR experiment were then imported into MATLAB where they underwent dynamic adaptive binning (Anderson et al., 2011), followed by manual

inspection and correction of the bins, and recursive segment-wise peak alignment (Veselkov et al., 2009) In total, 287 bins were created for this analysis.

Metabolites were identified using a combination of resources: Chenomx 8.2 NMR Suite (Chenomx Inc., Edmonton, Alberta, Canada), the Human Metabolome Database (HMBD), (Wishart et al., 2018), and the Human Serum Metabolome (Psychogios et al., 2011) containing a list of chemical classes of blood-based metabolites. Once the significant metabolites of interest were identified, they were used for metabolic pathway and visualization tests in MetaboanalystR (Chong et al., 2019). Topology Analysis was also conducted, which uses the list of significant metabolites, the Kyoto Encyclopedia of Genes and Genomes (KEGG), and the HMBD libraries (Wishart et al., 2018; Xia et al., 2010) to provide metabolite pathways that have been potentially altered due to differences following injury and at post-recovery.

Statistical Analysis

Multivariate statistical analysis was used to determine if blood-derived metabolite profiles could be used to distinguish between the initial and post-recovery samples. Prior to modelling, the data were normalized to the total metabolome, excluding the region corresponding to water, and pareto-scaled (Craig et al., 2006; Wiklund et al., 2008). Bins containing significant metabolites were sorted according to the F-ranked Variable Importance Analysis based on random Variable Combination (VIAVC) analysis (Yun et al., 2015). This MATLAB based statistical programming algorithm enables identification of significant metabolites based on the Receiver Operator Characteristic (ROC) test and the subsequent Area-Under-the-Curve (AUC) analysis (Fawcett et al., 2005). It also employs a binary matrix resampling method, which is a more robust method for randomly sampling

the data, and all multivariate supervised models were double ten-fold cross-validated (Szymanska et al., 2012). Univariate statistical tests were also conducted; either a paired T-test or paired Wilcoxon-Mann-Whitney test was used in the case of parametric or non-parametric data, respectively.

An orthogonal projection to latent structures discriminant analysis (OPLS-DA) was also conducted to visualize between-group separation as a function of within-group separation The advantage to using OPLS-DA is that the model is rotated where class separation or between-class, correlated variation is found in the first predictive component, and within-class, uncorrelated variation is seen in the orthogonal component (Wiklund et al., 2008). This was complemented by a Principal Components Analysis (PCA) which demonstrated the degree of separation between the groups without the presence of an algorithm, as well as unsupervised hierarchical clustering illustrated by the accompanying heat map.

Pearson R correlations were computed between concentrations of blood-derived metabolites and patient GCS scores (table 4). The significance is assessed based on the Bonferroni corrected *p*-value, obtained by dividing alpha<0.05 by the number of VIAVC F-ranked bins tested for each analysis (alpha<0.005, alpha<0.00093, and alpha<0.0021 for males, females, and together respectively) to obtain a more rigorous set of clinically relevant metabolites (Goodpaster et al., 2010).

RESULTS

Patient Characteristics

The number of patients with severe (n=4), moderate (n=4) and mild GCS (n=4) are summarized in Table 3, indicating TBI severity ranging from mild to severe at first visit. Patient performance at the Montreal Cognitive Assessment Test is summarized as follows. This test was conducted initially (n=4 patients with normal scores, n=8 patients with impairment) and at post-recovery (n=10 patients with normal scores, n=2 patients with impairment). In addition, patient performance was assessed at the Functional Independence Measure: This test was conducted initially (n=3 patients completely independent, n=3 patients mildly dependent and n=5 patients moderately dependent, n=1 no data) and at post-recovery (n=2 patients completely independent, n=10 patients mildly dependent). Additional patient results are summarized in Table 3.

Metabolomic Profiles are Robust Predictors of Recovery Following TBI

The bins found to be significant by either the paired T-test/Wilcoxon Mann-Whitney test (41 bins for males, 29 for females, and 59 for both males and females) or the VIAVC best subset (3 bins for males, 18 for females, and 8 for both males and females) were used for the analysis. PCA demonstrated a partial degree of unsupervised group separation for the males, with complete separation for the females, and comparable partial separation for males and females combined (Figures 4A, B, C). The OPLS-DA plot illustrates significant group separation between the initial injury and post-recovery samples for males ($R^2Y=0.794$, $p<0.01$; $Q^2=0.607$, $p<0.01$), females ($R^2Y=0.988$, $p<0.05$; $Q^2=0.935$, $p<0.05$), and males combined with females ($R^2Y=0.713$, $p<0.01$; $Q^2=0.533$, $p<0.001$; Figures 4D, E, F). This supervised model indicates a change in the metabolic profiles of patients over the course of the recovery process. Metabolites that contributed the most to the group separation for males, females, and combined are provided in

Appendix 2. Metabolites are ranked in order of significance according to the paired T-test/Wilcoxon Mann Whitney analysis.

ROC curves were also generated for males and females separately and combined. For males an area-under-the-curve equal to 0.844 was achieved, with a 95% confidence interval of 0.667-1 (Figure 5A). For females there were not enough variables generated by VIAVC to create a ROC curve since there is a small sample size (n=4). When males and females were combined, an area-under-the-curve equal to 0.901 was achieved, with a 95% confidence interval of 0.702-1 (Figure 5B).

Pathway topology analysis conducted separately for males, females, and both sexes combined (Figures 6A, B, C) illustrates the potential pathway impact based on changes to the patients' blood-derived metabolic profiles, presented in increasing order of impact. Metabolic pathways significantly affected amongst the male patients were phenylalanine, tyrosine, & tryptophan biosynthesis ($p<0.01$), pyruvate metabolism ($p<0.01$), aminoacyl-tRNA biosynthesis ($p<0.01$), alanine, aspartate, & glutamate metabolism ($p=0.01$), phenylalanine metabolism ($p<0.05$), glyoxylate & dicarboxylate metabolism ($p<0.5$), glycine, serine, & threonine metabolism ($p<0.05$), and the citrate cycle ($p<0.05$). The pathways significant amongst the female patients were phenylalanine, tyrosine, & tryptophan biosynthesis ($p=0.001$), aminoacyl-tRNA biosynthesis ($p<0.01$), phenylalanine metabolism ($p<0.01$), and arginine & proline metabolism ($p<0.05$). When male and female data were combined, significant pathways included glycine, serine, & threonine metabolism ($p<0.01$), pyruvate metabolism ($p<0.05$), alanine, aspartate, & glutamate metabolism ($p<0.05$), and glyoxylate & dicarboxylate metabolism ($p<0.05$). Pathway

analysis was based on bins significant by the VIAVC best subset, and the paired T-test/or the Wilcoxon-Mann-Whitney test.

Metabolomic Signatures Correlate with Injury Severity

Table 4 provides the Pearson R correlation values when comparing the change in concentration of each metabolite initially following injury and at 6-months to the GCS scores. L-Alanine (R= -0.63, $p<0.01$ negatively correlated to injury severity in males. Myoinositol (R= 0.97, $p<0.001$) and glycylproline (R= 0.95, $p<0.001$) positively correlated to injury severity in females and were both significant correlations by the Bonferroni threshold. When males and females were combined, L-lactic acid (R= -0.51, $p<0.05$) and methylcysteine (R= -0.42, $p<0.05$) presented with negative correlations.

DISCUSSION

The present study demonstrates that blood-derived biomarkers have the potential to predict recovery trajectories following TBI. Overlapping as well as different biochemical pathways were potentially altered amongst males, females, and when considered together, suggesting that both sex-independent and sex-dependent mechanisms of responses to injury. In addition, different metabolites presented with significant correlations to clinical outcomes across the three groups, again suggesting sex-specific metabolic fingerprints following TBI. These findings suggest that a metabolomics approach combined with machine learning analysis of blood samples is feasible and has the potential to provide robust metabolic profiles with respect to injury severity.

Pathway Analysis

The most significantly altered pathway for the male patient subgroup was phenylalanine, tyrosine, and tryptophan biosynthesis. The metabolites phenylalanine and tyrosine implicated in this pathway indicate disruptions to neurotransmitter signaling, as these amino acids are known precursors to catecholamine neurotransmitters, including dopamine and epinephrine. The large neutral amino acid transport (LNAA) system found at the blood brain barrier (BBB) is the gateway for uptake of these amino acids into the brain (Fernstrom, 1981). A TBI leads to disruption of the vessels within the BBB which can lead to ischemia in surrounding areas (Price et al., 2016). Thus, it is plausible that BBB disruption and ensuing changes in amino acid levels precipitate abnormalities in neurotransmitter production.

The second most affected pathway for the male subgroup was pyruvate metabolism. In a parallel study examining blood-derived biomarkers amongst male SCI patients, it was found that pyruvate metabolism was the most significantly altered pathway (Bykowski et al., in preparation). We postulated that this was due to aberrant insulin signaling; as the hormone that drives glycolysis and subsequent pyruvate formation, this pathway becomes dysregulated after SCI (Gorgey et al., 2012). A similar mechanism may be suspected following TBI, as synaptic insulin resistance has been found to be a pathological hallmark that is associated with increased susceptibility for Alzheimer's disease (Franklin et al., 2019). This overlapping characteristic of SCI and TBI warrants further investigation as a potential clinical feature for central nervous system trauma in general.

For the female patient subgroup, the most significantly altered pathway was also phenylalanine, tyrosine, and tryptophan biosynthesis. The observed overlap when males and females are considered separately also suggests a sex independent mechanism

involving aberrant neurotransmitter production to abnormalities in transport of amino acid precursors.

The second most affected pathway for females was aminoacyl tRNA biosynthesis. With a key role in protein biosynthesis, aminoacyl tRNA synthetases are programmed in the genetic code throughout the cells of the body. Their relevance to brain pathology has been documented- in neuronal diseases such as amyotrophic lateral sclerosis and Parkinson's disease, modifications to this translational machinery underlies pathological changes (Park et al., 2008). Perhaps a similar mechanism afflicts TBI mechanisms; however, this remains to be explored.

The pathway found to be most significantly for males combined with females was glycine, serine, and threonine metabolism. There is evidence that plasma amino acids tend to be higher in patients with skeletal muscle degeneration due to higher protein requirements (Elder et al., 2004). As a reputed symptom following SCI, skeletal muscle atrophy also appears to be a factor following TBI. In a previous study using a mouse model, it was shown that TBI induced atrophy in lower limb muscles, such as the soleus and tibialis anterior (Shahidi et al., 2017). Thus, changes in body composition following brain trauma may underlie these inferred changes in blood amino acid levels. The second most affected pathway was pyruvate metabolism. The fact that pyruvate metabolism for males only in addition to males combined with females suggests that synaptic insulin resistance may be a sex independent injury mechanism implicating this pathway.

Relationship Between Metabolite Profiles and GCS

The single clinically significant metabolite from the male subgroup was L-alanine, demonstrating a negative correlation to patient GCS outcomes. This indicates that an increase in serum L-alanine levels is associated with poorer GCS scores. L-alanine is a non-essential amino acid and is found in skeletal muscle. Following TBI, messages sent by cranial nerves do not reach their effector muscles the same way, which can lead to changes in activation of these muscles (Carron et al., 2016). As previously described, muscle atrophy was shown to be a consequence of TBI in a mouse model (Shahidi et al., 2017). Perhaps this effect is more pronounced for males compared to females, as males on average tend to have a greater proportion of muscle (Wells, 2007), and disrupted transmission along cranial nerves has a greater impact on their metabolic profile.

The female subgroup presented with significant positive correlations between myoinositol and glycylproline to GCS outcomes (table 4). Myoinositol is one of the most abundant metabolites in the human brain, found mainly in glial cells and also as a precursor to membrane phospholipids (Haris et al., 2011). Consequently, damage to myelin sheets can lead to increased concentrations of free myoinositol, as is likely to occur following TBI. Thus, myoinositol may have potential as a biomarker of membrane disruption in the brain following trauma and is especially evident amongst females.

The potential of glycylproline as a biomarker of TBI has also been previously examined. It was shown that TBI induced a decrease in proline concentrations, which is due to the fact that proline is the main component of the extracellular matrix and its concentrations fluctuate during vascular remodeling after head injury (Louin et al., 2007). In addition, proline is a substrate for gluconeogenesis, which is up-regulated following TBI due to reduced availability of glucose (Glenn et al.,2015). The positive correlation observed

for glycylproline (a modified form) may indicate attenuation of degeneration of extracellular matrix and indicate that regenerative processes are in progress; it may also indicate a persistent lack of glucose availability and use of alternative metabolic modes.

L-Lactate emerged as a clinically significant biomarker when males and females were combined, with a negative correlation to patient GCS scores (Table 4). It is well known that following cerebral trauma there is an elevation in extracellular lactate concentration and an inflated lactate to pyruvate ration (Carpenter et al., 2015). According to the "astrocyte neuron lactate shuttle hypothesis" (Magistretti and Pellerin, 1996), lactate can be used as an energy source by neurons during times of hypoxia and stress. Thus, the potential of l-lactate as a sex independent biomarker of metabolic changes following TBI has been previously studied and is corroborated by the present study as well.

Methylcysteine was also found to be a clinically significant biomarker across males and females combined, as it serum levels negatively correlated with patient GCS scores (Table 4). Although post-translationally modified with a methyl group, cysteine plays an important role in the body as a precursor to glutathione, which is an antioxidant in the brain, offering protection against reactive oxygen species (Dringen and Hirrlinger, 2003; Lu, 2010). The observed negative correlation, whereby increased serum methylcysteine is associated with lower GCS scores (worse clinical outcome) may indicate an increased need for neuroprotection by glutathione synthesis due to oxidative stress (Dringen, 2000). It is interesting to note that clinically significant metabolites presented with weaker Pearson R values when males and females were combined. This was also the case in the parallel study examining urinary metabolites amongst this same patient cohort (Bykowski et al., submitted), in which there were no significant metabolites when the sexes were combined.

Weaker correlations observed for the combined sexes strongly suggests that following TBI, there are unique pathological processes affecting males and females separately.

Metabolite Profiles and Sex Differences

The OPLS-DA comparisons likely indicate that there are sex dependent mechanisms at work, as greater group separation was achieved when the sexes were considered separately than when there were combined (Figures 4D-F). There is also evidence to suggest that blood may be a superior bio-fluid for examining metabolic changes amongst females, as greater separation initially and post-recovery was observed in the OPLS-DA in comparison to males (Figures 4B and E). In contrast, when urine samples were analyzed for this same group of patients, greater separation was observed for the males than for the females, suggesting that urine is a superior bio-fluid for examining metabolic changes amongst males (Bykowski et al., submitted). Thus, this exploratory pilot study provides substantiated evidence for the potential of metabolites in clinically available bio-fluids for prognosticating outcomes for males and females following TBI.

LIMITATIONS

Although the sample size was limited, the pairing of spinal cord injured subjects within this pilot study ensures that the regulation of metabolite concentrations is significant across the initial and post-recovery groups. Although sex differences were explored, further validation via an increased sample size would confirm whether the observed differences are due to inter-individual variability or are in fact sex specific. Although the patients' diets were not controlled, this potential confound is compensated for the fact that two serum samples were collected from each patient, and that significant changes to metabolite levels reflect a global increase or decrease across *paired* serum samples.

CONCLUSIONS

The present study identified endogenous blood-derived biomarkers that change over recovery following TBI, with correlations to injury severity. The results reveal sex differences in metabolite profiles, suggesting sex influences metabolites in blood which should be considered in future metabolomic studies. Although the sample size in the present proof-of-principle study was small, the present within-subject design ensured that the regulation of metabolite concentrations provides a robust indicator of change in TBI symptom severity. Further validation will ascertain the potential of the identified metabolites as proxy measures for clinical use.

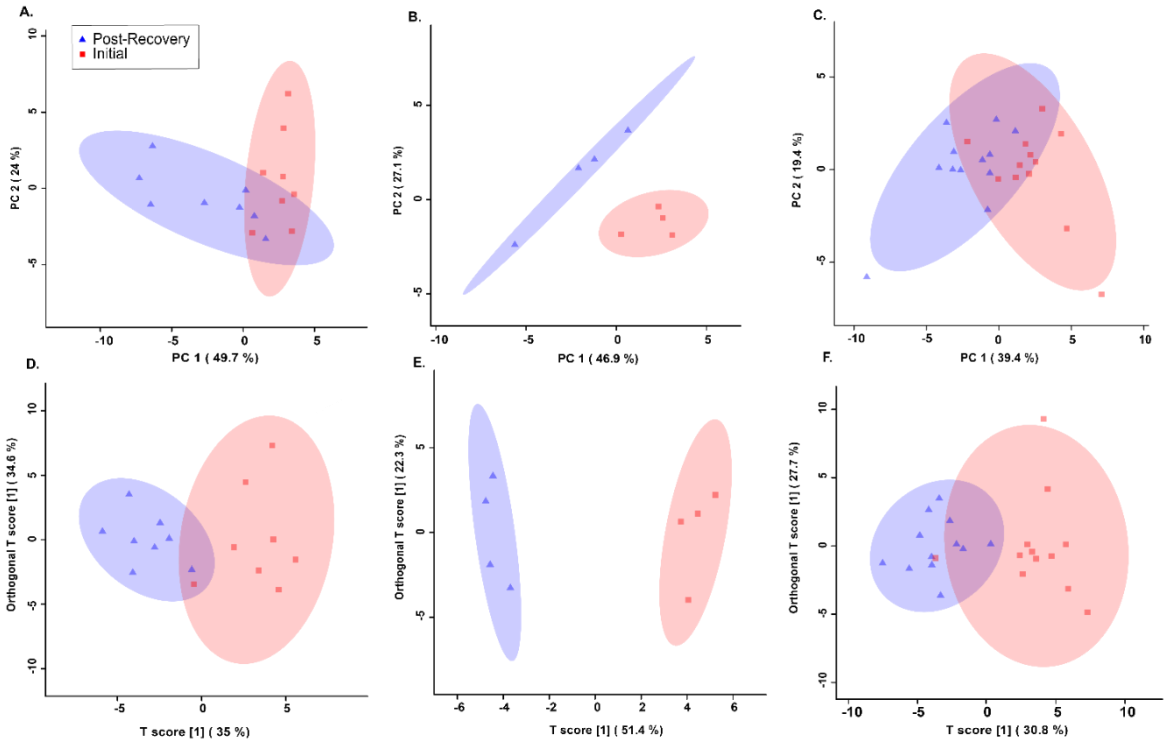

Figure 4. Principal Components Analysis (PCA) (A-C) and Orthogonal Projections to Latent Structures Discriminant Analysis (OPLS-DA) (D-F) scores plots for males (A and D), females (B and E) and both sexes combined (C and F). This analysis was carried out using a list of blood-derived metabolites found to be statistically significant by either paired t-test/Mann-Whitney or VIAVC testing. The 95% confidence interval is indicated by the shaded ellipses. In the case of the PCA scores plots the x- and y-axis show the data variance explained by principle component 1 and 2, respectively. In the case of the OPLS-DA scores plot the x- and y-axis show the predictive (between group) and orthogonal (within group) variation, respectively. The following are the cross-validation and permutation measures for the OPLS-DA figures: D - $R^2Y=0.794$ ($p<0.01$), $Q^2=0.607$ ($p<0.01$); E - $R^2Y=0.988$ ($p<0.05$), $Q^2=0.935$ ($p<0.05$); F - $R^2Y=0.713$ ($p<0.01$), $Q^2=0.533$ ($p<0.001$).

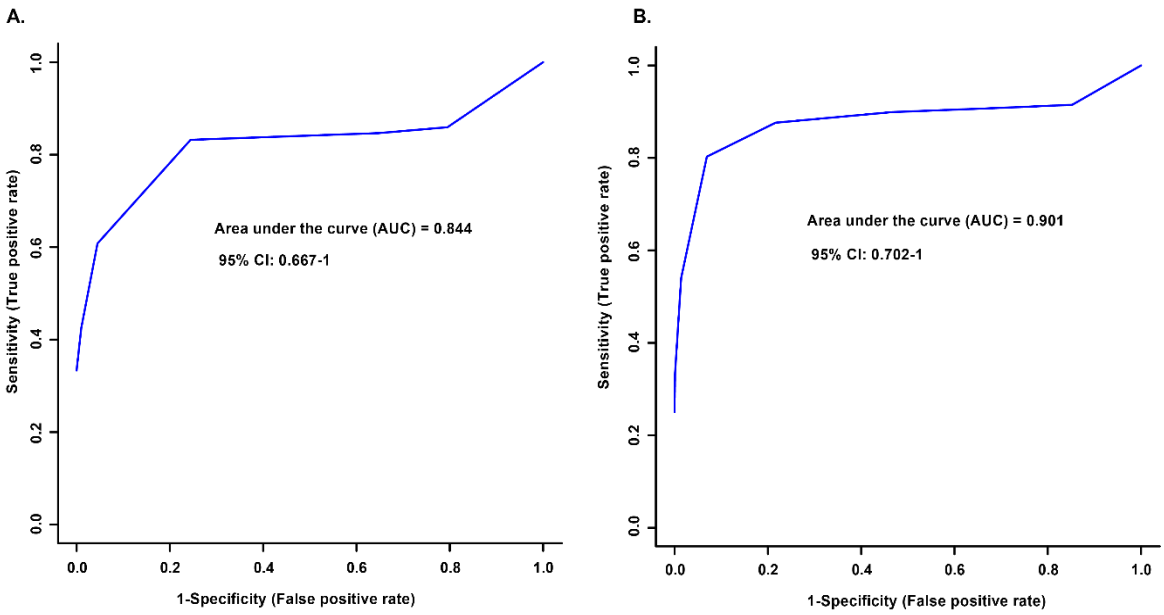

Figure 5. Receiver Operator Characteristic (ROC) curves for (A**)** males and (B) both sexes combined. The corresponding area under the curve (AUC) and confidence interval are indicated on each figure. These ROC curves were constructed using the metabolites determined to be significantly altered based on the VIAVC best subset which corresponds to 3 and 8 bins for figures A and B respectively. The predictive accuracy of males (A) and the combined sexes (B) is 86.3%and 86.5%, respectively, when all bins from the best subset are considered.

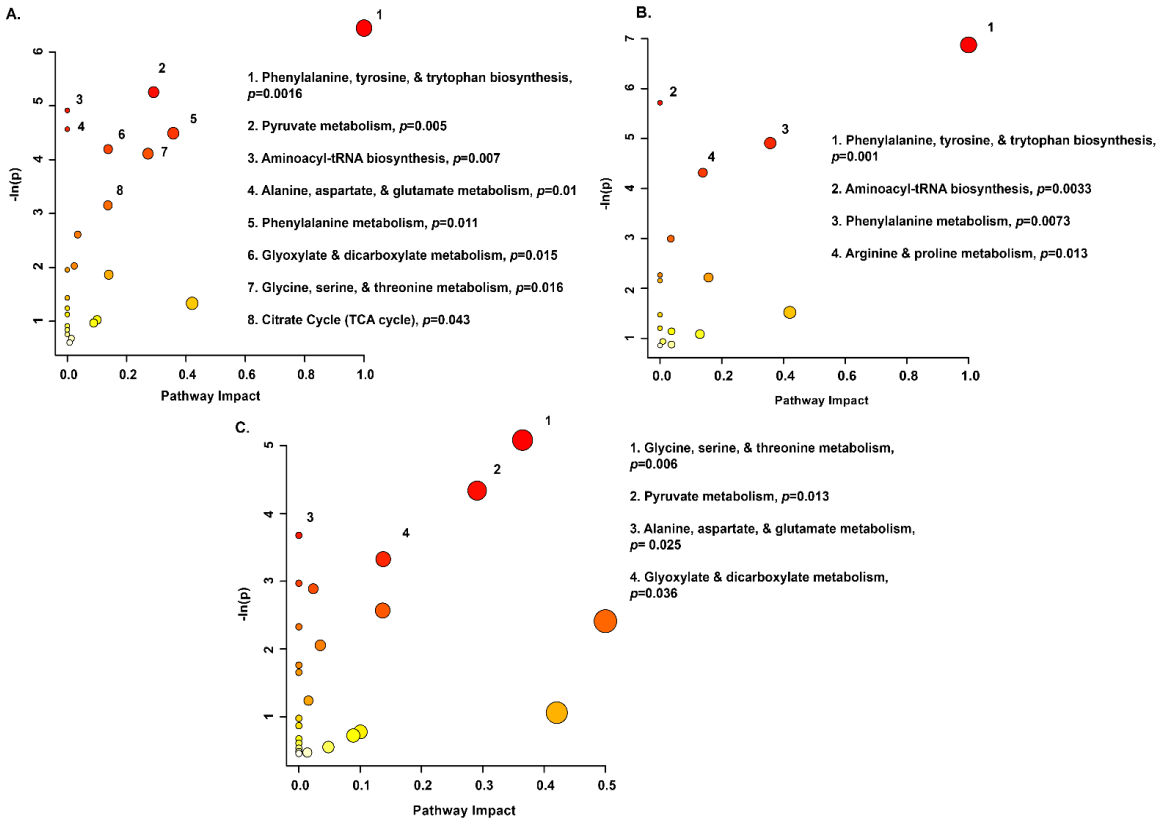

Figure 6. Metabolic Pathway Analysis for (A) males, (B) females, and (C) both sexes combined. A higher value on the y-axis indicates a lower *p*-value for the pathway and the x-axis provides the pathway impact, which is a measure of how affected each pathway is by the metabolites identified as significantly altered. Only pathways with a *p*-value less than 0.05 are labelled. This analysis was carried out using the list of metabolites that were identified to be significantly altered by the paired t-test/Mann-Whitney test or the VIAVC best subset.

Table 3. Patient characteristics table indicating the sex, age, and TBI type, as well as the initial Glasgow Coma Scale score and both the initial and post-recovery Montreal Cognitive Assessment and Functional Independence Measure scores.

Patient Code	Sex	Age	Glasgow Coma Scale score	TBI Type	Initial Montreal Cognitive Assessment score	Post-Recovery Montreal Cognitive Assessment score	Initial FIM Score	Post-Recovery FIM score
TBI_02	M	18	3	Frontal	25	30	126	126
TBI_03	M	49	10	Frontal	23	26	113	122
TBI_04	F	17	3	SDH/Intraparenchymal hemorrhage	27	28	126	123
TBI_07	M	18	6	SDH	26	27	124	125
TBI_10	F	52	9	SAH- Right	25	26	NaN	125
TBI_13	M	64	13	DAI- Left	20	27	112	121
TBI_19	M	46	8	SDH/SAH bifrontal	25	26	113	124
TBI_24	M	68	15	SDH/SAH	21	23	126	123
TBI_26	M	48	14	SDH/SAH	27	27	124	126
TBI_28	F	52	15	SAH	27	26	120	125
TBI_29	M	48	12	SAH- right frontal	23	23	115	122
TBI_30	F	22	3	DAI- left	22	29	106	124

Abbreviations: SDH = subdural hematoma, SAH= subarachnoid hemorrhage, DAI= diffuse axonal injury

Table 4. Pearson R values and associated p-values displayed for males and females for the change in metabolites (post-recovery concentration – initial concentration) correlated to the Glasgow Coma Scale score. For males, there was one metabolite with a p-value less than 0.05, but not significant according to the Bonferroni corrected threshold (alpha<0.005). For females there were two metabolites significant based on the Bonferroni threshold (alpha<0.00093) as indicated by the asterisk (*). For males combined with females, there were two metabolites with p-values less than 0.05, but not significant according to the Bonferroni threshold (alpha<0.0021).

SUBJECTS	CLINICAL TEST	Δ METABOLITES TO INITIAL INJURY SEVERITY (GCS)
MALES	Glasgow Coma Scale	L-Alanine R= -0.63, *p*= 0.0093
FEMALES	Glasgow Coma Scale	Myoinositol * R= 0.97, *p*= 0.000047 Glycylproline * R= 0.95, *p*= 0.0003
MALES AND FEMALES	Glasgow Coma Scale	L-Lactic Acid R= -0.51, *p*= 0.011 Methylcysteine R= -0.42, *p*= 0.042

REFERENCES

Allison D, Ditor D. (2015). Targeting inflammation to influence mood following spinal cord injury: a randomized clinical trial. *Journal of Neuroinflammation, 12*:204.

Anderson P, Mahle D, Doom T, Reo N, DelRaso N, Raymer M. (2011). Dynamic Adaptive Binning: an Improved Quantification Technique for NMR Spectroscopic Data. *Metabolomics, 7*(2): 179-190. https://link.springer.com/article/10.1007/s11306-010-0242-7 Accessed January 15, 2020.

Bykowski EA, Petersson JN, Dukelow S, Ho C, Debert CT, Montina T, Metz GAS. (In Preparation). Identification of serum metabolites as prognostic biomarkers in spinal cord injury.

Bykowski, E., Petersson, J., Dukelow, S., Ho, C., Debert, C., Montina, T., & Metz G.A.S. Urinary The relationship between Urinary Metabolomic Signatures and Injury Severity in Males and Females with Traumatic Brain Injury. *Journal of Head Trauma Rehabilitation,* submitted.

Carron SF, Alwis DS, Rajan R. (2016). Traumatic brain injury and neuronal functionality changes in sensory cortex. *Frontiers in Systems Neuroscience*, 10:47. Doi: 10.3389/fnsys.2016.00047.

Carpenter KL, Jalloh I, Hutchinson PJ. (2015). Glycolysis and the significance of lactate in traumatic brain injury. *Frontiers in Systems Neuroscience, 9*:112. Doi: 10.3389/fnins.2015.00112

Chong J, Wishart DS, Xia J. (2019). Using MetaboAnalyst 4.0 for Comprehensive and Integrative Metabolomics Data Analysis. *Current Protocols in Bioinformatics, 68*, e86 (128 pages). doi: 10.1093/nar/gky310.

Dewan M, Rattani A, Gupta S, et al. (2019). Estimating the global incidence of traumatic brain injury. *Journal of Neurology, 130*: 1080-1097.

Dringen R. (2000). Metabolism and functions of glutathione in brain. *Progress in Neurobiology*, *62*(6): 649-671.

Dringen R, Hirrlinger J. (2003). Glutathione pathways in the brain. *Biological Chemistry*, *384*(4): 505-516.

Elder C, Apple D, Bickel C, Meyer R, and Dudley, G. Intramuscular fat and glucose tolerance after spinal cord injury- a cross-sectional study. *Spinal Cord.* 711-716.

Fawcett T. (2005). An introduction to ROC analysis. *Pattern Recognition Letters*, *72*(8):861-874. https://doi.org/10.1016/j.patrec.2005.10.010 Accessed January 17, 2020.

Fernstrom, JD. (1981). Effects of precursors on brain neurotransmitter synthesis and brain functions. *Diabetologia*, 20: 281-289.

Franklin W, Krishnan B, Tagliatela G. (2019). Chronic synaptic insulin resistance after traumatic brain injury abolishes insulin protection from amyloid beta and tau

oligomer-induced synaptic dysfunction. *Scientific Reports*, 9:8228, https://doi.org/10/1038/s41598-019-44635-z

Gil R., Lehmann R., Schmitt-Kopplin P, Heinzmann, S. (2016). (1)H NMR-based metabolite profiling workflow to reduce inter-sample chemical shift variations in urine samples for improved biomarker discovery. *Analytical and Bioanalytical Chemistry, 408*(17): 4683-4691.

Glenn TC, Martin NA, Horning MA, McArthur DL, Hovda DA, Vespa P, Brooks GA. (2015). Lactate: brain fuel in human traumatic brain injury: a comparison with normal healthy control subjects. *Journal of Neurotrauma, 32*(11): 820-832. Doi: 10.1089/neu.2014.3483.

Goodpaster, A., Romick-Rosendale, L., Kennedy, M. (2010). Statistical significance analysis of nuclear magnetic resonance-based metabonomics data. *Analytical Biochemistry, 401*: 134-143.

Gorgey, A., Dolbow, D., Dolbow, J., Khalil, R., Castillo, C., and Gater, D. (2014). Effects of spinal cord injury on body composition and metabolic profile. *Journal of Spinal Cord Medicine, 37*(6): 693-702.

Haris M, Cai K, Singh A, Hariharan H, Reddy R. (2011). *In vivo* mapping of brain myo-inositol. *Neuroimage*, 54(3): 2079-2085. Doi: 10.1016/j.neuroimage.2010.10.017.

Kidd D, Stewart G, Baldry J, et al. (1995). The Functional Independence Measure: A comparative validity and reliability study. *Disability and Rehabilitation*, *17*(1): 10-14. Doi: 10.3109/09638289509166622

Louin G, Neveux N, Cynober L, Plotkine M, Marchand-Leroux C, Jafarian-Tehrani M. (2007). Plasma concentrations of arginine and related amino acids following traumatic brain injury: proline as a promising biomarker of brain damage severity. *Nitric Oxide*, 17(2): 91-97.

Lu S. (2010). Regulation of glutathione synthesis. *Mol Aspects Med*, 31(1-2): 42-59.

Magistretti PJ, Pellerin L. (1996). Cellular bases of brain energy metabolism and their relevance to functional brain imaging: evidence for a prominent role of astrocytes. *Cerebral Cortex, 6*(1): 50-61.

Nasreddine Z, Phillips N, Bedirian V,et al. (2005). The Montreal Cognitive Assessment, MoCA: A Brief Screening Tool for Mild Cognitive Impairment. *Journal of the American Geriatrics Society*, *53*(4): 695-699. Doi: 10.1111/j.1532-5415.2005.53221.x

Papa, L., Ramia, M.M., Edwards, D., Johnson, B.D., & Slobounov, S.M. (2015). Systematic review of clinical studies examining biomarkers of brain injury in athletes after sports-related concussion. *Journal of Neurotrauma, 32*(10): 661-673.

Park SG, Schimmel P, Kim S. (2008). Aminoacyl tRNA synthetases and their connections to disease. *PNAS*, 105(32): 11043-11049. https://doi.org/10.1073/pnas.0802862105.

Price L, Wilson C, Grant G. (2016). Chapter 4: Blood-brain barrier pathophysiology following traumatic brain injury. In: *Translational Research in Traumatic Brain Injury*. CRC Press/Taylor and Francis Group.

Psychogios, N., Hau, D., Peng, J., Guo, A., Mandal, R., Bouatra, S., et al. (2011). The human serum metabolome. *PLoS One, 6*(2): e16957.

Shahidi B, Shah SB, Esparza M, Head BP, Ward SR. (2018). Skeletal muscle atrophy and degeneration in a mouse model of traumatic brain injury. *Journal of Neurotrauma;* 35(2): 398-401. Doi: 10.1089/neu.2017.5172

Smelter, A., Rouchka, E., and Moseley, H. (2017). Detecting and accounting for multiple sources of positional variance in peak list registration analysis and spin system grouping. *Journal of Biomolecular NMR,* 68(4): 281-296.

Sternbach G. (2000). The Glasgow Coma Scale. *Journal of Emergency Medicine, 19*(1):67-71. Doi: 10.1016/s0736-4679(00)00182-7.

Szymanska E, Saccenti E, Smilde AK, Westerhuis JA. (2012). Double-check: validation of diagnostic statistics for PLS-DA models in metabolomics studies. *Metabolomics, 8*:S3-S16. doi: 10.1007/s11306-011-0330-3.

Veselkov K., Lindon J., Ebbels T., Crockford D., Volynkin V., et al. (2009). Recursive Segment-Wise Peak Alignment of Biological 1H NMR Spectra for Improved Metabolic Biomarker Recovery. *Analytical Chemistry, 81*(1): 56-66. Doi: 10.1021/ac8011544.

Wells, J. (2007). Sexual dimorphism of body composition. *Best Practice & Research Clinical Endocrinology & Metabolism, 21*(3): 415-430.

Wiklund, S., Johannsson, E., et al. (2008). Visualization of GC/TOF-MS-Based Metabolomics Data for Identification of Biochemically Interesting Compounds Using OPLS Class Models. *Analytical Chemistry, 80*(1): 115-122.

Wishart DS, Feunang YD, Marcu A, et al. (2018). HMBD 4.0- The human metabolome database for 2018. *Nucleic Acids Research*. Jan 4;*46*(D1): D609-17. 29140435. Doi: 10.1093/nar/gkx.1080.

Wu, G. (2009). Amino acids: metabolism, functions, and nutrition. *Amino Acids, 37*(1): 1-17.

Xia J, Wishart DS. (2010). MetPA: a web-based metabolomics tool for pathway analysis and visualization. *Bioinformatics, 26,* 2342-2344. Doi: 10.1093/bioinformatics/btq418.

Yun, Y., Liang, F., Deng, B., Lai, G., Goncalves, C., Lu, H., Yan, J., Huang, X., Yi, L., and Liang, Y. (2015). Informative metabolites identification by variable importance analysis based on random variable combination. *Metabolomics, 11*(6): 1539-1551.

CHAPTER 4: URINARY BIOMARKERS INDICATIVE OF RECOVERY FROM SPINAL CORD INJURY

INTRODUCTION

Spinal cord injuries (SCIs) can have long-term consequences for survivors and their families. In Canada, there are approximately 4,300 cases annually (Noonan et al., 2012) generating a significant economic burden to society. Rehabilitation represents the primary approach to promote long-term functional recovery after SCI, which can occur due to compression, incision, or contusion (Nas et al., 2015). Nevertheless, there is an urgent need to promote evidence-based rehabilitation therapies to optimize the potential for recovery. Currently, the American Spinal Cord Injury Association (ASIA) Impairment Scale serves as a measure of prognostic outcomes following SCI (Spiess et al., 2009). Additionally, computerized tomography and magnetic resonance imaging remain important imaging modalities for diagnosing and determining SCI severity (Metz et al., 2000); however, the large expenses and low throughput are major pitfalls associated with these technologies (Goeree et al., 2005; Krueger et al., 2013; Tator et al., 2016). Currently, there is no single "gold standard" prognostic biofluid marker to objectively determine if a patient has suffered an SCI and if so, the extent of physical and functional disability. This results in the demand for a high-throughput method that can rapidly diagnose SCI severity and optimize the potential for subsequent recovery.

The present study utilized metabolomics is a powerful approach to provide quantitative assessment of endogenous small molecules within biological fluids, such as urine (Nicholson et al., 2008). NMR has the most number of detectable (209) and unique (180) metabolites in human urine when compared to chromatography and mass

spectrometry techniques (Bouatra et al., 2013). Previous work from our laboratories has demonstrated that levels of metabolic compounds in bio-fluids can be used to effectively predict recovery following brain injury (Bykowski et al., submitted) and stress due to a natural disaster (Paxman et al., 2018). Similar changes in metabolism may also accompany SCI. Metabolic changes are accompanied by severe atrophy of denervated musculature, which leads to marked changes in body composition (Baumann & Spungen, 2000; Gorgey et al., 2013). Metabolic rates decline due to the loss of metabolically active lean body mass below the level of the lesion and a corresponding increase in adiposity (Giangregorio & McCartney, 2016). Accordingly, SCI diminishes whole body glucose transport, which is proportional to the reduction in muscle mass (Spungen et al., 2003) and can provoke disorders in carbohydrate and lipid metabolism (Baumann & Spungen, 1994). Following cervical SCI, disrupted glucose homeostasis may downregulate gene expression related to lipid oxidation and glycogen storage in skeletal muscle (Long et al., 2011). SCI is also accompanied by insidious delayed secondary tissue damage that can persist for months of years (Popovich et al., 2002; Donnelly & Popovich, 2007; Allan & Rothwell, 2003; Schwab & Bartholdi, 1996). Thus, knowledge of the biochemical pathways altered by SCI will inform about the natural changes following initial injury throughout the recovery process. A robust prognostic metabolic biomarker that reflects these changes would be valuable to improving SCI treatment and patient outcome.

Here, we identified a metabolic fingerprint in urine of SCI patients within 1 month of injury and at 6 months post-injury using nuclear magnetic resonance (NMR) spectroscopy. Using both univariate statistics and a machine learning multivariate approach, the present study determined (1) the metabolomics profile of SCI patients

initially and long-term after injury; (2) which metabolites lead to the observed differences; (3) which biochemical pathways contribute to these metabolomic alterations; (4) the accuracy of the identified metabolites as diagnostic SCI biomarkers; and (5) the prognostic value of the biomarker profiles in predicting personal clinical outcome.

METHODS

Patient Characteristics and Sample Collection

This study was embedded in a larger study entitled the UCAN Study, which follows patients with SCI, stroke, and traumatic brain injury throughout their recovery from one month to 6 months post-injury. Male patients with incomplete (n=4) and complete SCI (n=2) were recruited through the Foothills Medical Centre, University of Calgary (average age 55 +/- 20 years; Table 5). Pairs of fasting morning urine samples (acquired between 6am and 9am) were collected at two different time points: one month following injury and again at 6 months post-injury. Pairing the samples for this within-subject control study reduced the influence of confounding factors, such as diet and lifestyle, to raise the validity of the analysis. Urine samples were stored at -80°C until further processing.

We initially received seven pairs of urine samples, of which one was a female. To remove the effect of sex as a confounding factor, we removed this female from our multivariate/univariate statistical analysis. However, from a clinical standpoint, it is interesting to pursue the question of metabolic differences attributed to sex. For this reason, we retained the single female as a proof-of-principle approach. The present research was approved by the University of Calgary Conjoint Health Research Ethics Board (CHREB) and the University of Lethbridge Human Participant Research Committee in accordance to

the standards set forth by the Tri-Council Policy Statement: Ethical Conduct for Research Involving Humans.

Clinical Assessments

The Spinal Cord Independence Measure (SCIM) was completed for each patient at 1 month following injury and at 6 months follow-up. The SCIM, based on patient self-reports, includes the following areas of function: self-care (sub-score 0-20), respiration and sphincter management (0-40), and mobility (0-40) (Catz et al., 1997). The final score ranges from 0 (total dependence) to 100 (total independence). We also collected information on SCI type (complete or incomplete), ASIA score, sex, lesion location, co-morbidities, and age (see Table 5).

NMR Sample Preparation, Data Acquisition, and Processing

To control for pH and reduce positional noise within NMR-generated datasets (Gil et al., 2016; Smelter et al., 2017) urine samples were combined with buffer consisting of 4:1 ratio of dibasic potassium phosphate (K_2HPO_4) to monobasic potassium phosphate (KH_2PO_4) with a combined concentration of 0.625 M in dH_2O (pH 7.4), containing 3.75 mM NaN_3 anti-microbial agent and 0.375 M potassium fluoride (KF). For sample preparation, 400 µL of urine, 160 µL of buffer, and 40 µL of 0.02709 % weight/volume D_2O with trimethylsilyl propanoic acid (TSP) were pipetted into a microfuge tube. Each sample was centrifuged at 12,000 rpm for 5 min at 4°C to eliminate insoluble matter. 550 µL of supernatant was then transferred to an NMR tube, vortexed and loaded into the spectrometer.

A 700 MHz Bruker Avance III HD NMR spectrometer and a room-temperature TBO probe were used to acquire the NMR data. Three-dimensional and one-dimensional shimming experiments were conducted prior to NMR data acquisition to correct for any inhomogeneities in the static magnetic field. The data were acquired using a one-dimensional 1H Nuclear Overhauser Effect Spectroscopy experiment with water suppression, 128k points, and 128 scans. The data were processed using zero filling to 256k points, line broadening to 0.3 Hz, and automatic phase and baseline correction. The spectra were then imported into MATLAB where they underwent dynamic adaptive binning (Anderson et al., 2011) followed by manual inspection and correction of the bins, and recursive segment-wise peak alignment (Veselkov et al., 2009). In total, 505 bins were created for this analysis.

Metabolites were identified using a combination of resources: Chenomx 8.2 NMR Suite (Chenomx Inc., Edmonton, Alberta, Canada), the Human Metabolome Database (HMBD), (Wishart et al., 2018) and the Human Urine Metabolome (Bouatra et al., 2013) containing a list of NMR-derived urinary metabolites and their concentrations. Once the significant metabolites of interest were identified, they were used for metabolic pathway and visualization tests in MetaboanalystR (Chong et al., 2019). Topology analysis was also conducted based on the Kyoto Encyclopedia of Genes and Genomes (KEGG) and the HMBD libraries (Wishart et al., 2018; Xia et al., 2010) to identify modified metabolite pathways.

Statistical Analysis

Multivariate statistical analysis was used to determine if urinary metabolite profiles could be used to distinguish between the 1 month and 6 month-post-injury samples. Prior

to modelling, the data were normalized to the total metabolome, excluding the region corresponding to water, and pareto-scaled (Craig et al., 2006; Wiklund et al., 2008). Bins containing significant metabolites were sorted according to the F-ranked Variable Importance Analysis based on random Variable Combination (VIAVC) analysis (Yun et al., 2015) to identify significant metabolites based on the Receiver Operator Characteristic (ROC) and the subsequent Area-Under-the-Curve (AUC) analysis (Fawcett, 2005). It also employs a binary matrix resampling method as a robust method for random data sampling data, and all multivariate supervised models were double ten-fold cross-validated (Szymanska et al., 2012). Univariate statistical tests were also conducted; either a paired T-test or paired Wilcoxon-Mann-Whitney test was used in the case of parametric or non-parametric data, respectively.

An orthogonal projection to latent structures discriminant analysis (OPLS-DA) was conducted to visualize between-group separation as a function of within-group separation (Wiklund et al., 2008). This was complemented by a Principal Components Analysis (PCA), which demonstrated the degree of separation between the groups without the presence of an algorithm, as well as unsupervised hierarchical clustering illustrated by the accompanying heat map.

Pearson R correlations were computed between concentrations of urinary metabolites and SCIM patient scores (Table 6). Significance was based on the Bonferroni corrected *p*-value, obtained by dividing alpha<0.05 by the number of VIAVC F-ranked bins tested for this analysis (n=19), to obtain a rigorous set of clinically relevant metabolites (Goodpaster et al., 2010). The % difference for SCIM scores at the two different time points were computed as follows, based on the clinical data provided in Table 5:

$$\left(\frac{Post\ Recovery\ Score - Initial\ Score}{\left(\frac{Post\ Recovery\ Score + Inital\ Score}{2}\right)}\right) * 100\%$$

RESULTS

Metabolic Biomarkers Related to Functional Improvement

Clinical improvement was evident amongst the SCI patients at 6-months post-injury compared to the initial scores (1 month post-injury) for the SCIM. The average improvement was 10.8 +/- 10.4 points. To determine if initial metabolite concentrations can predict this functional improvement, Pearson R correlations, were computed between initial metabolite levels and % difference in SCIM scores, revealing three urinary metabolites with significant correlations: caffeine (R= -0.76, p<0.01), 3-hydroxymandelic acid (R= -0.85, p<0.001), and L-valine (R= 0.90, p<0.001; Table 6).

Metabolomic Profiles are Robust Predictors of Recovery Following SCI

The bins found to be significant by either the paired T-test/Wilcoxon Mann-Whitney test (n=44 bins) or the VIAVC best subset (n=3 bins) were used for subsequent analysis. The VIAVC best subset consisted of dopamine, Sumiki's acid, and caffeine. PCA and heat map illustration demonstrated a partial degree of unsupervised group separation (Figure 7A and B). The OPLS-DA plot (Figure 8) illustrates significant group separation at 1 month and 6 months (R^2Y=0.991, p<0.05; Q^2=0.808, p<0.01). This supervised model indicated a change in the metabolic profiles over the course of patient recovery in repeated samples. Metabolites that contributed the most to the group separation are shown in Appendix 3, ranked in order of significance according to the paired T-test/Wilcoxon Mann-Whitney test

A ROC curve was also generated for the male SCI patients. An area-under-the-curve equal to 1 was achieved, with a 95% confidence interval of 1-1 (Figure 9). The predictive accuracy for this curve when 2 bins re included was 92% and when all 3 bins were included was 100%. This analysis was based on the 3 bins significant by the VIAVC best-subset.

Pathway topology analysis (Figure 10) illustrated the impact of urinary metabolites on changes to the SCI patients' metabolic profiles, presented in increasing order of impact. Metabolic pathways significantly affected amongst the male patients were purine metabolism ($p<0.01$), followed by tyrosine metabolism ($p<0.01$). Pathway analysis was based on bins significant by the VIAVC best subset, paired T-test, and Wilcoxon-Mann-Whitney test.

To determine if the change in metabolite concentration served as a proxy measure of the degree of recovery, Pearson R correlations were also computed between the difference in metabolite concentrations and % difference in SCIM scores, revealing significant correlations for L-valine (R= -0.64, $p<0.05$) and N-methylhydantoin (R= -0.90, $p<0.001$; Table 6).

To investigate potential sex differences in biomarkers, the only available single female patient was included in the correlation analysis (Table 6). The inclusion of the female did not affect the correlation value for 3-hydroxymandelic acid and L-valine (delta to % difference). The absolute value of all other correlations was decreased when the female was included in the correlation, yet still retained a strong correlation.

DISCUSSION

Here we show that metabolomic profiles in urine change throughout recovery following SCI, and positively relate to SCIM scores. The most significant change occurred in metabolites that were part of the VIAVC best subset (dopamine, Sumiki's acid, and caffeine), suggesting that these metabolites present the most robust indicators of successful recovery in SCI. Their value as metabolic biomarkers of SCI severity was confirmed by a predictive accuracy of 100%. The main metabolic pathways altered by recovery following SCI included purine metabolism and tyrosine metabolism. Moreover, we showed that the degree of functional recovery is best predicted by caffeine, 3-hydroxymandelic acid, and L-valine. N-methylhydantoin and L-valine. Thus, a metabolomics approach combined with machine learning is able to provide clinically accessible biomarkers with high prognostic potential for SCI recovery.

Pathway Analysis

Purine metabolism presented as the most significantly affected pathway in SCI recovery. This follows from our previous work (Bykowski et al., submitted), which indicated that urinary purines and their derivatives may play a role in pathology arising from traumatic brain injury. Purines are known for their neuroprotective roles in the nervous system, with the ability to mitigate inflammatory responses (Jackson et al., 2016). Although it is well known that purine metabolism is disrupted in the wake of head trauma (Clark et al., 1997; Cronstein, 1994), there is less evidence for their dysregulation following SCI. However, a recent study in which hypoxia was induced in a SCI rat model led to an increase in extracellular purine derivatives, specifically adenosine and inosine (Takahashi et al., 2010). Inosine, which is implicated within the purine pathway in our study, was also

shown to be present at ten-fold higher concentrations than adenosine. The excretion of this purine in the urine reflects its presence within the body as an endogenous neuroprotective agent against inflammation. Furthermore, levels of purine derivatives were also shown to vary with intracellular calcium concentration within the spinal cord, whereby increased calcium activity promoted purine release (Liu et al., 2006). Increased osteoclast activity associated with bone fracture following SCI may a play a role in calcium fluctuations which influence purine release.

An alternative mechanism for purine release is associated with the inflammatory response following SCI, which is mediated by microglia. As the main active immune defense in the central nervous system, microglia respond to sites of injury via release of ATP (a purine derivative) from the injured area (Dou et al., 2012). This mechanism may also explain dysregulation of the purine pathway in the present study. Thus, urinary metabolites implicated in purine metabolism may be indicative of their neuroprotective action or their role in initiating immune system activation.

Evidence for tyrosine metabolites in the urine suggests low cellular uptake and excessive excretion of catecholamines produced along this pathway, including dopamine which was part of the VIAVC best subset. Although there have been few studies relating the role of dopamine to spinal cord functioning in humans, evidence in model systems such as the rodents, lamprey and *C. elegans* showed sources of dopamine in the spinal cord which modulate movement patterns (Sharples et al., 2014). Although this area of study is in its infancy, extrapolation of this finding to humans is plausible. The loss of dopaminergic as well as noradrenergic inputs to the spinal cord following SCI may contribute to the loss of rhythmic and autonomic movements (Han et al., 2007; Acton et al., 2018). Additionally,

it was shown that sources of dopamine in the dorsal horn of the rat spinal cord modulate the bladder reflex, and underlies micturition following SCI (Hou et al., 2016). Thus, spinally derived dopamine in animal models increases the possibility of a similar mechanism in human patients.

Relationship Between Metabolite Profiles and SCIM

Caffeine presented as a clinically significant metabolite, with a negative correlation to patient SCIM scores. It has been shown that SCI patients experience a reduced metabolic rate as a result of skeletal muscle atrophy and lower levels of activity (Graham-Paulson et al., 2017). Delayed caffeine absorption was found to be greater for tetraplegic than for paraplegic SCI patients, owing to a greater loss of skeletal muscle and subsequent reduction in resting metabolic rate (Graham-Paulson et al., 2017). In tetraplegia, gastrointestinal emptying times are prolonged, with effects experienced as soon as three days after sustaining an SCI injury (Qualls-creekmore et al., 2009). Therefore, caffeine likely serves as a biomarker of metabolic slowing, and a higher risk of adiposity associated with a reduced decreased metabolic rate due to the loss of metabolically active lean body mass. Clinical intervention requires ways to boost the metabolic state of patients to prevent this downstream effect. With rehabilitation and an increase in patient mobility, increase muscle strength may out-weigh atrophy, and with improved metabolism and absorption of nutrients, the ensuing decrease in urinary caffeine levels may indicates recovery.

In correlation with functional recovery, 3-hydroxymandelic acid revealed a negative relationship to improved recovery, as its levels decreased. In a previous study, it was found that elevated excretion of 3-hydroxymandelic is associated with tyrosine intake (Fell et al., 1979). Excretion of this catecholamine metabolite is additional evidence

supporting dysregulation of the tyrosine metabolic pathway as indicated in the pathway analysis for this study. This suggests a corresponding decrease in excretion of tyrosine derivatives as recovery progresses, as inferred from the negative correlation.

Lastly, L-valine, an essential amino acid, L-valine is a building block for muscle tissue, presented with a positive correlation to % difference measurements at the SCIM. Muscle atrophy is a cardinal feature of SCI (Giangregorio & McCartney, 2016); it is likely that excretion of L-valine in the urine is indicative of muscle breakdown following SCI, and overall liberation of its constituent amino acids. The fact that an initial increase in its levels is associated with recovery likely underlies the body's subsequent demands for protein building blocks to restore muscle tissue.

This study also aimed to determine if the change in metabolite concentration could serve as a proxy measure of the degree of recovery. L-valine again presented as a significant metabolite for this comparison, but with a negative correlation. Neuronal death following SCI is triggered by an elevation in intracellular calcium levels (Tymianski et al., 1993), and L-valine is postulated to be a part of this pathway (Simpson et al., 1990). As an excitatory, branched chain amino acid implicated in the cascade that leads to calcium-induced neuronal cell death, it follows that a decrease in its levels is associated with an improvement in patient recovery.

A negative correlation was also observed for N-methylhydantoin levels compared to the % difference SCIM scores. N-methylhydantoin is a by-product of the degradation of creatinine by bacteria (Seifter, 2014). Creatinine is a breakdown product of creatine phosphate in the muscle, and therefore indicates muscle atrophy. Unlike most polar substances, creatinine is not reabsorbed by the kidneys, and is filtered out to be excreted in

the urine (Levey et al., 1998). Decreased levels of N-methylhydantoin post-injury may indicate a decrease in skeletal muscle atrophy, via reduced creatinine levels.

Metabolite Profiles and Sex Differences

There were differences observed when the female was included for correlation to clinical SCIM outcomes. With the exception of 3-hydroxymandelic acid and L-valine, all of the metabolites listed within Table 6 decreased in significance. This indicates that 3-hydroxymandelic acid and L-valine are implicated in processes that are not sex-dependent, and therefore have potential as sex-independent biomarkers. As a catecholamine metabolite derived from tyrosine, it can be inferred that 3-hydroxymandelic acid implicated in dysregulation of the tyrosine pathway is of similar relevance to both sexes; however, there is a paucity of literature to reinforce this claim. With respect to L-valine's role as a metabolic indicator of muscular atrophy, this condition afflicts males and females, however disproportionately. The higher average muscle mass of males compared to females (Wells, 2007) would predict differences in levels of this metabolite. Therefore, the comparable levels provides an unexpected yet intriguing finding that muscle atrophy is significant in both male and female SCI patients.

LIMITATIONS

Although the sample size was limited, the pairing of spinal cord injured subjects within this pilot study ensures that the regulation of metabolite concentrations is significant across the initial and post-injury groups. Identification of unique urinary metabolic signatures is validated via this paired analysis, which increases statistical power. Another limitation to this pilot study is that patients' diets were not controlled while in hospital or

following release. The effects of this potential confound are minimized by the fact that two urine samples were collected from each patient, and that significant changes to metabolite levels reflect a global increase or decrease across *paired* urine samples.

CONCLUSION

The identified biomarkers and metabolic pathways may represent attractive therapeutic targets and have potential for clinical translation. Metabolites with statistically significant correlations to SCIM outcomes represent a window of opportunity for neurotherapeutic intervention amongst spinal cord injured patients. Caffeine, 3-hydroxymandelic acid, and L-valine may have the ability to predict recovery outcomes, whereas N-methylhydantoin and L-valine have potential to serve as measures of the change in metabolic profiles over time.

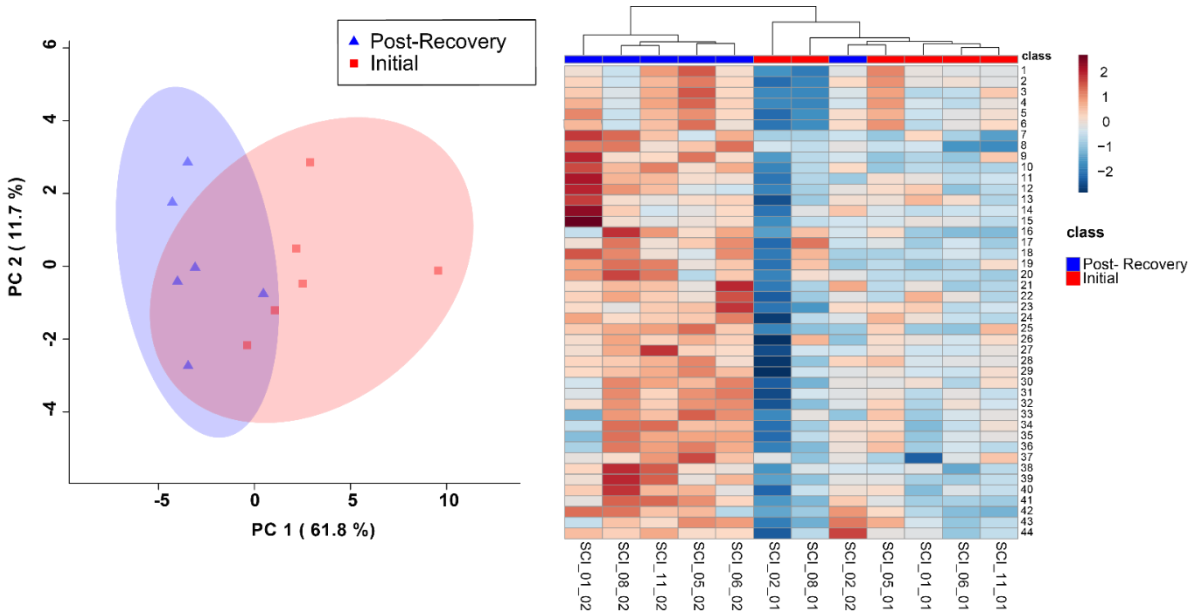

Figure 7. Principal Components Analysis (PCA) (left) and heat maps (right) representing unsupervised separation and hierarchical clustering analysis of male SCI patients' metabolic profiles. The legend indicates the class label: initially initially after SCI and 6 months post-recovery. The heat maps illustrate up-regulation versus down-regulation of metabolites significant by the VIAVC best subset (n=3 bins) and paired T-test/Wilcoxon Mann-Whitney Test (n=44 bins). Appendix 3 provides the name of the metabolite corresponding to each of the numbers provided to the right of the heat map.

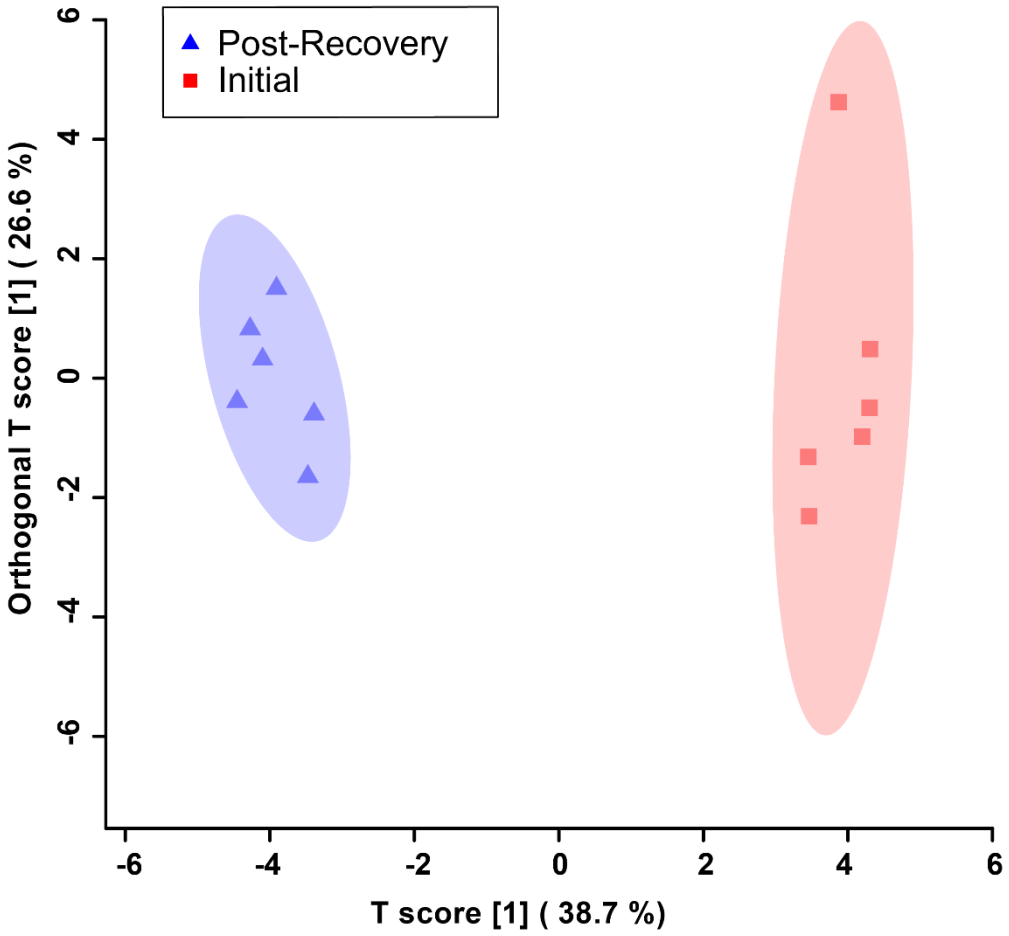

Figure 8. Orthogonal Projections to Latent Structures Discriminant Analysis (OPLS-DA) score plot showing supervised separation between male SCI patients initially (red/squares) and 6 months post-recovery (indigo/triangles). This analysis was carried out using a list of urinary metabolites found to be statistically significant by either the paired T-test/Mann-Whitney or VIAVC testing. The 95% confidence interval is indicated by the shaded ellipses. The x- and y-axis show the predictive (between group) and orthogonal (within group) variation, respectively. The following are the cross-validation and permutation measures for the OPLS-DA figures: $R^2Y=0.991$, $p=0.011$; $Q^2=0.808$, $p=0.002$.

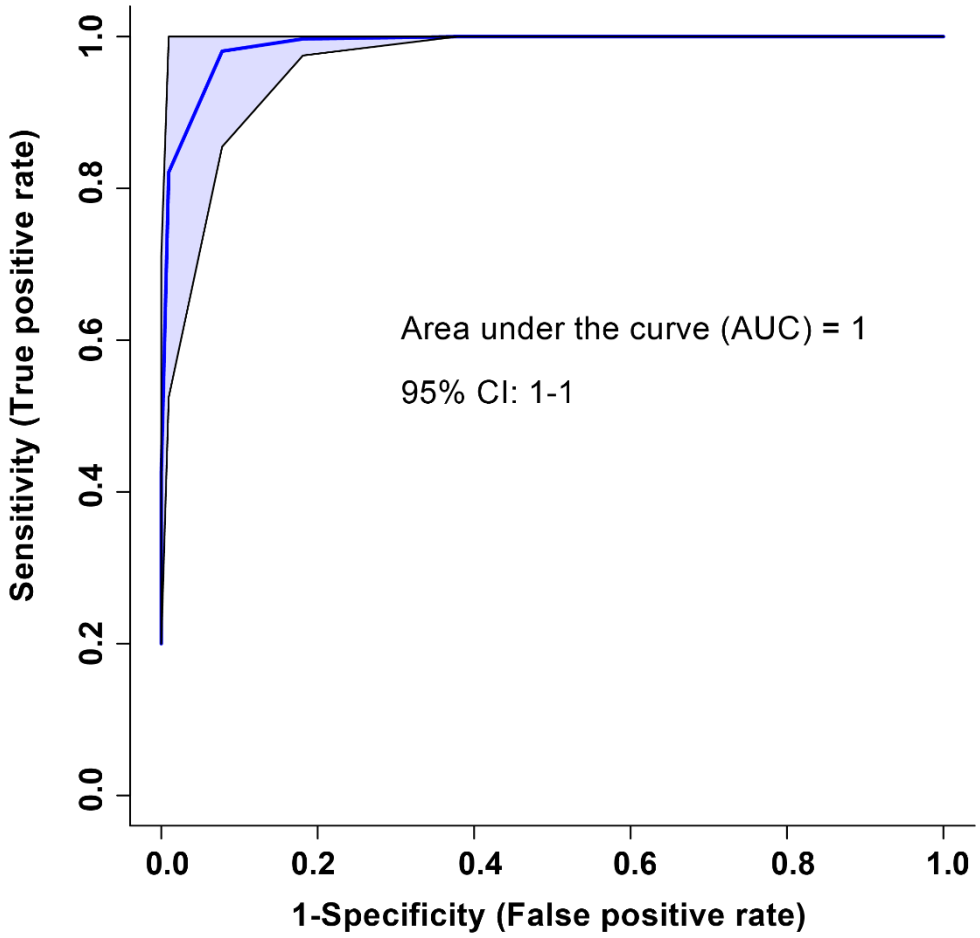

Figure 9. The Receiver Operator Characteristic (ROC) curve represents a high sensitivity and specificity of the group separation between initial and post-recovery samples. The corresponding area under the curve (AUC) and confidence interval are indicated on each figure. The ROC curve was constructed using the metabolites determined to be significantly altered based on the VIAVC best subset, which corresponds to 3 bins.

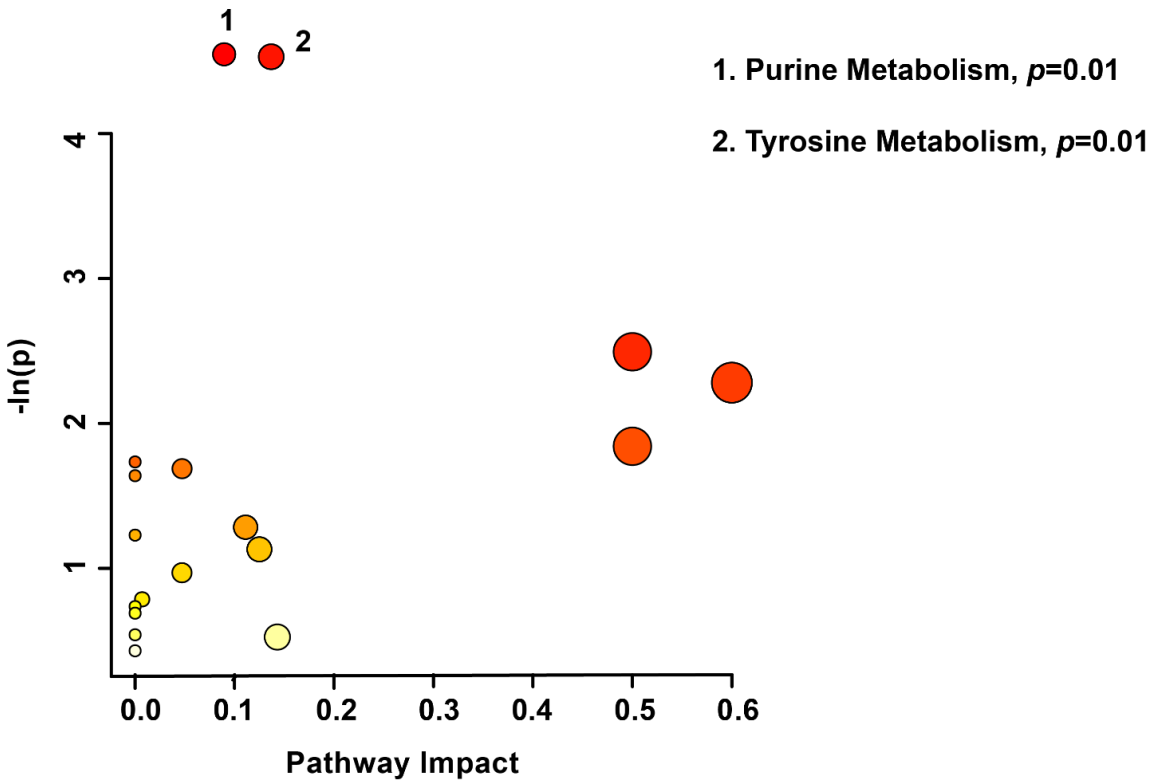

Figure 10. Metabolic pathway analysis conducted based on spectral bins that are significant by either the VIAVC best subset or the paired T-test/Wilcoxon Mann-Whitney test. A higher value on the y-axis indicates a lower *p*-value for the pathway and the x-axis provides the pathway impact, which is a measure of how affected each pathway is by the metabolites identified as significantly altered. Only pathways with a *p*-value less than 0.05 are labeled.

Table 5. Patient characteristics table indicating the sex, age, lesion location, co-morbidities, and SCI type, as well as both the initial and post-recovery SCIM scores.

Patient Code	SCI Type	ASIA Score	Sex	Lesion Location	Co-Morbidities	Age	Pre SCIM	Post SCIM
SCI_01	Incomplete	D	Male	Central Cord		80	84	89
SCI_02	Complete	A	Male	T7		29	70	70
SCI_05	Incomplete	D	Male	C4		38	72	92
SCI_06	Complete	A	Male	T6		50	49	66
SCI_07	Complete	A	Female	C7		16	36	44
SCI_08	Incomplete	D	Male	C6-C7		59	100	100
SCI_11	Incomplete	B	Male	C2-C4	UTI, C2-C3 spinal artery infarct	73	77	100

Table 6. Pearson R correlation values and associated p-values displayed for males only and with the female patient included for 'initial to % difference' and 'delta to % difference' comparisons. P-values with a star indicates significance based on the Bonferroni corrected threshold (alpha=0.0026).

Metabolite	Males only (n=6)		Female subject included (n=7)	
Initial to % Diff SCIM	Pearson R	*p*-value	Pearson R	*p*-value
Caffeine	-0.76	0.0039	-0.69	0.006
3-hydroxymandelic acid	-0.85	0.00045*	-0.85	0.00013*
L-Valine	0.90	0.000066*	0.84	0.00015*
Delta to % Diff SCIM				
L-Valine	-0.64	0.03	-0.65	0.012
N-methylhydantoin	-0.90	0.00008*	-0.85	0.0001*

REFERENCES

Acton, D., Broadhead, M.J., & Miles, G.B. (2018). Modulation of spinal motor networks by astrocyte-derived adenosine is dependent on D1-like dopamine receptor signaling. *Journal of Neurophysiology, 120*(3): 998-1009. Doi: 10.1152/jn.00783.2017.

Anderson, P., Mahle, D., Doom, T., Reo, N., DelRaso, N., & Raymer M. (2011). Dynamic adaptive binning: an improved quantification technique for NMR spectroscopic data. *Metabolomics, 7*(2): 179-190. https://link.springer.com/article/10.1007/s11306-010-0242-7 Accessed January 15, 2020.

Allan, S. & Rothwell, N. (2003). Inflammation in central nervous system injury. *Philosophical Transactions of the Royal Society B Biological Sciences, 358*(1438): 1669-1677.

Baumann, W., & Spungen, A. (1994). Disorders of carbohydrate and lipid metabolism in veterans with paraplegia or quadriplegia: a model of premature aging. *Metabolism, 43*(6): 749-756.

Baumann, W., & Spungen, A. (2000). Metabolic changes in persons after spinal cord injury. *Physical Medicine and Rehabilitation Clinics of North America, 11*(1): 109-140.

Bouatra, S., Aziat, F., Mandal, R., Guo, A.C., Wilson, M.R., Knox, C., & Wishart, D.S. (2013). The human urine metabolome. *PLOS ONE, 8*(9), 1-28.

Bykowski, E., Petersson, J., Dukelow, S., Ho, C., Debert, C., Montina, T., & Metz G.A.S. Urinary The relationship between Urinary Metabolomic Signatures and Injury Severity in Males and Females with Traumatic Brain Injury. *Journal of Head Trauma Rehabilitation,* submitted.

Catz, A., Itzkovich, M., Agranov, E., Ring, H., and Tamir, A. (1997). SCIM- spinal cord independence measure: a new disability scale for patients with spinal cord lesions. *Spinal Cord, 35*: 850-56.

Chong, J., Wishart, D.S., & Xia J. (2019). Using metaboAnalyst 4.0 for comprehensive and integrative metabolomics data analysis. *Current Protocols in Bioinformatics, 68,* e86 (128 pages). doi: 10.1093/nar/gky310.

Clark, R., Carcillo, J., Kochanek, P, et al. (1997). Cerebrospinal fluid adenosine concentration and uncoupling of cerebral blood flow and oxidative metabolism after severe head injury in humans. *Neurosurgery, 41*(6): 1284-1292. Doi: 10.1097/0000613-199712000-00010

Craig, A., Cloarec, O., Holmes, E., Nicholson, J.K., & Lindon, J.C. (2006). Scaling and normalization effects in NMR spectroscopic metabonomic data sets. *Analytical Chemistry*, 78: 2262-2267.

Cronstein, B. (1994). Adenosine, an endogenous anti-inflammatory agent. *Journal of Applied Physiology, 76*(1): 5-13. Doi: 10.1152/jappl.1994.76.1.5

Donnelly, D., & Popovich, P. (2007). Inflammation and its role in neuroprotection, axonal regeneration and functional recovery after spinal cord injury. *Experimental Neurology, 209*(2): 378-388.

Dou, Y., Wu, H.J., Li, H.Q., Qin, S., Wang, Y.E., Li, J.,…Duan, S. (2012). Microglial migration mediated by ATP-induced ATP release from lysosomes. *Cell Research,* 22(6): 1022-1033.

Fawcett, T. (2005). An introduction to ROC analysis. *Pattern Recognition Letters*, *72*(8):861-874. https://doi.org/10.1016/j.patrec.2005.10.010 Accessed January 17, 2020.

Fell, V., Greenway, A.M., & Hoskins, J.A. (1979). The metabolism of L-*m*-tyrosine in man. *Biochemical Medicine*, 22(2): 46-55. Doi: 10.1016/0006-2944(79)90010-3.

Giangregorio, L., & McCartney, N. (2016). Bone loss and muscle atrophy in spinal cord injury: epidemiology, fracture prediction, and rehabilitation strategies. *The Journal of Spinal Cord Medicine, 29*(5): 489-500.

Gil, R., Lehmann, R., Schmitt-Kopplin, P., & Heinzmann, S. (2016). (1)H NMR-based metabolite profiling workflow to reduce inter-sample chemical shift variations in urine samples for improved biomarker discovery. *Analytical and Bioanalytical Chemistry*, *408*(17): 4683-4691.

Goeree, R., Blackhouse, G., Petrovic, R., & Salama, S. (2005). Cost of stroke in Canada: a 1-year prospective study. *Journal of Medical Economics, 8*(4): 147-167. DOI: 10.3111/200508147167

Goodpaster, A., Romick-Rosendale, L., & Kennedy, M. (2010). Statistical significance analysis of nuclear magnetic resonance-based metabonomics data. *Analytical Biochemistry*, *401*: 134-143.

Gorgey, A., Dolbow, D., Dolbow, J., Khalil, R., Castillo, C., & Gater, D. (2013). Effects of spinal cord injury on body composition and metabolic profile. *Journal of Spinal Cord Medicine, 37*(6): 693-702.

Graham-Paulson, T., Paulson, T., Perret, C., Tolfrey, K., Cordery, P., & Goosey-Tolfrey, V. (2017). Spinal cord injury level influences acute plasma caffeine responses. *Medicine & Science in Sports & Exercise*, *49*(2): 363-370.

Han, P., Nakanishi, S.T., Tran, M.A., & Whelan, P. (2007). Dopaminergic modulation of spinal neuronal excitability. *The Journal of Neuroscience, 27*(48): 13192-13204. https://doi.org/10.1523/JNEUROSCI.1279-07.2007.

Hou, S., Carson, D.M., Wu, D., Klaw, M.C., Houle, J.D., & Tom, V.J. (2016). Dopamine is produced in the rat spinal cord and regulates micturition reflex after spinal cord injury. *Experimental Neurology*, 285(Pt. B): 136-146. Doi: 10.1016/j.expneurol.2015.12.001

Jackson, E., Boison, D., & Kochanek, P. (2016). Purines: forgotten mediators in traumatic brain injury. *Journal of Neurochemistry*, *137*(2): 142-153.

Krueger, H., Noonan, V., Trenaman, L., Joshi, P., & Rivers, C. (2013). The economic burden of traumatic spinal cord injury in Canada. *Chronic Diseases and Injuries in Canada, 33*(3): 113-122.

Levey, A., Perrone, R., & Madias, N. (1988). Serum creatinine and renal function. *Annual Review of Medicine, 39*: 465-490.

Liu, G.J., Kalous, A., Werry, E., & Bennett, M. (2006). Purine Release from Spinal Cord Microglia after Elevation of Calcium by Glutamate. *Molecular Pharmacology*, 70(3): 851-859.

Long, Y., Kostovski, E., Boon, H., Hjeltnes, N., Krook, A., & Widegren, U. (2011). Differential expression of metabolic genes essential for glucose and lipid metabolism in skeletal muscle from spinal cord injured subjects. *Journal of Applied Physiology, 110*(5): 1204-1210.

Metz, G.A.S., Curt, A., van de Meent, H., Klusman, I., Schwab, M.E., & Dietz V. (2000). Validation of the weight-drop contusion model in rats: a comparative study of human spinal cord injury. *Journal of Neurotrauma*, 17(1):1-17.

Nas, K., Yazmalar, L., Sah, V., Ayudin, A., & Ones, K. (2015). Rehabilitation of spinal cord injuries. *World Journal of Orthopedics, 18*(6): 8-16. Doi: 10.5312/wjo.v6.il.8

Nicholson, J.K., & Lindon, J.C. (2008). Systems biology: metabonomics. *Nature, 455*(7216), 1054–1066.

Noonan, V.K., Fingas, M., Farry, A., Baxter, D., Singh, A., Fehlings, M.G., & Dvorak, M.F. (2012). Incidence and prevalence of spinal cord injury in Canada: A National Perspective. *Neuroepidemiology, 38*(4): 219-226.

Paxman, E.J., Boora, N.S., Kiss, D., Laplante, D.P., King, S., Montina, T., & Metz, G.A.S. (2018). Prenatal maternal stress from a natural disaster alters urinary metabolomic profiles in project ice storm participants. *Scientific Reports, 8*(1): 12932.

Popovich, P., Guan, Z., McGaughy, V., Fisher, L., Hickey, W., & Basso, D. (2002). The neuropathological and behavioral consequences of intraspinal microglial/macrophage activation. *Journal of Neuropathology and Experimental Neurology, 61*(7): 623-633.

Qualls-creekmore, E., Tong., M., & Holmes, G. (2009). Time-course of recovery of gastric emptying and motility in rats with experimental spinal cord injury. *Journal of Neurogastroenterology and Motility, 22*(1): 62-e28.

Seifter, J. (2014). Urinary creatinine-splitting bacteria after ileal-loop diversion causing underestimate of glomerular filtration rate. *The American Journal of Medicine: Clinical Communication to the Editor, 27*(12).

Schwab, M.E.., & Bartholdi, D. (1996). Degeneration and regeneration of axons in the lesioned spinal cord. (1996). *Physiological Reviews*, 76(2): 916-70.

Sharples, S., Koblinger, K., Humphreys, J., & Whelan, P. (2014). Dopamine: a parallel pathway for the modulation of spinal locomotor networks. *Front Neural Circuits*, 16(8): 55. Doi: 10.3389/fncir.2014.00055.

Simpson, R., Robertson, C., & Goodman, C. (1990). Spinal cord ischemia-induced elevation of amino acids: extracellular measurement with microdialysis. *Neurochemical Research, 15*(6): 635-639.

Smelter, A., Rouchka, E., & Moseley, H. (2017). Detecting and accounting for multiple sources of positional variance in peak list registration analysis and spin system grouping. *Journal of Biomolecular NMR, 68*(4): 281-296.

Spiess, M.R., Muller, R.M., Rupp, R., Schuld, C., EM-SCI Study Group, van Hedel, H.J. (2009). Conversion in ASIA impairment scale during the first year after traumatic spinal cord injury. *Journal of Neurotrauma, 26*(13): 2027-36. Doi: 10.1089/neu.2008.0760.

Spungen, A.M., Adkins, R.H., Stewart, C.A., Wang, J., Pierson, R.N. Jr., Waters, R.L., & Baumann, W.A. (2003). Factors influencing body composition in persons with spinal cord injury: a cross-sectional study. *Journal of Applied Physiology, 95*(6): 2398-407. Doi:10.1152/japplphysiol.00729.2002.

Szymanska, E., Saccenti, E., Smilde, A.K., & Westerhuis, J.A. (2012). Double-check: validation of diagnostic statistics for PLS-DA models in metabolomics studies. *Metabolomics, 8*:S3-S16. doi: 10.1007/s11306-011-0330-3.

Takahashi, T., Osguguro, K., Ohta, T., & Ito S. Adenosine and inosine release during hypoxia in the isolated spinal cord of neonatal rats. (2010). *British Journal of Pharmacology, 16*(1): 1806-1816.

Tator, C., Logan, L., and Stringer, K. (2016). Action needed to address the rising cost of concussions in Canada. Published in *The Ottawa Sun.* Retrieved September 30, 2018.

Tymianski, M., Charlton, M.P., Carlen, P.L., & Tator, C.H. (1993). Source specificity of early calcium neurotoxicity in cultured embryonic spinal neurons. *Journal of Neuroscience, 13*(5): 2085-2104.

Veselkov, K., Lindon, J., Ebbels, T., Crockford, D., Volynkin V.V., Holmes, E.,….Nicholson, J.K. (2009). Recursive segment-wise peak alignment of biological 1H NMR spectra for improved metabolic biomarker recovery. *Analytical Chemistry, 81*(1): 56-66. Doi: 10.1021/ac8011544.

Wells, J. (2007). Sexual dimorphism of body composition. Best Practice & Research Clinical *Endocrinology & Metabolism, 21*(3): 415-430.

Wiklund, S., Johansson, E., Sjostrom, L., Mellerowicz, E.J., Edlund, U., Shockcor, J.P.,…Trygg, J. (2008). Visualization of GC/TOF-MS-based metabolomics data for identification of biochemically interesting compounds using OPLS class models. *Analytical Chemistry, 80*(1): 115-122.

Wishart, D.S., Feunang, Y.D., Marcu, A., Guo AC, Liang K, Vazquez-Fresno, R.,…Scalbert, A. (2018). HMBD 4.0- The human metabolome database for 2018. *Nucleic Acids Res, 4*;*46*(D1): D608-17. 29140435. Doi: 10.1093/nar/gkx.1080.

Xia, J., & Wishart, D.S. (2010). MetPA: a web-based metabolomics tool for pathway analysis and visualization. *Bioinformatics, 26*, 2342-2344. Doi: 10.1093/bioinformatics/btq418.

Yun, Y., Liang, F., Deng, B., Lai, G., Goncalves, C., Lu, H.,…Liang, Y. (2015). Informative metabolites identification by variable importance analysis based on random variable combination. *Metabolomics, 11*(6): 1539-1551.

CHAPTER 5: IDENTIFICATION OF SERUM METABOLITES AS PROGNOSTIC BIOMARKERS IN SPINAL CORD INJURY

INTRODUCTION

Spinal cord injury (SCI) is a devastating neurological condition that occurs when some or all of the spinal pathways are transected or crushed leading to disrupted motor, sensory, and autonomic function. Depending on the level of injury, a SCI patient will experience loss of functional independence to varying degrees, and lesion extent is the main determinant of recovery (Kirshblum et al., 2011; Nas et al., 2015). Although there is greater potential for recovery following incomplete compared to complete injury (Metz et al., 2000; Marino et al., 2016), recovery is limited by the presence of inhibitory growth factors controlling nervous system myelination (Schwab et al., 1996). Effective rehabilitation therapy is crucial to regain/compensate for reduced motor function and to minimize the secondary damage that occurs in the weeks to months following injury (Allan & Rothwell, 2003). The current methods for diagnosing and prognosticating SCI outcomes are challenged by a lack of objective, cost-effective approaches, creating growing demand for a high-throughput method for rapid diagnosis and prediction of outcomes.

SCI patients endure an array of significant metabolic disturbances, including glucose intolerance, insulin resistance, and decreased lean body mass (Spungen et al., 2003; Gorgey et al., 2014). A key pathological hallmark evident in the weeks to months following a SCI is the increase in adipose tissue, particularly surrounding the abdominal regions (Gorgey et al., 2015). Bone marrow adipose tissue accumulation shows an inverse relationship with bone mineral density, which underlies the susceptibility to osteoporosis that afflicts SCI patients (Tan et al., 2013). Furthermore, increased adiposity amongst SCI

patients adversely affects the liver. Liver adiposity has been shown to be positively related to inflammation, and the release of inflammatory mediators TNF-alpha and interleukin-6, which propagate metabolic stress (Park et al., 2010). In addition, when autonomic innervation to the liver is disrupted following SCI, this raises the risk of adiposity and glucose intolerance as the liver is a key regulator of glucose homeostasis (Mizuno & Ueno, 2017). The latter can potentially increase the risk of disorders in carbohydrate and lipid metabolism in SCI patients (Baumann & Spungen, 1994).

Blood as a biofluid is especially amenable to detecting glucose intolerance since by-products of the liver's metabolism directly enter the bloodstream via the hepatic portal vein. Nuclear magnetic resonance (NMR) spectroscopy is capable of detecting 49 different compounds in blood serum, 20 of which are unique to NMR and cannot be detected by gas chromatography-mass spectrometry (Psychogios et al., 2011). An informative biomarker that indicates when such pathologies arise could be used to inform clinical practice as to what therapies should be implemented to target these pathologies in the acute stages of SCI.

The present longitudinal study used nuclear magnetic resonance (NMR) spectroscopy and both univariate statistics and multivariate machine learning to identify a metabolic fingerprint in serum of SCI patients. The design of the study assessed a metabolomics profile of SCI patients initially following injury and at post-recovery to determine which metabolites lead to the observed differences and which biochemical pathways contribute to these metabolomic alterations. The findings demonstrate the potential for NMR spectroscopy to identify metabolites as diagnostic and predictive SCI biomarkers.

MATERIALS AND METHODS

Patient Characteristics and Sample Collection

This research was part of the UCAN Study at the University of Calgary, which follows SCI patients throughout their recovery from initial injury to 6 months post-injury. Male patients with incomplete (n=5) and complete SCI (n=2) were recruited through the Foothills Medical Centre, University of Calgary (average age 54 +/- 18 years; Table 7). Pairs of fasting morning blood samples (acquired between 6am and 9am) were collected at two different time points, within 21-90 days following SCI and again at 6 months post-injury. The pairwise analyses in this within-subject control study reduces the impact of confounding individual lifestyle factors. We initially received seven pairs of blood samples from males and one pair from a female SCI patient. Because it is interesting to pursue the question of metabolic differences attributed to sex from a clinical standpoint, we retained the single female for discussion of metabolic pathways.

The present protocols were reviewed and approved by the University of Calgary Conjoint Health Research Ethics Board (CHREB) and the University of Lethbridge Human Participant Research Committee in accordance to the standards set forth by the Tri-Council Policy Statement: Ethical Conduct for Research Involving Humans.

Clinical Assessment

The Spinal Cord Independence Measure (SCIM) was completed for each patient at 1 week and 6 months following SCI. The SCIM, based on patient self-reports, includes the following areas of function: self-care (subscore 0-20), respiration and sphincter management (0-40), and mobility (0-40) (Catz et al., 1997), where 0 indicates high disability and 100 indicates low disability. Patients were also evaluated using the American

Spinal Cord Association (ASIA) Impairment Scale to determine the severity of the SCI and whether it was complete or incomplete (Table 7).

NMR Sample Preparation, Data Acquisition, and Processing

Whole blood samples were centrifuged to isolate the serum and stored at -80℃. K_2HPO_4 buffer (4:1) was prepared with a combined concentration of 0.625 M in dH_2O (pH 7.4), containing 3.75 mM NaN_3 anti-microbial agent and 0.375M KF (Gil et al., 2016; Smelter et al., 2017). Amicon 0.5 mL 3 kDa centrifuge filters were used to isolate water soluble components from the protein-rich component. Reverse pipetting was used to add 300 µL of metabolomics buffer into each of the Amicon centrifuge filters. Then, 200 µL of serum was pipetted and centrifuged at 14,000 g for 30 min at 4℃. For NMR sample preparation, 380 µL of serum filtrate, 100 µL of phosphate buffer and 120 µL of 0.02709 % weight/volume D_2O with TSP were centrifuged at 12,000 rpm for 5 min at 4℃. 550 µL of buffered sample was transferred to an NMR tube to be loaded into the spectrometer. Samples were vortexed prior to loading to ensure that the serum was mixed prior to spectral acquisition.

A 700 MHz Bruker Avance III HD NMR spectrometer and a room-temperature TBO probe were used with three-dimensional and one-dimensional shimming experiments prior to NMR data acquisition. The data were acquired using a one-dimensional ^1H Nuclear Overhauser Effect Spectroscopy experiment with water suppression, 128k points, and 128 scans. The data were processed using zero filling to 256k points, line broadening to 0.3 Hz, and automatic phase and baseline correction. The spectra obtained from the NMR experiment were then imported into MATLAB where they underwent dynamic adaptive binning (Anderson et al., 2011), followed by manual inspection and correction of the bins,

and recursive segment-wise peak alignment (Veselkov et al., 2009; Kiss et al., 2016; Paxman et al., 2018). In total, 287 bins were created for this analysis.

Metabolites were identified using a combination of resources: Chenomx 8.2 NMR Suite (Chenomx Inc., Edmonton, Alberta, Canada), the Human Metabolome Database (HMBD), (Wishart et al., 2018), and the Human Serum Metabolome (Bouatra et al., 2013) containing a list of NMR-derived urinary metabolites and their concentrations. Once the significant metabolites of interest were identified, they were used for metabolic pathway and visualization tests in MetaboanalystR (Chong et al., 2019). Topology analysis was also conducted based on the Kyoto Encyclopedia of Genes and Genomes (KEGG) and the HMBD libraries (Wishart et al., 2018; Xia et al., 2010) to identify modified metabolite pathways.

Statistical Analysis

Multivariate statistical analysis was used to determine if blood-derived metabolite profiles could be used to distinguish between the initial and post-recovery samples. Prior to modelling, the data were normalized to the total metabolome, excluding the region corresponding to water, and pareto-scaled (Craig et al., 2006; Wiklund et al., 2008). Bins containing significant metabolites were sorted according to the F-ranked Variable Importance Analysis based on random Variable Combination (VIAVC) analysis (Yun et al., 2015) based on the Receiver Operator Characteristic (ROC) test and the subsequent Area-Under-the-Curve (AUC) analysis (Fawcett et al., 2005). It also employed a binary matrix resampling method and all multivariate supervised models were double ten-fold cross-validated (Szymanska et al., 2012). Univariate statistical tests included paired T-tests or paired Wilcoxon-Mann-Whitney tests.

An orthogonal projection to latent structures discriminant analysis (OPLS-DA) was conducted to visualize between-group separation as a function of within-group separation (Wiklund et al., 2008). This was complemented by hierarchical clustering illustrated by the heat map, which demonstrated the degree of separation between the groups without the presence of an algorithm.

Pearson R correlations were computed between concentrations of blood-derived metabolites and patient SCIM scores (Table 8). The significance was assessed based on the Bonferroni corrected *p*-value, obtained by dividing alpha<0.05 by the number of VIAVC F-ranked bins tested for this analysis (n=13), to obtain a more rigorous set of clinically relevant metabolites (Goodpaster et al., 2010). The % difference for scores at the two different time points were computed as follows, based on the clinical data provided in Table 7:

$$\left(\frac{Post\ Recovery\ Score - Initial\ Score}{\left(\frac{Post\ Recovery\ Score + Inital\ Score}{2}\right)}\right) * 100\%$$

RESULTS

Patient Characteristics

Clinical improvement was evident amongst the male SCI patients at 6-months post-injury with respect to the initial scores for the SCIM. The average improvement was 13.71 +/- 12.16 points, in which a higher "post" score indicates greater recovery (Table 7). There were three patients with complete injury and five patients with incomplete injury.

Metabolomic Profiles are Robust Predictors of Recovery Following SCI

The bins found to be significant in male SCI patients by either the paired T-test/Wilcoxon Mann-Whitney test (17 bins) or the VIAVC best subset (5 bins) were used for the analysis. The VIAVC best subset consists of the following metabolites: citric acid, 1,3,7-trimethyluric acid, and acetyl phosphate. Heat map illustration demonstrated a partial degree of unsupervised group separation (Figure 11). The OPLS-DA plot (Figure 12) illustrates significant group separation initially and post-recovery ($R^2Y=0.921$, $p<0.01$; $Q^2=0.687$, $p<0.01$). This supervised model indicated a change in the metabolic profiles over the course of patient recovery in repeated samples. Metabolites that contributed the most to the group separation are shown in Appendix 4, ranked in order of significance, based on the paired T-test/Wilcoxon Mann-Whitney test. An ROC curve achieved an equal to 1, with a 95% confidence interval of 1-1 (Figure 13), with a predictive accuracy of 66.5% when 2 bins are included, 95% when 3 bins are included, 96.5% when 4 bins are included, and 99% when all 5 bins are included. This analysis was based on the 5 bins significant by the VIAVC best subset.

Pathway topology analysis (Figure 14) illustrates the impact of individual metabolites on changes to the SCI patients' metabolic profiles, presented in increasing order of impact. Metabolic pathways significantly affected included pyruvate metabolism ($p<0.001$), the citrate cycle ($p<0.01$), glycolysis/gluconeogenesis ($p<0.05$), alanine, aspartate, & glutamate metabolism ($p<0.05$), and glyoxylate & dicarboxylate metabolism ($p<0.05$). Pathway analysis was also based on bins significant by the VIAVC best subset, the paired T-test, and the Wilcoxon Mann-Whitney test.

Metabolic Biomarkers as Predictors of Functional Improvement

To determine if initial metabolite concentrations can predict patients' functional improvement, Pearson R correlations were computed between initial metabolite levels and % difference in SCIM scores, revealing acetyl phosphate with significant correlations: R=-0.66, $p<0.05$ (Table 8). To determine if the change in metabolite concentration serves as a proxy measure of the degree of recovery, Pearson R correlations were also computed between the difference in metabolite concentrations and % difference in SCIM scores, revealing significant correlations for 1,3,7- trimethyluric acid (R=0.57, $p<0.05$), 1,9-dimethyluric acid (R=0.76, $p<0.01$), and acetic acid (R=0.74, $p<0.01$) (Table 8).

To investigate potential sex differences in biomarkers, the only available single female patient was included in the correlation analysis (Table 8). The inclusion of the female caused the absolute value of all the correlations (with the exception of acetyl phosphate) to decrease, yet still retained a strong correlation. However, none of the correlations achieved significance based on the Bonferroni threshold (alpha=0.0038). In addition, 1,9-dimethyluric acid again achieved the strongest Pearson R value.

DISCUSSION

The present study shows that metabolomic signatures in serum provide novel biomarkers that predict recovery trajectories following SCI. The most significant change occurred in metabolites that were part of the VIAVC best subset (citric acid, 1,3,7-trimethyluric acid, and acetyl phosphate), suggesting that these metabolites present the most robust indicators of successful recovery in SCI. Their value as metabolic biomarkers of SCI severity was confirmed by a predictive accuracy of 99%. The main metabolic pathways altered by recovery following SCI included pyruvate metabolism, the citrate cycle, glycolysis/gluconeogenesis, alanine, aspartate, & glutamate metabolism, and

glyoxylate & dicarboxylate metabolism Moreover, we show that the degree of functional recovery and optimal response is best predicted by acetyl phosphate. 1,3,7-trimethyluric acid, 1,9-dimethyluric acid and acetic acid serve as good measures of treatment efficacy. Thus, a metabolomics approach combined with machine learning is able to provide clinically accessible biomarkers with high prognostic potential for SCI recovery and treatment success. Moreover, it allows to distinguish between the degenerative events of injury and beneficial changes linked to recovery.

Pathway Analysis

Pyruvate metabolism presented as the most significantly affected pathway amongst the present SCI subjects (Figure 14). In glycolysis, two pyruvate molecules are generated from the breakdown of glucose, which are later used to generate ATP energy via the citric acid cycle. Insulin stimulates glycolysis and the formation of pyruvate, by promoting the expression of enzymes phosphofructokinase and pyruvate kinase which drive this pathway. However, over time SCI patients experience insulin resistance attributed to increased adiposity (Gorgey et al., 2012), and consequently some cells may fail to respond to insulin and glucose is not metabolized as quickly. This is characteristic of type 2 diabetes, in which patients present with elevated blood glucose levels due to impaired insulin signaling. Consequently, it is likely that pyruvate metabolism is down-regulated amongst SCI patients, as they begin to experience symptoms akin to type 2 diabetes.

Presence of the intermediates succinate and citrate in the patients' serum indicates dysregulation of the citric acid cycle. As the second most significantly altered pathway, disruptions to the citric acid cycle may indicate a metabolic switch from aerobic respiration to anaerobic respiration (Das et al., 1987). Normally in the presence of oxygen, cells prefer

to undergo aerobic respiration which, due to the citric acid cycle and electron transport chain, produces a larger ATP yield compared to anaerobic respiration. However, following SCI with contusion or compression of nerves and vasculature, ensuing hemorrhage creates a depletion in blood flow around surrounding tissues, which can lead to different degrees of ischemia (Mautes et al., 2000). Consequently, anaerobic glycolysis may prevail leading to accumulation of lactate, which was a significantly altered metabolite in the present serum samples (Appendix 4). Damage to blood vessels underlies the secondary injury events that follow the initial mechanical insult, which leads to neuronal death (Mautes et al.,2000); thus, leakage of metabolic intermediates into the blood suggests a shift in metabolic mode and secondary tissue damage.

The third most significantly affected pathway was glycolysis or gluconeogenesis. Gluconeogenesis and glycolysis are reciprocally regulated pathways, controlled by two competing hormones, insulin that drives glycolysis, and glucagon that drives gluconeogenesis (Qaid, et al., 2016). Gluconeogenesis largely occurs in hepatocytes and is a pathway used by the body to create glucose from other molecules. Insulin is the most important hormone for this pathway that suppresses gluconeogenic enzymes (Barthel & Schmoll, 2003). However, in the case of SCI where cells do not respond to insulin, this regulation of gluconeogenesis is lost, and consequently the rate of hepatic gluconeogenesis is considerably increased. This claim is reinforced by a recent study which demonstrated that in individuals with compromised insulin signaling, insulin failed to suppress hepatic gluconeogenesis, even in the fed state (Hatting et al., 2018). Therefore, it is likely that gluconeogenesis is up-regulated after SCI. Complementary to gluconeogenesis is glycolysis, which functions to break down glucose into two pyruvate molecules to derive

ATP cellular energy. A previous rodent study has shown that suppression of glycolysis occurs in diabetic hepatocytes, at a rate 40% of the rate of normal hepatocytes (Henly et al., 1996). Since SCI patients experience altered insulin sensitivity, down-regulation of their glycolysis is highly probable.

The fourth most significant pathway implicated within our patients' samples was alanine, aspartate, and glutamate metabolism. Prior studies have shown that levels of excitatory amino acids, including aspartate and glutamate, are up-regulated in response to trauma to the brain and spinal cord (Faden et al., 1989; Panter et al., 1990). Specifically, glutamate levels transiently increase within the first three hours following an SCI (Park et al., 2004). Neurons are especially susceptible to the damaging effects of glutamate excitotoxicity since they express a full complement of glutamate receptors (Oyinbo, 2011), and oligodendrocytes within the white matter are especially sensitive (Xu et al., 2004). Reduced intracellular aspartate levels in the cervical spinal cord of a rat model suggests release of this excitatory amino acid in response to injury (Watanabe et al., 1998). Unlike glutamate and aspartate, the amino acid alanine is inhibitory. It has been shown that cell damaging conditions such as ischemia, oxidative stress, and free radical formation, trigger its release to protect against neurotoxicity (Saransaari and Oja, 1999). Thus, degenerative mechanisms following SCI may trigger the release of metabolites implicated in this pathway.

The fifth pathway modified by SCI was glyoxylate and dicarboxylate metabolism. Recent evidence discusses the potential of glyoxylate as biomarker of type 2 diabetes, with changes that predetermine glucose levels (Nikiforova et al., 2014). As SCI patients experience altered sensitivity to insulin, evidence of this pathway within the serum may

indicate initial development of this pathology. Also relevant is the fact that a glyoxylate shunt is activated during oxidative stress and provides an alternative metabolic route to the citric acid cycle (Ahn et al., 2016). Oxidative stress following SCI may lead to use of this alternative pathway.

Relationship Between Metabolite Profiles and SCIM

Acetyl phosphate is a clinically significant metabolite, given that initial levels of this biomarker correlated to the % difference measurements for SCIM performance (Table 8). The negative correlation indicates improved recovery as levels of this metabolite decrease. Evidence suggests that acetyl phosphate serves as a marker of mitochondrial activity, with a postulated role as a reaction intermediate in the generation of precursors for the citric acid cycle (Xu et al., 2018). It is known that changes in mitochondria activity within skeletal muscle underlies the development of insulin resistance (Porter and Wall, 2012). Insulin resistance is a prevalent issue afflicting SCI patients (Yekutiel et al., 1989), likely due to the ensuing changes in the amount of muscle tissue. The observed decrease in blood acetyl phosphate levels may indicate attenuation of muscle atrophy and subsequent decrease in breakdown of organelles such as mitochondria, leading to the observed improvement in patient recovery.

The present findings indicate that changes in blood metabolites, especially 1,3,7-trimethyluric acid, 1,9-dimethyluric acid, and acetic acid, may serve as robust proxy measures for SCIM scores. The positive correlation indicates that improvement in patient outcomes is paralleled by increased blood 1,3,7-trimethyluric acid levels. As a breakdown product of purines, 1,3,7-trimethyluric acid may serve as a biomarker of the neuroprotective action of purines in the nervous system (Jackson et al., 2016). It has been shown that plasma

uric acid, a type of purine, was negatively correlated with the incidence of neurodegenerative disease by promoting neuronal glutathione synthesis (Aoyama et al., 2011), a major antioxidant (Dringen, 1999). This same framework could also explain the presence of 1,9-dimethyluric acid, another purine derivative that is positively correlated to patient SCIM outcomes and reflective of neuroprotective mechanisms.

A positive correlation was also seen for changes in acetic acid levels compared to the % difference in SCIM scores. Again, this indicates that patient recovery is paralleled by increased blood acetic acid levels. Acetic acid, whose conjugate base is acetate, is a precursor to glucose production within the tricarboxylic acid cycle (TCA cycle). Via a thioester linkage, acetic acid is bound to coenzyme A, which serves as the starting material for energy production within the TCA cycle, common to all types of cells (Akram, 2014). Increasing levels associated with patient recovery may indicate a greater metabolic demand for glucose, likely due to muscle rebuilding and restoration, which are very metabolically active (Richter & Hargreaves, 2013). This highlights the importance of exercise rehabilitation in developing muscle tissue to stimulate glucose metabolism. In fact, a previous study showed that physical exercise prevents insulin resistance by inhibiting pro-inflammatory signaling pathways (Lambernd, et al., 2012). Therefore, higher acetic acid levels may indicate higher glucose demand, which emphasizes the importance of exercise interventions to attenuate insulin resistance.

Metabolite Profiles and Sex Differences

Including the single female reduced Pearson R values indicating that the respective metabolites represent sex-dependent biomarkers. As males have a greater average proportion of muscle tissue compared to females (Wells, 2007), the ensuing loss of lean

tissue after SCI will be greater for males than for females. This is reflected in acetyl phosphate and acetic acid levels, which are implicated in pathways involving muscle degradation. As for 1,3,7-trimethyluric acid and 1,9-dimethyluric acid, their postulated roles in neuroprotection may be additional evidence of differences in neuroimmune signaling as has been shown to be a sexually dimorphic trait (McCarthy et al., 2017).

LIMITATIONS

Although the sample size of the present study was limited, the longitudinal design revealed significant regulation of metabolite concentrations across initial and post-recovery time points allowed the identification of unique blood-derived metabolic signatures. Another limitation to this pilot study is that SCI patients were not on a strict diet regimen. The effects of this potential confound were minimized, however, by collecting two blood samples from each patient so that significant metabolite changes reflect a global change across *paired* blood samples.

CONCLUSIONS

Rehabilitation interventions that capitalize on mobilizing the patient from the acute stage would be prudent for limiting the extent of inflammatory degradation, minimizing patient adiposity, and improving glucose tolerance. The identified biomarkers and metabolic pathways may represent attractive therapeutic targets and have prognostic potential for clinical translation. Metabolites with statistically significant correlations to SCIM outcomes represent a window of opportunity for neurotherapeutic intervention for SCI patients. Acetyl phosphate has the ability to predict recovery and outcomes, whereas 1,3,7-trimethyluric acid, 1,9-dimethyluric acid, and acetic acid have potential to serve as

proxy biomarkers of recovery. Furthermore, significant group separation in metabolite profiles was observed before and after rehabilitation, where the subset of metabolites part of the VIAVC best-subset correctly classified metabolic profiles with a predictive accuracy of 99%.

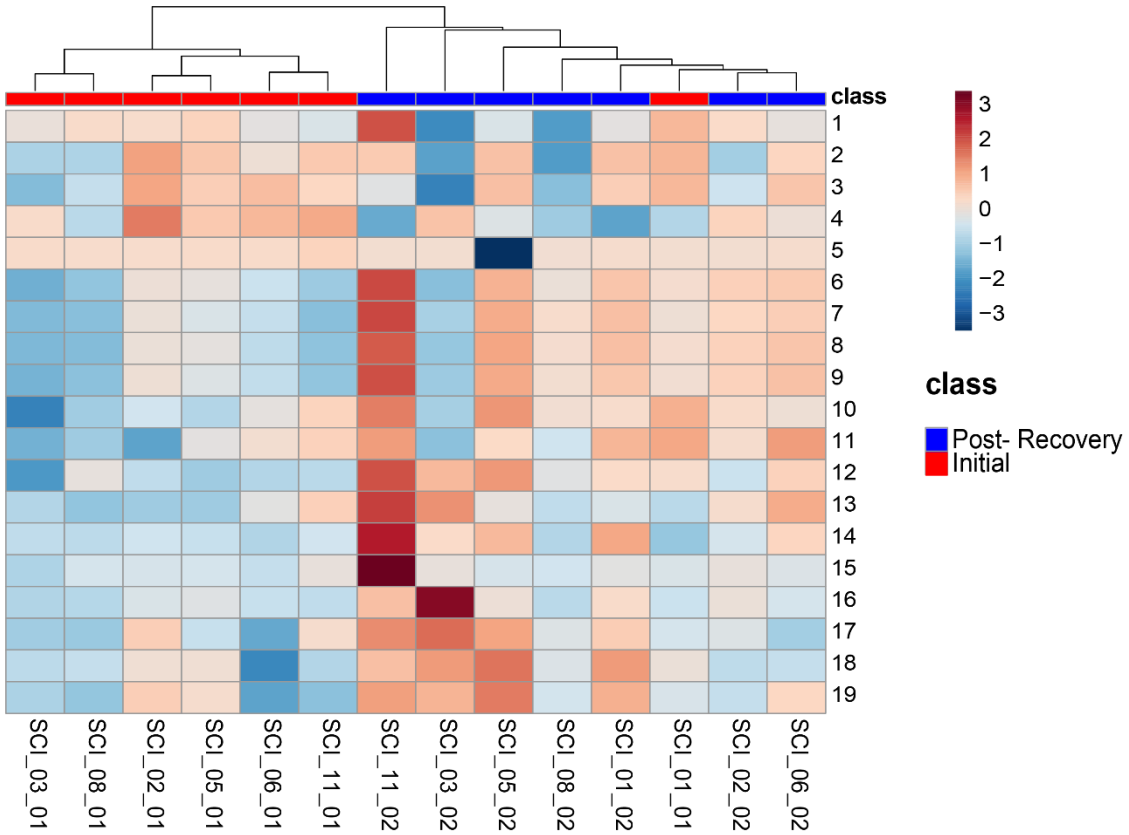

Figure 11. Heat map illustrating unsupervised separation and hierarchical clustering analysis of metabolic profiles in male SCI patients initially and at 6 months post-recovery. The heat map depicts up-regulation versus down-regulation of metabolites determined significant by the VIAVC best subset (5 bins) and paired T-test/Wilcoxon Mann-Whitney test (17 bins). Appendix 4 provides the name of the metabolite corresponding to each of the numbers provided to the right of the heat map.

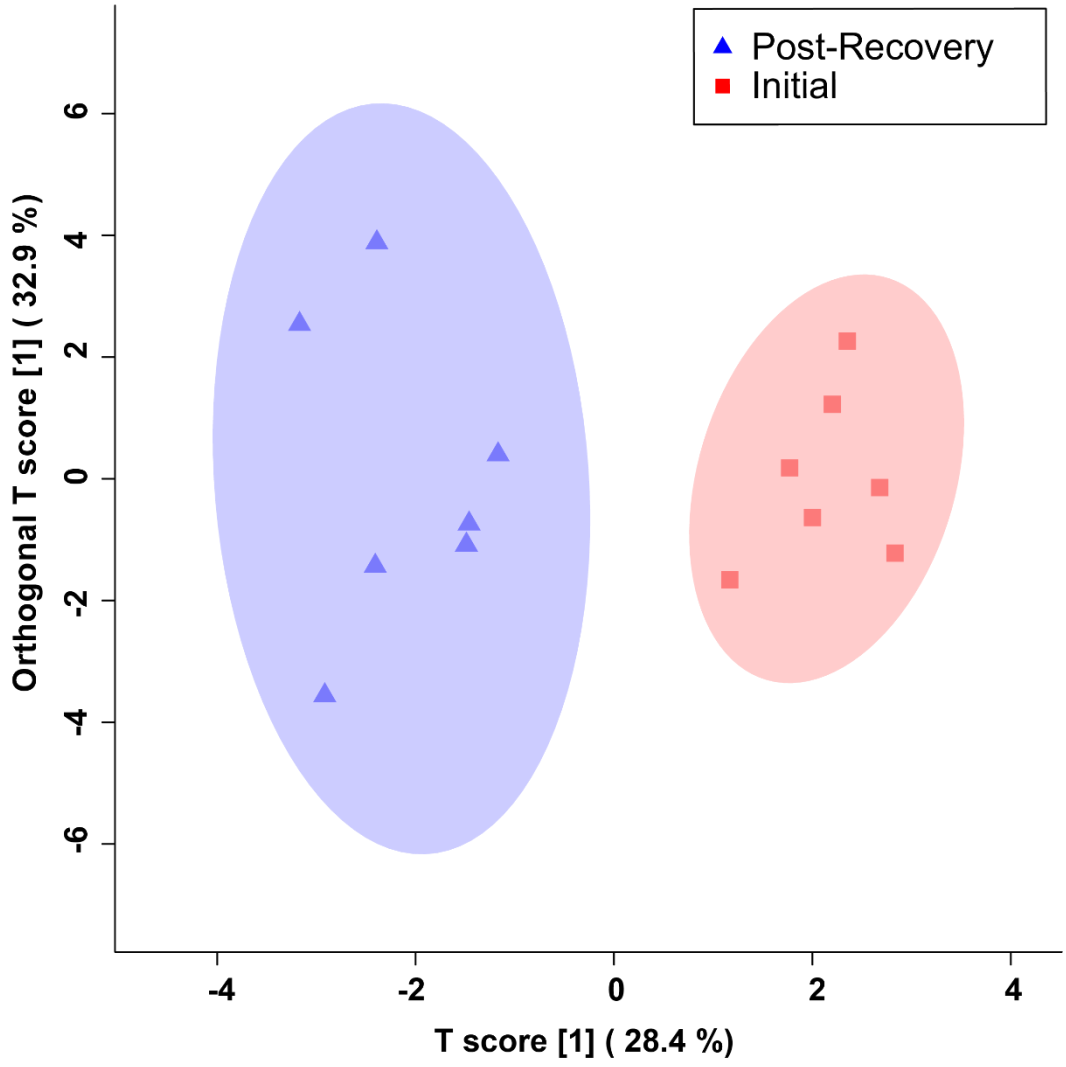

Figure 12. Orthogonal Projections to Latent Structures Discriminant Analysis (OPLS-DA) score plot showing supervised separation for male SCI patients initially (red/squares) and 6 months post-recovery (indigo/triangles). This plot was created using a list of blood-derived metabolites found to be significantly altered by either paired T-test/Mann-Whitney or VIAVC testing. The 95% confidence interval is indicated by the shaded ellipses. The x- and y-axes show the predictive (between group) and orthogonal (within group) variation, respectively. Cross-validation and permutation measures for the OPLS-DA was R^2Y=0.921, p=0.006; Q^2=0.687, p=0.002.

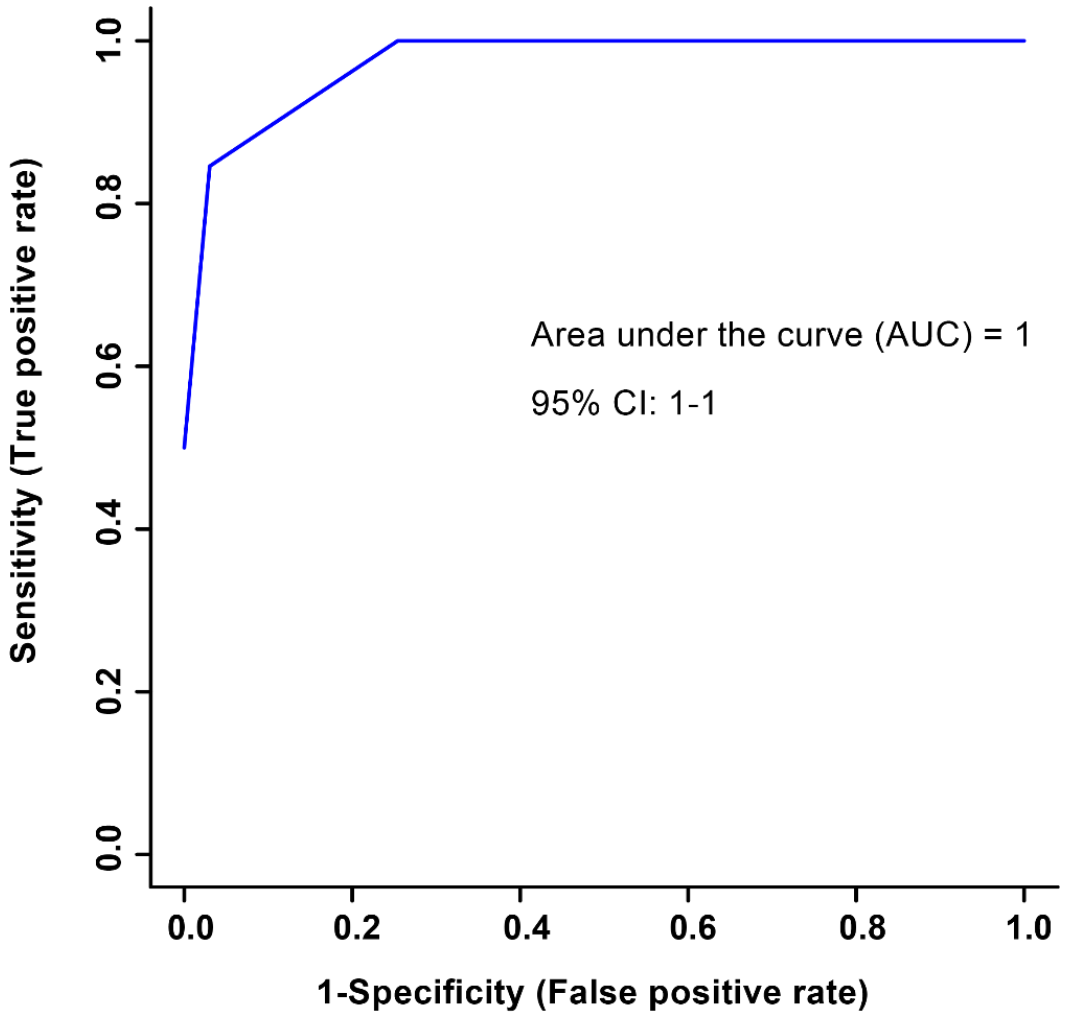

Figure 13. The Receiver Operator Characteristic (ROC) curve representing high sensitivity and specificity of the group separation between initial and post-recovery samples. The corresponding area under the curve (AUC) and confidence interval are indicated. The ROC curve was constructed using the metabolites determined to be significantly altered based on the VIAVC best subset, which corresponds to 5 bins.

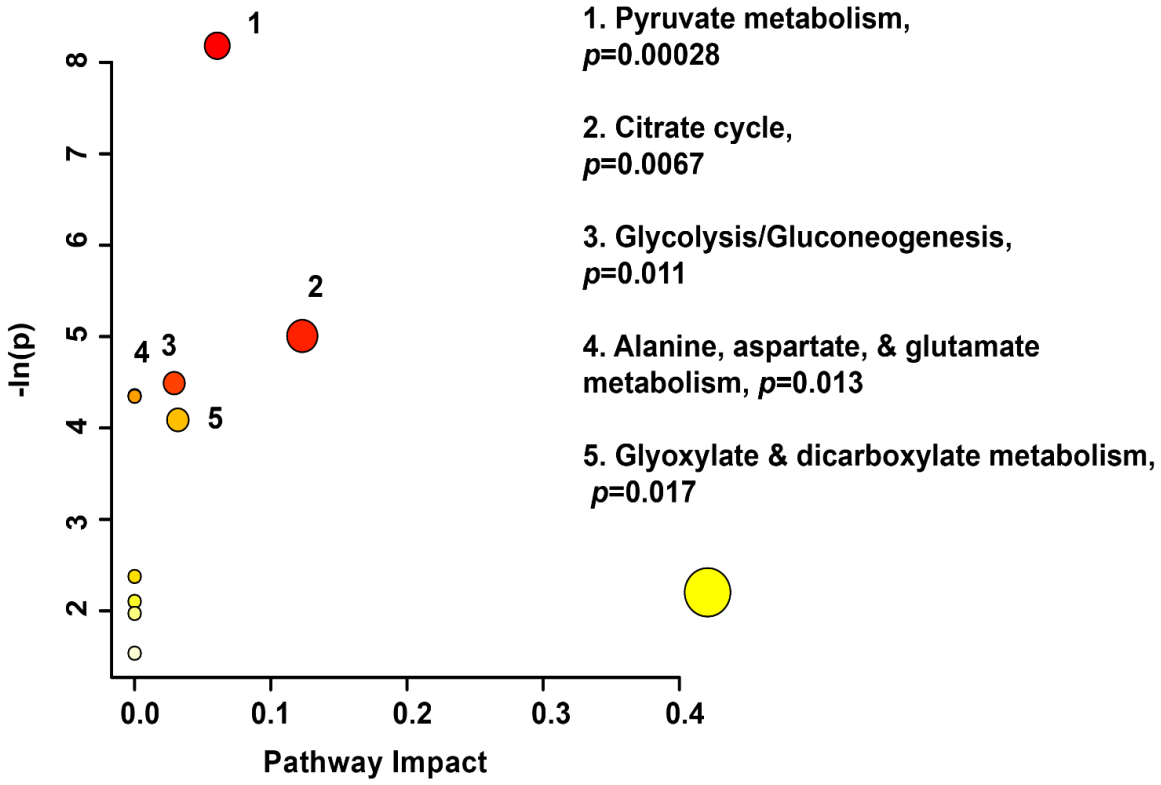

Figure 14. Metabolic pathway analysis conducted based on spectral bins that were significant in the VIAVC best subset and paired T-test/Wilcoxon Mann-Whitney test. A higher value on the y-axis indicates a lower *p*-value for the pathway. The x-axis provides the pathway impact as a measure of how affected each pathway is by the metabolites identified as significantly altered. Only pathways with a *p*-value less than 0.05 are labeled.

Table 7. Patient characteristics table indicating the sex, age, lesion location, co-morbidities, and SCI type, as well as both the initial and post-recovery SCIM scores.

Patient Code	SCI Type	ASIA Score	Sex	Lesion Location	Co-Morbidities	Age	Pre SCIM	Post SCIM
SCI_01	Incomplete	D	Male	Central Cord		80	84	89
SCI_02	Complete	A	Male	T7		29	70	70
SCI_03	Incomplete	D	Male	Central Cord		48	66	97
SCI_05	Incomplete	D	Male	C4		38	72	92
SCI_06	Complete	A	Male	T6		50	49	66
SCI_07	Complete	A	Female	C7		16	36	44
SCI_08	Incomplete	D	Male	C6-C7		59	100	100
SCI_11	Incomplete	B	Male	C2-C4	UTI, C2-C3 spinal artery infarct	73	77	100

Table 8. Pearson R correlation values and associated p-values displayed for males only and with the female patient included for 'initial to % difference' and 'delta to % difference' comparisons. P-values with a star indicates significance based on the Bonferroni corrected threshold (alpha=0.0038).

Metabolite	Males only (n=7)		With female subject included (n=8)	
Initial to % Diff SCIM	Pearson R	*p*-value	Pearson R	*p*-value
Acetyl phosphate	-0.66	0.011	-0.63	0.01
Delta to % Diff SCIM				
1,3,7-Trimethyluric Acid	0.57	0.035	0.48	0.06
1,9-Dimethyluric Acid	0.76	0.002*	0.68	0.0041
Acetic Acid	0.74	0.0026*	0.61	0.013

REFERENCES

Ahn, S., Jung, J., Jang, I., Madsen, E., & Park, W. (2016). Role of glyoxylate shunt in oxidative stress response. *The Journal of Biological Chemistry, 291*(22): 11928-11938. Doi: 10.1074/jbc.M115.708149.

Allan, S., & Rothwell, N. (2003). Inflammation in central nervous system injury. *Philosophical Transactions of the Royal Society B: Biological Sciences, 358*(1438): 1669-1677.

Anderson, P., Mahle, D., Doom, T., Reo, N., DelRaso, N., & Raymer, M. (2011). Dynamic Adaptive Binning: an Improved Quantification Technique for NMR Spectroscopic Data. *Metabolomics, 7*(2): 179-190. https://link.springer.com/article/10.1007/s11306-010-0242-7 Accessed January 15, 2020.

Aoyama, K., Matsumura, N., Watabe, M., Wang, F., Kikuchi-Utsumi, K., & Nakaki, T. (2011). Caffeine and uric acid mediate glutathione synthesis for neuroprotection. *Neuroscience*, *181*(5): 206-215.

Akram, M. (2014). Citric acid cycle and role of its intermediates in metabolism. *Cell Biochemistry and Biophysics, 68*(3): 475-478.

Barthel, A., & Schmoll, D. (2003). Novel concepts in insulin regulation of hepatic gluconeogenesis. *American Journal of Physiology: Endocrinology and Metabolism, 285*(4): E685-E692.

Catz, A., Itzkovich, M., Agranov, E., Ring, H., & Tamir, A. (1997). SCIM- spinal cord independence measure: a new disability scale for patients with spinal cord lesions. *Spinal Cord, 35*: 850-56.

Chong, J., Wishart, D.S., & Xia J. (2019). Using metaboAnalyst 4.0 for comprehensive and integrative Metabolomics Data Analysis. *Current Protocols in Bioinformatics, 68,* e86 (128 pages). doi: 10.1093/nar/gky310.

Craig, A., Cloarec, O., Holmes, E., Nicholson, J.K., & Lindon, J.C. (2006). Scaling and normalization effects in NMR spectroscopic metabonomic data sets. *Analytical Chemistry*, *78*: 2262-2267.

Das, D.K., Engelman, R.M., Rousou, J.A., & Breyer, R.H. (1987). Aerobic vs anaerobic metabolism during ischemia in heart muscle. *Annales chirurgiae et gynaecologiae*, *76*(1): 68-75.

Dringen, R. (1999). Metabolism and functions of glutathione in brain. *Progress in Neurobiology*, 62: 649-671.

Faden, A., Demediuk, P., & Vink, R. (1989). The role of excitatory amino acids and NMDA receptors in traumatic brain injury. *Science*, 244(4906): 798-800. Doi: 10.1126/science.2567056

Fawcett, T. (2005). An introduction to ROC analysis. *Pattern Recognition Letters, 72*(8):861-874. https://doi.org/10.1016/j.patrec.2005.10.010 Accessed January 17, 2020.

Gil, R., Lehmann, R., Schmitt-Kopplin, P., & Heinzmann, S. (2016). (1)H NMR-based metabolite profiling workflow to reduce inter-sample chemical shift variations in urine samples for improved biomarker discovery. *Analytical and Bioanalytical Chemistry, 408*(17): 4683-4691.

Goodpaster, A., Romick-Rosendale, L., & Kennedy, M. (2010). Statistical significance analysis of nuclear magnetic resonance-based metabonomics data. *Analytical Biochemistry, 401*: 134-143.

Gorgey, A.S., Dolbow, D., Dolbow, J., Khalil, R., Castillo, C., & Gater, D. (2014). Effects of spinal cord injury on body composition and metabolic profile. *Journal of Spinal Cord Medicine, 37*(6): 693-702.

Gorgey, A.S., Wells, K.M., & Austin, T.L. (2015). Adiposity and spinal cord injury. *World Journal of Orthopedics, 6*(8): 567-576. Doi: 10.5312/wjo.v6.i8.567.

Hatting, M., Tavares, C., Sharabi, K., Rines, A., & Puigserver, P. (2018). Insulin regulation of gluconeogenesis. *Annals of New York Academy of Sciences, 1411*(1): 21-35.

Henly, D., Phillips, J., & Berry, M. (1996). Suppression of glycolysis is associated with an increase in glucose cycling in hepatocytes from diabetic rats. *The Journal of Biological Chemistry, 271*(19): 11268-11271.

Jackson, E., Boison, D., & Kochanek, P. (2016). Purines: forgotten mediators in traumatic brain injury. *J Neurochem, 137*(2): 142-153.

Kirshblum, S., Burns, S., Biering-Sorenson, F., Donovan, W., Graves, D., Jha, A.,…Waring, W. (2011). International standards for neurological classification of spinal cord injury. *The Journal of Spinal Cord Medicine, 34*(6): 535-546.

Lambernd, S., Taube, A., Schober, A., Platzbecker, B., Gorgens, B., Schlich, R.,…Eckel, J. (2012). Contractile activity of human skeletal muscle cells prevents insulin resistance by inhibiting pro-inflammatory signalling pathways. *Diabetologia, 55*(4): 1128-39.

Marino, R., Barros, T., Biering-Sorensen, F., Burns, S., Donovan, W., Graves, D.,…Priebe, M. (2016). International standards for neurological classification of spinal cord injury. *The Journal of Spinal Cord Medicine, 26*: sup1, S50-S56, doi:10.1080/10790268.2003.11754575.

Mautes, A., Weinzierl, M., Donovan, F., & Noble, L.J. (2000). Vascular events after spinal cord injury: contribution to secondary pathogenesis. *Physical Therapy, 80*(7): 673-687.

McCarthy, M.M., Nugent, B.M., & Kathryn, M.L. (2017). Neuroimmunology and neuroepigenetics in the establishment of sex differences in the brain. *Nature Reviews Neuroscience, 18*(8): 471-484. Doi: 10.1038/nrn.2017.61

Mizuno, K., & Ueno, Y. (2017). Autonomic nervous system and the liver. *Hepatology Research, 47:* 160-165.

Nas, K., Yazmalar, L., Sah, V., Ayudin, A., & Ones, K. (2015). Rehabilitation of spinal cord injuries. *World Journal of Orthopedics, 18*(6): 8-16.

Nikiforova, V., Giesbertz, P., & Wiemer, J. Glyoxylate, a new marker metabolite of type 2 diabetes. *Journal of Diabetes Research,* 2014; http://doi. Org/10,1155/2014/685204.

Oyinbo, C. (2011). Secondary injury mechanisms in traumatic spinal cord injury: a nugget of this multiply cascade. *Acta Neurobiologiae Experimentalis, 71*(2): 281-299.

Panter, S.S., Yum, S.W., & Faden, A.I. (1990). Alteration in extracellular amino acids after traumatic spinal cord injury. *Annals of Neurology, 27*(1): 96-99.

Park, E., Lee, J., Yu, G., He, G., Ali, S., Holzer, R.,…Karin,M. (2010). Dietary and genetic obesity promote liver inflammation and tumorigenesis by enhancing IL-6 and TNF expression. *Cell, 140*(2): 197-208.

Park, E., Velumian, A., & Fehlings, M. (2004). The role of excitotoxicity in secondary mechanisms of spinal cord injury: a review with an emphasis on the implications for white matter degeneration. *Journal of Neurotrauma, 21*(6): 754-774.

Porter, C., & Wall, B. (2012). Skeletal muscle mitochondrial function: is it quality of quantity that makes the difference in insulin resistance? *The Journal of Physiology, 590* (Pt 23): 5935-5936. Doi: 10.1113/jphysiol.2012.241083.

Psychogios, N., Hau, D., Peng, J., Guo, A., Mandal, R., Bouatra, S.,…Wishart, D.S. (2011). The human serum metabolome. *PLoS One, 6*(2): e16957.

Qaid, M., & Abdelrahman, M. (2016). Role of insulin and other related hormones in energy metabolism- A review. *Cogent Food & Agriculture, 2*: 1267691.

Richter, E., and Hargreaves, M. (2013). Exercise, GLUT4, and skeletal muscle glucose uptake. *Physiological Reviews, 93*(3): 993-1017.

Saransaari, P., & Oja, S.S. (1999). Beta-alanine release from the adult and developing hippocampus is enhanced by ionotropic glutamate receptor agonists and cell-damaging conditions. *Neurochemical Research, 24*(3): 407-414.

Schwab, M.E.., & Bartholdi, D. (1996). Degeneration and regeneration of axons in the lesioned spinal cord. (1996). *Physiological Reviews*, 76(2): 916-70.

Smelter, A., Rouchka, E., & Moseley, H. (2017). Detecting and accounting for multiple sources of positional variance in peak list registration analysis and spin system grouping. *Journal of Biomolecular NMR*, 68(4): 281-296.

Szymanska, E., Saccenti, E., Smilde, A.K., & Westerhuis, J.A. (2012). Double-check: validation of diagnostic statistics for PLS-DA models in metabolomics studies. *Metabolomics*, *8*:S3-S16. doi: 10.1007/s11306-011-0330-3.

Tan, C., Battaglino, R., & Morse, L. (2013). Spinal cord injury and osteoporosis: causes, mechanisms, and rehabilitation strategies. *International Journal of Physical Medicine and Rehabilitation, 1*:127.

Veselkov, K., Lindon, J., Ebbels, T., Crockford, D., Volynkin V.V., Holmes, E.,….Nicholson, J.K. (2009). Recursive segment-wise peak alignment of biological 1H NMR spectra for improved metabolic biomarker recovery. *Analytical Chemistry, 81*(1): 56-66. Doi: 10.1021/ac8011544

Watanabe, M., Fujimara, Y., Nakamura M., Yato, Y., Ohta, K., Okai, H., & Ogawa, Y. (1998). Changes of amino acid levels and aspartate distribution in the cervical spinal cord after traumatic spinal cord injury. *Journal of Neurotrauma, 15*(4): 285-293. Doi: 10.1089/neu.1998.15.285.

Wells, J. (2007). Sexual dimorphism of body composition. *Best Practice & Research Clinical Endocrinology & Metabolism, 21*(3): 415-430.

Wiklund, S., Johansson, E., Sjostrom, L., Mellerowicz, E.J., Edlund, U., Shockcor, J.P.,…Trygg, J. (2008). Visualization of GC/TOF-MS-based metabolomics data for identification of biochemically interesting compounds using OPLS class models. *Analytical Chemistry, 80*(1): 115-122.

Wishart, D.S., Feunang, Y.D., Marcu, A., Guo AC, Liang K, Vazquez-Fresno, R.,…Scalbert, A. (2018). HMBD 4.0- The human metabolome database for 2018. *Nucleic Acids Research*, *4;46*(D1): D608-17. 29140435. Doi: 10.1093/nar/gkx.1080.

Wu, G. (2009). Amino acids: metabolism, functions, and nutrition. *Amino Acids*, *37*(1): 1-17.

Xia, J., & Wishart, D.S. MetPA: a web-based metabolomics tool for pathway analysis and visualization. *Bioinformatics*, 2010;*26*, 2342-2344. Doi: 10.1093/bioinformatics/btq418.

Xia, J., & Wishart, D.S. MetPA: a web-based metabolomics tool for pathway analysis and visualization. (2010). *Bioinformatics*, *26*, 2342-2344. Doi: 10.1093/bioinformatics/btq418.

Xu, G.Y., Hughes, M.G., Ye, Z., Hulsebosch, C.E., & McAdoo, D.J. (2004). Concentrations of glutamate released following spinal cord injury kill oligodendrocytes in the spinal cord. *Experimental Neurology, 187*(2): 329-336. Doi: 10.1016/j.expneuro.2004.01.029.

Xu, W.J., Wen, H., Kim, H.S., Ko, Y.J., Dong, S.M., Park, I.S.,…Park, S. (2018). Observation of acetyl phosphate formation in mammalian mitochondria using real-time in-organelle NMR metabolomics. *PNAS, 115*(16): 4152-4157.

Yekutiel, M., Brooks, M.E., Ohry, A., Yarom, J., & Carel, R. (1989). The prevalence of hypertension, ischaemic heart disease and diabetes in traumatic spinal cord injured patients and amputees. *Spinal Cord, 27*: 58-62.

Yun, Y., Liang, F., Deng, B., Lai, G., Goncalves, C., Lu, H.,…Liang Y. (2015). Informative metabolites identification by variable importance analysis based on random variable combination. *Metabolomics, 11*(6): 1539-1551.

CHAPTER 6: GENERAL CONCLUSIONS AND FUTURE DIRECTIONS

The present thesis evaluated urine and blood-derived biomarkers with potential for clinical application amongst two groups of patients with trauma to the central nervous system. For all four studies presented, significant group separation was observed when comparing samples collected at initial time of injury with samples collected post-recovery after both TBI and SCI. Unsupervised separation exhibited by the PCA figure/heat maps demonstrate partial separation of metabolites in urine and blood samples of SCI patients. Partial separation was also seen for the urine of TBI females, and for urine and blood when males and females were considered together. Complete unsupervised separation was observed for the urine of TBI males and for the blood of TBI females. As for supervised separation exhibited by the OPLS-DA figures, partial separation was seen for the urine of TBI females, the blood of TBI males, and for urine and blood when males and females were considered together. Complete supervised separation was observed for the urine and blood of SCI patients, for the urine of TBI males and TBI females, and for the blood of TBI females.

An emerging trend from the present data is that better group separation is observed for male subjects in urinary compared to blood-based metabolic profiles. This is seen when comparing the SCI urine study to the SCI blood study (see Figure 8 and Figure 12) and when comparing the TBI urine study to the TBI blood study (see Figures 1A, 1D and Figures 4A, 4D). Although an intriguing result, further investigative work will be needed to validate whether urine is a superior bio-fluid for analyzing metabolic responses of males. In contrast, better group separation is observed for female subjects in blood-based compared to urinary metabolic profiles. This is seen when comparing the TBI blood study

to the TBI urine study (see Figure 1B,E and Figure 4B,E). This implies that blood may be a superior bio-fluid for examining the metabolic responses of females in the wake of TBI. The nature of the sex-dependent metabolites uncovered in this study is reinforced by the fact that poorer group separation results when males and females are considered together during analysis of TBI urine and blood (as is seen in Figures 1C, 1F and Figures 4C, 4F).

The Receiver Operator Characeristic curves presented in each chapter demonstrate that the metabolites selected by the VIAVC best-subset have a high predictive ability for SCI urine (100%), SCI blood (99%), males for TBI urine (99.7%), males & females for TBI urine (93.5%), males for TBI blood (86.3%), and males & females for TBI blood (86.5%) when all bins are included. The exceptional ability of these metabolites to classify metabolic profiles initially and post-recovery reinforces their translational potential into the clinical setting.

It is interesting to note that there were no overlapping biomarkers with correlation to clinical outcomes between bio-fluids and across both types of injury. This indicates that urine and blood yield unique metabolic fingerprints, and together they offer a more holistic picture of homeostatic disturbances that occur in response to injury. Based on the theory of homeostatic regulation, it stands to reason that an increase in excretion of a urinary metabolite would lead to a corresponding decrease in the same blood-derived metabolite (Modell et al., 2015). However, physiological systems are not mutually exclusive, and this does not rule out potential overlap between biomarkers that are present in the urine and blood. A previous study presented the argument that early pathological changes in the acute stage of a disease would be better reflected in the urine and that during later stages, changes caused by the disease cannot be effectively removed from the blood and therefore would have similar representation in both urine and blood (Gao, 2015). Perhaps it is for this reason

that in our study, which follows patients for only 6 months post-injury, more severe metabolic changes expressed in the urine are not yet equally evident in the blood, and we observe differences in metabolic profiles between bio-fluids. It is equally interesting that for TBI, there was no significant correlation to metabolites for males combined with females in the urine, but there were two significant correlations for males combined with females in the blood (see Table 2 and 4). This may indicate that blood has the potential to serve as a more sensitive biomarker for detecting metabolic disturbances following TBI when considering both sexes together.

With respect to the biochemical pathways identified, there were both unique as well as overlapping instances. When comparing SCI urine to SCI blood, there were no overlapping pathways. When comparing TBI urine to TBI blood, there was one overlapping pathway- phenylalanine, tyrosine, and trytophan biosynthesis (urine: males and males + females; blood: males and females as separate groups). As this pathway is implicated in neuortransmitter production and brain signalling, repeated occurrences of this pathway strongly suggests that disruption of neurotransmitters is a pathological process in the wake TBI, and that perhaps levels of dopamine, epinephrine, and serotonin are associated with severity of injury.

The presented studies within my thesis represent one-third of the broader UCAN Study, which is following patients with SCI, stroke, and TBI, throughout the recovery process while collecting fMRI imaging and rehabilitation robotics data in addition to biomarker profiles (Mercier et al., 2020). In the future, it would be worthwhile to examine whether there are similarities in the types of biomarkers present between TBI and stroke, as there are overlapping pathological mechanisms between the two injuries including

oxidative stress and inflammation (Patterson & Holahan, 2012; Anrather & Iadecola, 2016).

Although NMR spectroscopy is an amenable technique to identifying bio-fluid biomarkers, there are alternative metabolomics techniques, such as liquid and gas phase chromatography, that have the ability to identify metabolites that are not detectable by NMR (Bouatra et al., 2013). Thus, use of multiple metabolomics platforms would provide a more comprehensive library of potential metabolites for predicting injury severity and evaluating treatment efficacy.

It would also be prudent to expand the female sample to further substantiate claims regarding sex differences. This would especially provide insight as to how female and male spinal cord injuries vary, and would enable multivariate statistical analysis in addition to the qualitative approach we took with respect to the clinical correlation data for SCI. In addition, having an equal number of male and female TBI patients would also reinforce the potential of differentiating biomarkers we observed.

The present studies were "within-subject control" design studies, whereby two urine/blood samples were collected and the same patients served as their own controls. Although this design improves study efficiency, a future suggestion would be to separately recruit control subjects with impairments that allow isolation of a particular pathology. For instance, orthopedic patients with bone fracture could be compared to spinal cord injured patients to elucidate the significance of osteoblast/osteoclast activity in the wake of SCI, and disturbances in calcium signalling. Also, patients with musculoskeletal abnormalities could be compared to SCI as well to determine the significance of the extent of muscle atrophy. The only comparative studies to date examining TBI and SCI evaluated living outcomes and quality of life following these injuries (Harker et al., 2002; Nolt et al., 2014).

The absence of physiological data comparing these two injuries is filled by the present thesis, which aims to bridge this gap in the literature by evaluating the pathological mechanisms as evidenced by biomarker profiles.

REFERENCES

Anrather, J. & Iadecola, C. (2016). Inflammation and stroke: an overview. *Neurotherapeutics, 13*(4): 661-670. doi: 10.1007/s13311-016-0483-x.

Bouatra, S., Aziat, F., Mandal, R., Guo, A.C., Wilson, M.R., Knox, C., & Wishart, D.S. (2013). The human urine metabolome. *PLOS ONE, 8*(9), 1-28.

Gao, Y. (2015). Differences in blood and urine biomarker discovery. *MOJ Proteomics & Bioinformatics, 2*(5): 143. Doi: 10.15406/mojpb.2015.02.00058.

Harker , W.F., Dawson, D.R., Boschen, K.A., & Stuss, D.T. (2002). A comparison of independent living outcomes following traumatic brain injury and spinal cord injury. *International Journal of Rehabilitation Research, 25*(2): 93-102. doi: 10.1097/00004356-200206000-00003.

Mercier, L.J., Fung, T.S., Harris, A.D., Dukelow, S.P., & Debert, C.T. (2020). Improving symptom burden in adults with persistent post-concussive symptoms: a randomized aerobic exercise trial protocol. *BMC Neurology, 20*(1): 46. doi: 10.1186/s12883-020-1622-x.

Modell, H., Cliff, W., Michael, J., McFarland, J., Wenderoth, M.P., & Wright, A. (2015). A physiologist's view of homeostasis. *Advances in Physiology Education, 39*(4): 259-266. Doi: 10.1152/advan.00107.2015.

Nolt, M.T., Baguley, I.J., Heriseanu, R., Weber, G., Middleton, J.W., Meares, S.,…Chilko, S. (2014). Effects of concomitant spinal cord injury and brain injury on medical and functional outcomes and community participation. *Topics in Spinal Cord Rehabilitation, 20*(3): 225-235. doi: 10.1310/sci2003-225.

Patterson, Z.R. & Holahan, M.R. (2012). Understanding the neuroinflammatory response following concussion to develop treatment strategies. *Frontiers in Cellular Neuroscience, 6*:58. doi: 10.3389/fncel.2012.00058.

APPENDIX 1: List of Metabolites Recovered in the Urine of TBI Patients

Sex	Metabolite	Paired T/Wilcoxon *p* value	% Difference	Regulation
Male	Melatonin ††	< 0.0001	-136.25	Down
	4-Hydroxyphenylpyruvic acid ††	< 0.0001	-158.79	Down
	Citric acid †	< 0.0001	87.34898	Up
	Acetylcholine †	< 0.0001	-151.853	Down
	Protocatechuic acid	0.0002	-96.9686	Down
	Methylcysteine †	0.0002	-134.185	Down
	1,3,7-Trimethyluric acid	0.0008	24.09453	Up
	Glyoxaline †	0.0009	-94.0182	Down
	Citric acid	0.0011	76.41326	Up
	Cholate	0.0013	63.46951	Up
	Allose	0.0016	-84.8046	Down
	1,3-Dimethylurate †	0.0016	51.36264	Up
	Homovanillate	0.0017	-54.407	Down
	Trimethylamine	0.0024	55.37988	Up
	pi-Methylhistidine †	0.0026	49.41367	Up
	2-Hydroxy-2-methylbutyric acid	0.0026	58.24272	Up
	3-Hexenedioic acid †	0.0034	64.79384	Up
	Creatinine	0.0035	35.31012	Up
	Dimethylglycine †	0.0046	52.76268	Up
	5-Hydroxyindoleacetic acid	0.0047	-25.6671	Down
	N-Methylhydantoin	0.005	33.54566	Up
	Threonate	0.0057	27.37477	Up
	3-Methylxanthine	0.0058	66.92104	Up
	Pipecolic acid	0.0059	34.09519	Up
	Pipecolic acid †	0.0065	46.25453	Up
	Adenosine	0.0072	60.67166	Up
	Sialic acid †	0.0073	51.77948	Up
	Pseudouridine	0.0078	43.44568	Up
	L-Phenylalanine ††	0.0078 (W)	-126.706	Down
	Homovanillate	0.0078	-80.314	Down
	N-Acetylmannosamine ††	0.0078	-185.297	Down
	Hippurate †	0.0078	63.5273	Up
	Homovanillate †	0.0078	-63.9118	Down
	Sarcosine	0.0078	-77.9993	Down
	Dihydrothymine	0.0078	39.72076	Up
	Creatinine	0.0078	34.10535	Up
	Dimethylsulfide †	0.0078	33.15424	Up
	Methionine ††	0.0078	57.12011	Up
	Methylsuccinic acid †	0.0078	50.9002	Up
	Alpha-hydroxyisobutyric acid †	0.0078	44.45365	Up
	Trigonelline	0.0081	113.743	Up

	Vanylglycol	0.0082	45.327	Up
	Hippurate	0.0084	96.62101	Up
	Malic acid	0.0087	26.77034	Up
	Thymine †	0.0087	-54.3628	Down
	5-Hydroxymethyl-4-methyluracil	0.0089	90.68059	Up
	3-Methyladenine	0.0092	38.65713	Up
	Cholate	0.0092	34.70276	Up
	Glucarate	0.0094	42.57561	Up
	Hippurate	0.0097	83.59827	Up
	Hippurate	0.0098	77.84831	Up
	Galactonic acid	0.0098	38.60495	Up
	Hippurate	0.0102	53.68158	Up
	Pipecolic acid	0.0109	51.73468	Up
	Tiglylglycine	0.0111	41.62273	Up
	Hippurate	0.0119	80.74044	Up
	Hippurate	0.0123	77.93489	Up
	5-Aminolevulinic acid	0.0123	43.61245	Up
	3-Hydroxymethylglutaric acid	0.0123	32.47485	Up
	N-Phenylacetylglycine	0.0128	36.73919	Up
	Sialic acid	0.0141	45.7653	Up
	Trigonelline	0.0142	100.2471	Up
	Hippurate	0.0156	77.56293	Up
	Xanthosine	0.0156	48.65283	Up
	Phosphocreatine	0.0156	-29.6518	Down
	3-Hexenedioic acid	0.0156	39.84437	Up
	3-Mercaptopyruvic acid	0.0156	33.49985	Up
	2,2-Dimethylsuccinic acid †	0.0156	55.32883	Up
	Citric acid	0.0156	86.55253	Up
	4-Pyridoxate	0.0156	81.44929	Up
	Acetylcysteine †	0.0156	43.83722	Up
	2-Hydroxy-2-methylbutyric acid	0.0156	54.42666	Up
	2-Hydroxy-2-methylbutyric acid	0.0156	48.37049	Up
	Pipecolic acid	0.0156	58.2001	Up
	Citric acid	0.0157	78.45996	Up
	Hippurate	0.0168	83.15095	Up
	Xanthosine	0.0168	71.77428	Up
	1,7-Dimethylxanthine †	0.0177	54.69981	Up
	3-Hydroxymethylglutaric acid	0.0177	23.92794	Up
	Pipecolic acid	0.0178	33.25033	Up
	Methylmalonic acid	0.0178	30.7996	Up
	Acetate	0.0184	36.77968	Up
	3-Methyladenine	0.0188	92.40711	Up
	Trehalose	0.0194	-34.085	Down
	N-Phenylacetylglycine	0.0197	-47.4382	Down
	Chlorogenic acid	0.0202	30.31143	Up
	ADP	0.0211	89.02829	Up

	2-Furoylglycine	0.0221	124.8848	Up
	Sialic acid	0.0223	35.46899	Up
	2,5-Furandicarboxylic acid ††	0.0229	-118.329	Down
	2-Furoylglycine ††	0.0234	115.0578	Up
	Dehydroascorbic acid	0.0234	49.43591	Up
	Dimethylsulfone	0.0234	31.65632	Up
	Unidentified	0.0234	130.4394	Up
	3-Mercaptopyruvic acid	0.0236	35.50818	Up
	3-Methylphenylacetic acid	0.0244	29.33842	Up
	Sebacic acid	0.0247	32.54021	Up
	Nicotinic acid adenine dinucleotide	0.0251	113.5006	Up
	Hypoxanthine	0.0259	49.2272	Up
	Deoxyinosine	0.0261	61.21619	Up
	Xanthurenic acid	0.0269	-45.8466	Down
	3,7-Dimethyluric acid	0.0277	-78.2102	Down
	1-Methyladenine	0.0281	69.69346	Up
	5-Methylcytidine	0.0287	106.2379	Up
	Guanosine	0.0289	37.6496	Up
	Hypoxanthine	0.0293	32.3095	Up
	Vanillate ††	0.0295	70.03194	Up
	1-Methyluric acid	0.0314	32.00227	Up
	1-Methylnicotinamide	0.0326	45.14991	Up
	m-Cresol	0.0331	46.23026	Up
	Trans-Aconitic Acid	0.0338	-42.4723	Down
	Xanthine	0.0345	63.43318	Up
	1-Methylnicotinamide	0.0347	62.3589	Up
	Hydroxyacetone	0.0352	69.24272	Up
	Deoxyadenosine triphosphate	0.0356	103.8414	Up
	3-Furoic acid ††	0.0369	47.73458	Up
	2-Phenylglycine	0.0375	-39.5166	Down
	3-Hexenedioic acid	0.0382	44.46205	Up
	Trigonelline	0.0391	108.543	Up
	FAPy-adenine ††	0.0391	56.38613	Up
	3-Furoic acid	0.0391	73.01136	Up
	2-Furoate ††	0.0391	91.53704	Up
	Riboflavin	0.0391	168.6219	Up
	3-Hexenedioic acid	0.0391	72.46143	Up
	Pipecolic acid	0.0391	47.00136	Up
	Citramalic acid	0.0392	47.97462	Up
	Unidentified	0.0398	51.83979	Up
	3-Hydroxymethylglutaric acid	0.0411	28.46693	Up
	Glyoxaline	0.0416	-56.9783	Down
	1-Methylguanosine	0.0419	32.15302	Up
	Methanol	0.0426	22.62963	Up
	Citraconate	0.0441	34.25105	Up

	4-Aminohippuric acid	0.0444	55.67541	Up
	Acetate	0.0488	26.69932	Up
Female	1-Methylnicotinamide	0.0061	90.5887	Up
	Unidentified	0.0142	89.90024	Up
	Inosine	0.0174	44.05605	Up
	1-Methyladenine	0.0181	72.89333	Up
	Unidentified	0.0242	40.08145	Up
	4-Hydroxy-3-methylbenzoic acid	0.0269	73.568	Up
	Galactonate	0.0300	66.90381	Up
	O-Cresol	0.0310	-66.3256	Down
	Anserine	0.0317	77.3389	Up
	2-Furoylglycine	0.0364	110.9238	Up
	S-Adenosylhomocysteine †	0.0372	44.05605	Up
	Riboflavin	0.0376	-116.546	Down
	Hydroxyacetone †	0.0392	97.38142	Up
	Guanosine †	0.0447	79.59892	Up
Male and Female	4-Hydroxyphenylpyruvic acid	<0.0001	-110.954	Down
	Glyoxaline	0.0001	-80.6225	Down
	L-Phenylalanine ††	0.0005 (W)	-115.191	Down
	Melatonin	0.0010 (W)	-118.783	Down
	2,5-Furandicarboxylic acid	0.0010	-98.2494	Down
	Sarcosine	0.0010 (W)	-68.2029	Down
	Methylcysteine	0.0010 (W)	-116	Down
	Acetylcholine	0.0010 (W)	-114.564	Down
	Quinic acid ††	0.0010 (W)	-60.1084	Down
	3-Methylxanthine	0.0014	48.89025	Up
	2-Furoylglycine †	0.0015 (W)	121.754	Up
	5-Hydroxymethyl-4-methyluracil	0.0015	88.60888	Up
	1-Methyladenine	0.0022	70.15323	Up
	Protocatechuic acid	0.0024 (W)	-77.0304	Down
	N-Acetylmannosamine	0.0024 (W)	-82.1738	Down
	Nicotinic acid adenine dinucleotide	0.0027	108.4384	Up
	Hydroxyacetone †	0.0027	81.77733	Up
	1-Methylguanosine	0.0027	50.67365	Up
	2-Phenylglycine	0.0029	-46.0792	Down
	Trans-Aconitic Acid	0.0033	-47.1949	Down
	Glyoxaline	0.0034 (W)	-64.1649	Down
	Allose	0.0034 (W)	-71.1363	Down
	5-Methylcytidine †	0.0041	98.07964	Up
	Melatonin	0.0041	-49.5651	Down
	Trigonelline	0.0044	92.98839	Up
	ADP	0.0046	77.31586	Up
	Deoxyinosine	0.0049 (W)	66.78409	Up
	Deoxyadenosine triphosphate †	0.0049 (W)	92.50578	Up
	Guanosine †	0.0049 (W)	73.15467	Up

	Guanosine	0.0049 (W)	70.74163	Up
	Vanylglycol	0.0052	65.50244	Up
Male and Female	Trigonelline	0.0057	83.01762	Up
	Xanthosine	0.0058	131.4733	Up
	N-methylnicotinamide	0.0059	60.26205	Up
	Homovanillate	0.0063	-47.4043	Down
	3-Furoic acid †	0.0068 (W)	64.87697	Up
	1-Methylnicotinamide	0.0068 (W)	73.73425	Up
	N-Phenylacetylglycine †	0.0069	-44.8828	Down
	Deoxyinosine	0.0075	61.14409	Up
	Dehydroascorbic acid	0.0081	69.48773	Up
	1-Methyladenine	0.0085	61.52399	Up
	Xanthosine	0.0092	119.1483	Up
	Glycerate	0.0093	29.31449	Up
	Phosphocreatine	0.0093 (W)	-30.6515	Down
	m-Cresol	0.0100	39.22118	Up
	Adenosine	0.0109	39.85581	Up
	Inosine	0.0122 (W)	58.54596	Up
	Xanthine	0.0127	48.77765	Up
	3-Methyladenine	0.0128	73.93608	Up
	Xanthurenic acid	0.0131	-37.2447	Down
	Trimethylamine	0.0131	40.66431	Up
	Vanillate †	0.0140	59.79043	Up
	1-Methyladenine	0.0147	39.30408	Up
	5-Aminolevulinic acid	0.0147	33.89688	Up
	Histidine	0.0161 (W)	48.40674	Up
	Cinnamic acid	0.0161 (W)	93.06875	Up
	Unidentified	0.0168	57.7468	Up
	Citicoline	0.0172	59.54046	Up
	2-Furoylglycine	0.0175	104.5104	Up
	Deoxyinosine	0.0182	40.88759	Up
	2,2-Dimethylsuccinic acid †	0.0188	49.7713	Up
	1-Methylnicotinamide	0.0198	47.5794	Up
	Hippurate	0.0208	59.83024	Up
	Trigonelline	0.0210 (W)	86.72517	Up
	Galactonate ††	0.0210 (W)	38.39573	Up
	1,3,7-Trimethyluric acid	0.0210 (W)	25.5829	Up
	Hippurate	0.0233	50.0585	Up
	N-Methylnicotinamide	0.0253	41.9966	Up
	5-Hydroxyindoleacetic acid	0.0255	-26.2021	Down
	L-Malic acid	0.0259	45.91603	Up
	Hippurate	0.0289	51.01796	Up
	Homovanillate	0.0319	-60.5568	Down
	Hippurate	0.0336	46.35172	Up
	Hippurate	0.0342 (W)	54.23087	Up
	Dehydroascorbic acid †	0.0342 (W)	38.82031	Up

	Homovanillic acid ††	0.0342 (W)	-63.5781	Down
	Malic acid	0.0342 (W)	23.72859	Up
Male and Female	1,3-dimethylurate †	0.0349	42.85411	Up
	Homoveratric acid †	0.0352	-34.5104	Down
	4-Aminohippuric acid †	0.0353	44.1898	Up
	Hippurate	0.0367	46.80818	Up
	Unidentified	0.0376	33.81275	Up
	3-Methyladenine	0.0381	28.66381	Up
	Anserine	0.0396	47.97782	Up
	Unidentified	0.0425 (W)	86.33283	Up
	Dimethylglycine	0.0425 (W)	40.01964	Up
	3-Mercaptopyruvic acid	0.0425 (W)	30.10323	Up
	Citric acid †	0.0425 (W)	73.31139	Up
	Citric acid †	0.0425 (W)	69.59278	Up
	tau-Methylhistidine	0.0445	44.01973	Up
	Histamine	0.0454	49.7772	Up
	Hippurate	0.0467	47.14561	Up
	Hippurate	0.0481	46.07529	Up
	1,7-Dimethylxanthine	0.0494	41.6028	Up

APPENDIX 2: List of Metabolites Recovered in the Blood of TBI Patients

Sex	Bin/Metabolite	Paired T/Wilcoxon *p* value	% Difference	Regulation
Male	L-Phenylalanine	0.0002	-60.140	Down
	1,9-Dimethyluric Acid	0.0005	25.651	Up
	Phosphonoacetate	0.0012	42.262	Up
	P-Cresol	0.0013	-84.436	Down
	L-Phenylalanine	0.0031	-30.914	Down
	Glycine	0.0031	18.260	Up
	Citric Acid	0.0040	35.800	Up
	Phosphonoacetate	0.0045	37.428	Up
	1,3-Dimethyluric Acid	0.0046	22.159	Up
	p-Cresol	0.0050	-65.625	Down
	2-Hydroxybutyrate ††	0.0050	-79.804	Down
	Glycine	0.0061	19.568	UP
	Trimethylamine-N-Oxide	0.0066	26.092	Up
	3-Methyl-2-Oxovaleric Acid	0.0066	-75.379	Down
	Creatinine	0.0078 (W)	21.179	Up
	Levulinate †	0.0089	20.412	Up
	Unidentified	0.0107	-53.026	Down
	Citramalic Acid	0.0112	18.255	Up
	4-Pyridoxate	0.0153	16.975	Up
	1,5-Anhydrosorbitol	0.0156 (W)	27.891	Up
	1,3-Dimethyluric Acid †	0.0156 (W)	20.480	Up
	Citramalic Acid †	0.0158	17.716	Up
	Pyruvic Acid	0.0169	17.951	Up
	L-Alanine ††	0.0172	35.621	Up
	1,5-Anhydrosorbitol	0.0178	20.012	Up
	Guanidoacetate †	0.0209	15.256	Up
	5-Hydroxyindole-3-acetate	0.0221	20.959	Up
	Tyrosine	0.0234	-33.767	Down
	Glucose	0.0274	-14.882	Down
	Glucose	0.0322	-9.187	Up
	Unidentified	0.0352	-86.139	Down
	D-Mannose	0.0391 (W)	-76.053	Down
	Hydroxyphenylacetylglycine	0.0391 (W)	11.043	Up
	Theophylline	0.0421	14.543	Up
	Lactate	0.0428	25.843	Up
	Glucose	0.0438	-7.688	Down
	Pi-methylhistidine	0.0449	18.003	Up
	Could not identifty	0.0476	15.001	Up
	Creatinine	0.0487	24.941	UP
	Acetylphosphate	0.0490	14.059	Up

	Methylsuccinic Acid	0.0497	13.903	Up
Female	1,3-Dimethyluric Acid ††	0.0110	32.479	Up
	1,9-Dimethyluric Acid ††	0.0487	39.374	Up
	3-Methyl-2-Oxovaleric Acid †	0.0299	-67.343	Down
	4-Hydroxyproline ††	0.0497	34.010	Up
	Citramalic Acid †	0.0300	10.393	Up
	Creatinine †	0.0006	20.098	Up
	Ethanol	0.0226	-49.084	Down
	Glycylproline †	0.0131	21.828	Up
	Glycylproline	0.0050	15.135	Up
	Glycylproline	0.0165	10.039	Up
	Malic Acid †	0.0093	22.987	Up
	Methylcysteine †	0.0019	23.663	Up
	Myoinositol ††	0.0069	45.528	Up
	N-Isovaleroylglycine †	0.0233	35.847	Up
	Phenyllactic Acid †	0.0381	22.491	Up
	Proline †	0.0297	20.453	Up
	Proline †	0.0132	33.980	Up
	Proline †	0.0075	29.734	Up
	Proline †	0.0138	26.758	Up
	Proline	0.0125	26.243	Up
	Proline	0.0086	30.491	Up
	Proline	0.0351	31.222	Up
	Proline	0.0276	31.005	Up
	Proline	0.0228	28.518	Up
	Proline †	0.0449	29.477	Up
	Thymine	0.0398	17.238	Up
	Thymine †	0.0134	27.550	Up
	Trimethylamine	0.0203	19.590	Up
	Trimethylamine	0.0132	18.705	Up
Male and Female	1,9-Dimethyluric Acid	<0.0001	30.852	Up
	Phosphonoacetate	<0.0001	46.250	Up
	2-Hydroxybutyrate ††	0.0002	-75.559	Down
	Citric Acid	0.0003	42.831	Up
	1,3-Dimethyluric Acid	0.0004	28.353	Up
	Phosphonoacetate	0.0004	41.805	Up
	Creatinine	0.0005 (W)	20.826	Up
	3-Methyl-2-Oxovaleric Acid ††	0.0005	-67.803	Down
	Glycine	0.0006	19.779	Up
	Trimethylamine-N-Oxide	0.0009	28.210	Up
	Citramalic Acid	0.0015	16.278	Up
	Glycine	0.0018	21.694	Up
	1,3-Dimethyluric Acid	0.0020	28.382	Up
	Unidentified ††	0.0021	-44.862	Down
	1,5-Anhydrosorbitol	0.0023	23.615	Up
	Citramalic Acid	0.0024 (W)	17.722	Up

	Levulinate	0.0027	16.325	Up
	Pyruvic Acid	0.0034	15.338	Up
	4-Pyridoxate	0.0037	14.546	Up
	1,5-Anhydrosorbitol	0.0039	29.655	Up
	Guanidoacetate	0.0042	19.464	Up
	5-Hydroxyindole-3-Acetate	0.0048	23.728	Up
	Glucose	0.0062	-16.667	Down
	Methylsuccinic Acid	0.0068 (W)	12.168	Up
	Hydroxyphenylacetylglycine	0.0076	13.010	Up
	L-Lactic Acid †	0.0084	33.000	Up
	1,3-Dimethyluric Acid	0.0085	21.837	Up
	1,3,7-Trimethyluric Acid †	0.0094	24.861	Up
	Citramalic Acid	0.0103	19.410	Up
	3-Methyl-2-Oxovaleric Acid	0.0105	-47.904	Down
	L-Alanine	0.0111	27.355	Up
	Creatinine ††	0.0125	32.605	Up
	Creatine Phosphate	0.0161 (W)	34.138	Up
	Citric Acid	0.0161 (W)	25.547	Up
	5-Hydroxyindole-3-Acetate	0.0162	12.424	Up
	Theophylline	0.0162	13.415	Up
	Sarcosine	0.0188	21.829	Up
	Dimethylsulfide	0.0197	10.577	Up
	Unidentified	0.0202	-109.814	Down
	Unidentified	0.0210 (W)	29.902	Up
	Acetyl phosphate	0.0211	12.028	Up
	Isoleucine	0.0229	14.124	Up
	Methylimidazoleacetic Acid	0.0233	-8.026	Down
	p-Cresol	0.0269 (W)	-24.353	Down
	Glucose	0.0320	-7.002	Down
	L-Lactic Acid	0.0342	25.520	Up
	Unidentified	0.0342 (W)	9.523	Up
	Methylcysteine †	0.0342 (W)	17.445	Up
	Lactate	0.0402	21.776	Up
	p-Cresol	0.0425 (W)	-25.365	Down
	Glucose	0.0433	-7.184	Down
	Succinylacetone	0.0438	-71.220	Down
	1-Methylguanine	0.0444	-7.493	Down
	Glucose	0.0445	-7.579	Down
	Glycocholic Acid	0.0450	-32.092	Down
	Pi-Methylhistidine	0.0482	17.576	Up
	Glycerophosphocholine	0.0490	-8.102	Down
	L-Alanine	0.0490	21.832	Up
	Methylcysteine	0.0493	13.136	Up

APPENDIX 3: List of Metabolites Recovered in the Urine of Male SCI Patients

Heat Map Number	Metabolite	Paired T/Wilcoxon *p* value	Regulation
4	4-Pyridoxic Acid	0.0011	Up
19	Nicotinurate	0.0015	Up
41	Sumiki's acid ††	0.0029	Up
25	Methylimidazoleacetic Acid	0.0036	Up
3	Imidazole	0.0038	Up
7	Gluconic acid †	0.0059	Up
32	Adenosine Monophosphate	0.0065	Up
38	4-Hydroxy-3-Methylbenzoic Acid	0.0071	Up
42	N-Methylhydantoin †	0.0078	Up
20	Xanthosine	0.0081	Up
34	3,4-Dihydroxybenzeneacetate	0.0089	Up
18	Indoxyl Sulfate	0.0113	Up
17	Guanosine	0.0129	Up
36	Isoferulic Acid	0.0141	Up
39	2-Furoic Acid	0.0149	Up
40	3-Methylhistamine †	0.0163	Up
11	Hydroxycobalamin	0.0164	Up
16	Formate	0.0195	Up
5	Acetoacetate	0.0215	Up
21	Dopamine ††	0.0216	Up
1	Glutarylglycine	0.0218	Up
9	N-Acetyltyrosine †	0.0269	Up
12	L-Trytophan	0.0275	Up
35	Kynurenic Acid	0.0277	Up
22	D-Glucuronic Acid	0.0284	Up
33	Inosine	0.0295	Up
37	Imidazole †	0.0295	Up
26	2-Furoylglycine	0.0313 (W)	Up
31	ADP	0.0313 (W)	Up
29	Pyroglutamic Acid	0.0313 (W)	Up
13	Fructose	0.0313 (W)	Up
27	Riboflavin	0.0313 (W)	Up
10	Indole-3-lactate †	0.0313 (W)	Up
14	Imidazole †	0.0313 (W)	Up
15	2-Isopropylmalic acid †	0.0313 (W)	Up
8	Caffeine ††	0.0313 (W)	Up
24	2,2-Dimethylsuccinic Acid	0.0318	Up
30	6-Hydroxynicotinate	0.0371	Up
6	Succinylacetone	0.038	Up
28	Pyroglutamic Acid	0.0421	Up
23	4-Methylcatechol	0.0435	Up

44	Deaminotyrosine †	0.0474	Up
43	Homovanillate	0.0484	Up
2	N-Acetylmannosamine	0.0488	Up

APPENDIX 4: List of Metabolites Recovered in the Blood of Male SCI Patients

Heat Map Number	Metabolite	Paired T/Wilcoxon *p* value	Regulation
13	Acetic Acid †	0.0022	Up
16	Dimethyl Sulfone	0.0156 (W)	Up
9	Citric Acid †	0.0187	Up
8	Citric Acid ††	0.0192	Up
7	Citric Acid ††	0.0202	Up
14	Acetic Acid †	0.0247	Up
18	1,9-Dimethyluric Acid	0.027	Up
6	Citric Acid ††	0.028	Up
19	1,9-Dimethyluric Acid †	0.0306	Up
12	1,5-Anhydrosorbitol	0.0361	Up
11	Succinic Acid	0.0361	Up
17	Methanol	0.04	Up
3	1,3,7-Trimethyluric Acid	0.0435	Down
4	D-Glucose	0.0445	Down
5	D-Mannose	0.0469 (W)	Down
15	Cannot be identified	0.0469 (W)	Up
10	Lactate	0.0484	Up
2	1,3,7-Trimethyluric Acid ††	>0.05	Down
1	Acetylphosphate ††	>0.05	Down
	Pantothenic Acid †	>0.05	Up
	Acetylphosphate †	>0.05	Down
	Acetylphosphate †	>0.05	Down
	1,5-Anhydrosorbitol †	>0.05	Up